Statistical Analysis of Integrated Circuits using Decoupled Polynomial Chaos

by

Xiaochen Liu

Thesis submitted to the
Faculty of Graduate and Postdoctoral Studies
In partial fulfillment of the requirements
For the M.A.Sc degree in
Electrical and Computer Engineering

School of Electrical Engineering and Computer Science
Faculty of Engineering
University of Ottawa

Abstract

One of the major tasks in electronic circuit design is the ability to predict the performance of general circuits in the presence of uncertainty in key design parameters. In the mathematical literature, such a task is referred to as uncertainty quantification. Uncertainty about the key design parameters arises mainly from the difficulty of controlling the physical or geometrical features of the underlying design, especially at the nanometer level. With the constant trend to scale down the process feature size, uncertainty quantification becomes crucial in shortening the design time.

To achieve the uncertainty quantification, this thesis presents a new approach based on the concept of generalized Polynomial Chaos (gPC) to perform variability analysis of general nonlinear circuits. The proposed approach is built upon a decoupling formulation of the Galerkin projection (GP) technique, where the large matrix is transformed into a block-diagonal whose diagonal blocks can be factorized independently. The proposed methodology provides a general framework for decoupling the GP formulation based on a general system of orthogonal polynomials. Moreover, it provides a new insight into the error level that is caused by the decoupling procedure, enabling an assessment of the performance of a wide variety of orthogonal polynomials. For example, it is shown that, for the same order, the Chebyshev polynomials outperforms other commonly used gPC polynomials.

Acknowledgements

I would like to express my sincerely gratitude to my supervisor, Professor Emad Gad, who offered me the chance to work on this interesting topic as well as the huge support and encouragement he gave me even before the day I started my research with him. I'm truly grateful for his valuable advises and inspirations, which were key to me finishing this thesis. I also appreciate Prof. Michel Nakhla for the solid background knowledge learned in his courses.

I wish to thank my colleagues Seyed and Kevin(Gao Kai) for their help and advice not only in research, but also in my graduate life.

More over, I want to give my special thanks to my wife, Jie Hao, for her understanding, respect, companionship and happiness she continuous to bring to me. It is her love that has helped me to overcome so many difficulties and problems. I'd also like to thank my parents for their unconditional love and support.

Finally, I would like to thank everyone in the community that my wife and I stayed with as they treat us like their children, especially my landlords Mr. and Mrs. Fridriksson and our neighbors Mr. and Mrs. Poland, when we are far from our homeland.

Table of Contents

List of Acronyms vii

List of Symbols viii

List of Tables xi

List of Figures xiii

1 Introduction 1

1.1 Background 1

1.2 Motivation 5

1.3 Contribution 5

1.4 Organization of the Thesis 6

2 Notations and Mathematical Formulation 7

2.1 Notation 7

2.2 Mathematical Formulation 8

2.2.1 Mathematical Formulation of Linear Circuits 8
2.2.2 Mathematical Formulation of Nonlinear Circuits 10
2.3 Mathematical Formulation with Uncertainty 12
2.4 Statistical Analysis of Circuit Performance 13

3 Background on Statistical Analysis **14**
3.1 Background on Probability Theory and Random Variable 15
3.2 Functions of Random Variables 21
3.3 Background on Statistical Analysis methods 23
3.3.1 The Monte Carlo Methods 24
3.3.2 The Generalized Polynomial Chaos 25
3.4 Discussion 39

4 Proposed Decoupling Approach **40**
4.1 Introduction 40
4.2 The Generalized Decoupling Approach 42
4.2.1 Theoretical Basis 42
4.2.2 Decoupling Approach: FD Analysis for Single Random Case 50
4.2.3 Decoupling Approach: FD Analysis for Multi-random Case 53
4.2.4 Decoupling Approach: TD Analysis for Multi-random Case 54
4.2.5 Summary 57

4.3 Non-Askey-Wiener Polynomials 58

4.4 Study of the Decoupling Error 61

5 Numerical Examples **64**

5.1 Examples for Decoupling approach 65

5.1.1 Example 1 65

5.1.2 Example 2 66

5.1.3 Example 3 74

5.2 CPU Time Comparison 79

6 Conclusion and Future Work **81**

6.1 Conclusion 81

6.2 Future Work 82

APPENDICES **84**

A Coefficients Conversion **85**

References **90**

List of Acronyms

Acronyms	Definition
BE	Backward Euler
CAD	computer-Aided Desugn
CPU	central processing unit
EM	Electromagnetic
FD	Frequency-domain
GP	Galerkin projection
gPC	generalized Polynomial Chaos
MC	Monte Carlo
MNA	Modified Nodal Analysis
MTLs	Multi-conductor Transmission Lines
Noc	number of coefficients
PC	Polynomial Chaos
PDF	probability distribution function
pdf	probability density function
RV(s)	Random variable(s)

SC	Stochastic collocation
ST	Stochastic Testing
TD	Time-domain

List of Symbols

Symbols	Definition
μ	mean value
σ	standard deviation
var	variance
ξ	single random variable
$\boldsymbol{\xi}$	set of multi-random variable
$<,>$	inner product
$H_n(\xi)$	Hermite polynomial of degree n
$P_n(\xi)$	Legendre polynomial of degree n
$L_n^{(\alpha)}(\xi)$	Generalized Laguerre polynomial of degree n with index α
$J_n^{\alpha,\beta}(\xi)$	Jacobi polynomial of degree n with index α and β
$T_n(\xi)$	Chebyshev polynomial of degree n
α, β, γ	single-dimensional indices
$\boldsymbol{\alpha}, \boldsymbol{\beta}, \boldsymbol{\gamma}$	multi-dimensional indices
α_i	i^{th} component of $\boldsymbol{\alpha}$
$\lvert\boldsymbol{\alpha}\rvert$	rank of a multi-index $\boldsymbol{\alpha}$

Υ_Q	a set of indices based on Tensor order truncation scheme
$\phi_\alpha(\xi)$	single-dimensional polynomial with degree α
$\phi_{\boldsymbol{\alpha}}(\boldsymbol{\xi})$	multi-dimensional polynomials with degree $\boldsymbol{\alpha}$
$w(\xi)$	weighting function for single-dimensional polynomial
$\boldsymbol{w}(\boldsymbol{\xi})$	weighting function for multi-dimensional polynomials
$\delta_{i,j}$	Kronecker delta function
$\delta(x)$	Dirac delta function
$\boldsymbol{G}$	matrix describing the memoryless elements in the circuit
$\boldsymbol{C}$	matrix describing the memory elements in the circuit
s	frequency variable of the circuit
$\boldsymbol{Y}(s)$	$\boldsymbol{Y}(s) = \boldsymbol{G} + s\boldsymbol{C}$
$\boldsymbol{X}(s)$	circuit response in frequency-domain
$\boldsymbol{x}(t)$	circuit response in time-domain
$\boldsymbol{U}(s)$	vector representing the independent stimulus of a circuit in frequency-domain
$\boldsymbol{b}(t)$	vector representing the independent stimulus of a circuit in time-domain
$\boldsymbol{f}(\boldsymbol{x}(t))$	the vector of nonlinear algebraic function that capture the nonlinear elements in the circuit.
$\hat{\boldsymbol{A}}_{\boldsymbol{\beta}}$	polynomial chaos basis expansion coefficients of $\boldsymbol{A}$
$\breve{\boldsymbol{A}}_{\boldsymbol{\beta}}$	Taylor series expansion coefficients of $\boldsymbol{A}$
$[\boldsymbol{A}]_{p,q}$	a scalar entry in matrix $\boldsymbol{A}$ located at p^{th} row and q^{th} column

$\{\boldsymbol{A}\}_{p,q}^{n}$	a block of size $n \times n$ in the matrix $\boldsymbol{A}$ that occupies rows p through $p+n-1$ and columns q through $q+n-1$
$\otimes$	the Kronecker product operator

List of Tables

3.1 gPC polynomial basis for different probability distribution 30

3.2 Orthogonality of commonly used gPC polynomial basis 31

3.3 Example of multi-index and multi-dimensional OP when $d = 2$, $M_1 = M_2 = 2$ (the distribution of two random variables are Gaussian and Uniform respectively . 32

4.1 ratio between the Frobenius norm of $\boldsymbol{\Delta}_\beta$ and $\boldsymbol{K}_\beta$ for the case of single random variable problem (d=1), $\beta = 2, 3, 4$ and $M = 2, 3, 4$ for different gPC basis . . . 63

5.1 Computational complexity comparison of three methods 79

5.2 CPU time comparison 80

List of Figures

2.1 A simple linear circuit example. 9

2.2 A simple nonlinear circuit example. 11

3.1 Examples of the pdf of Gamma Distribution. 20

3.2 Examples of the pdf of Beta Distribution. 21

4.1 Gaussian and Uniform distributions with same mean and variance 59

5.1 Schematic of RLC circuit used in Example 1. 65

5.2 pdf Comparison between Hermite and Chebyshev expansion for Gaussian distribution. 67

5.3 pdf Comparison between Legendre and Chebyshev expansion for Uniform distribution. 68

5.4 pdf Comparison between Laguerre and Chebyshev expansion for Uniform distribution. 69

5.5 Schematic of low-pass filter for example 2. 70

5.6 OpAmp subsircuit model. 70

5.7 pdf Comparison between multi-dimensional Chebyshev expansion and gPC basis expansion. 72

5.8 Distribution and the mean value of the output voltage. 73

5.9 Variance of the output voltage. 73

5.10 Schematic of low-pass filter for example 3. 74

5.11 pdf Comparison between multi-dimensional Chebyshev expansion and gPC basis expansion at 4 GHz. 75

5.12 pdf Comparison between multi-dimensional Chebyshev expansion and gPC basis expansion at 6 GHz. 76

5.13 pdf Comparison between multi-dimensional Chebyshev expansion and gPC basis expansion at 8 GHz. 77

5.14 Distribution and mean value of the output voltage. 78

5.15 Variance of the output voltage. 78

Chapter 1

Introduction

1.1 Background

In today's world, electronics, such as computers and cell-phones, are already becoming an indivisible part of our life. The one main fact that enabled the greater integration of electronics into society and daily consumer's life is the rapid progress in process technology which allowed reducing feature size of the transistor quite dramatically. Yet, this reduction in feature size to the nanometer level has not come without tremendous challenges to the Computer-Aided Design (CAD) community. The challenges for CAD research community stem from the fact that at the nanometer scale, process variability becomes too significant to ignore. This fact meant that CAD tools now need to treat circuits and system not as deterministic design, but rather consider them as the stochastic process, whose performance is fraught with uncertainty due to the uncertainty of variability in the fabrication process.

Thus, one of the main challenges in nano-scale designs is predicting the effect of the inher-

ent process variability of geometrical and physical parameters on the general performance of integrated circuits. The lack of predictability arises mainly from the difficulty of controlling the physical and geometrical parameters during the fabrication process. This effectively makes the numerical values for those parameters subject to significant uncertainty, which, in turn, produces uncertainty in the electrical performance of the circuit.

Traditionally, Monte Carlo (MC)[1] simulations have been used in the commercial circuit and Electromagnetic (EM) simulations for predicting the statistical distribution of the circuit and system performance. However, the slow convergence for MC has become a computational burden, especially in simulating large circuits. This fact has prompted wide interest in exploring alternative approaches to the problem of statistical analysis of the performance of electronic circuits.

A recent approach based on the notion of generalized polynomial chaos (gPC) was developed and showed a great computational advantage over the standard MC-based analysis [2]. This approach has been used in estimating the statistical properties of different types of circuits. Earlier polynomial chaos (PC) approaches focused on characterizing the variability analysis of interconnects [3] and multi-conductor transmission lines in the presence of process variations [4]. Further work addressed the problem of variability in generic multiport linear circuits [5]. It was also expanded to nonlinear circuits in [6] and to transmission line circuits terminated by nonlinear loads in [7]. The basic idea in the gPC approach is to expand the circuit response in a series of the Askey-Wiener type of orthogonal polynomials, e.g, Hermite polynomials, and then use a numerical method to compute the coefficients of the series. Typically, those coefficients are used to extract statistical information about the circuit response, e.g. mean and variance.

Several techniques have been available or recently proposed to compute the PC series numerically. The widest classification scheme in which those techniques may be classified is intrusive versus non-intrusive approaches.

The intrusive approach works by expanding the circuit equations into a larger system of equations whose solution directly yields the values for those PC coefficients. The non-intrusive approach approaches the task of computing the coefficients in a two-phase process. In the first phase, the circuit response is computed (typically, by a commercial simulator) at a grid points in the space spanned by the random parameters. In the second phase, the solutions found at those grid points are assembled to compute the PC series coefficients for few selected states of the circuit response. The stochastic technique based on the Galerkin projection (GP) is the best-known example of the intrusive approach, whereas the stochastic collocation-based (SC) is clearly a non-intrusive approach.

The major drawback in the SG is the requirement to solve a larger system of equations with dense Jacobian matrix. This drawback limits the applicability of this technique to problems with few random variables. By contrast, the first phase in the SC requires solving the original circuit equations at independent grid points in random space. This fact represents an advantage since it can be efficiently implemented on parallel platforms, and involves factorizing a sparse Jacobian matrix that typically from the sparse circuit connectivity. Recent development also proposed using sparse grid in the random space to increase the efficiency of the collocation approach [8].

Nevertheless, the intrusive approach presents an important and a rather subtle advantage over the collocation-based non-intrusive approach, when the task at hand is the statistical characterization of a time-domain response of the circuit variables, where PC coefficients are time-dependent

and, therefore, can only be computed at the discrete set of time points. That fact poses a unique challenge for the collocation approach that is a non-sequitur in the intrusive one. This is because the length of the time step is adaptively adjusted (by the commercial simulator in the first phase) with each new time point. This means that the discrete time-domain points chosen for a particular grid point in the random space will, more likely than not, be different from other grid points, and the challenge then becomes which set of discrete time points to use in the second phase for computing the coefficients. While interpolation may be used to reach a common discrete set of time-domain points, it can be a source of errors for the high-order PC coefficients [9].[1]

Combining the advantages in both approaches appears to have been first proposed in the formulation of the collocation method presented in [11]. While this formulation results in a larger system of equations, the resulting Jacobian matrix can be transformed into a (decoupled) block diagonal form, where the diagonal blocks can be factorized independently, effectively matching the desirable computational complexity of the collocation approach while alleviating its main problem of finding a common set of discrete time points. However, this formulation remained limited by the fact that it required the PC coefficients to be truncated in the tensor order, which grows exponentially with the number of random variables. Overcoming this problem was then proposed in the idea of Stochastic Testing (ST) [9], which is collocation-based intrusive method aiming at constructing a PC truncation scheme based on the total order, thereby, reducing significantly the number of diagonal blocks that need to be factorized.

A more recent approach [12], [13] considered the Galerkin based intrusive method and proposed a method to decouple its Jacobian matrix. This approach relies on developing a new

[1] In addition to the above advantage, a recent independent study comparing SC to GP indicated that GP "gives higher accuracy per stochastic degree of freedom" [10]

general formula that characterizes the structure of the augmented Jacobian matrix and shows that this structure can be decoupled into smaller matrices that can be factorized independently. That approach, however, still remains limited to PC problems described by Hermite polynomials, which limit the simulation only if the uncertain parameters has a Gaussian distribution.

1.2 Motivation

The main motivation of this work stems from the basic observation that uncertain parameters are not always Gaussian. This fact has limited the domain of applications of the decoupling approach presented in [12]. The basic objective of this thesis, has, therefore, been to seek a generalization methodology for the diagonalization and decoupling approach within a more general framework of non-Gaussian types of uncertainty. Achieving this goal would not only benefit the particular area of circuit simulation, but should also make it possible to be applied for uncertainty quantification in other fields.

1.3 Contribution

The main contribution of this work is to generalize the decoupling approach so that it can handle any type or system of orthogonal polynomials. The proposed methodology provides a general framework for decoupling the GP formulation based on a general system of orthogonal polynomials. Moreover, it provides a new insight into the error level that is caused by the decoupling procedure, enabling an assessment of the performance of a wide variety of orthogonal polynomials. For example, it is shown that, for the same order, the Chebyshev polynomials outperform

other commonly used gPC polynomials.

The preliminary idea of the generalized decoupling approach related to the special case of a single random parameter has been presented in [14]. This work presents the details for the case of multi-random parameters and provides the necessary proofs. Part of this work has also been submitted to a journal publication [15].

1.4 Organization of the Thesis

The rest of the thesis is organized as follows: Chapter 2 provide the mathematical framework for this thesis as well as the necessary notation. In chapter 3, the background of uncertainty quantification is provided, including the background of probability theory and random variable (RV) in section 3.1 and background on statistical analysis methods in section 3.3. The principle of proposed decoupled approach can be found in Chapter 4. The numerical examples and the summary of this thesis plus the future research options are in Chapter 5 and Chapter 6 respectively.

Chapter 2

Notations and Mathematical Formulation

In this chapter, the first section will present the basic notations used in this thesis. This will be followed by a brief review of mathematical formulation for circuit simulation for both the situations with and without uncertainty parameters.

2.1 Notation

A key part of the notation in this thesis is the concept of a multi-index which is a vector, e.g. $\boldsymbol{\alpha} \in \mathbb{N}^d$ of d non-negative integers. In the following treatment, a multi-index written in non-bold font with subscript i, α_i is used to denote the i^{th} component of the multi-index $\boldsymbol{\alpha}$.

A common task often associated with the notion of multi-index is defining a finite set of multi-indices. One such idea is based on the notion of tensor order which defines a set of multi-indices by only allowing all multi-indices $\boldsymbol{\alpha} \in \mathbb{N}^d$ whose components satisfy $\alpha_i \leq M_i$ (for a set of positive integers M_i) to be included in the set. A set of indices defined in this manner will

have Q multi-index elements, where $Q = \prod_{i=1}^{d}(M_i+1)$. In this thesis, a set formed based on the tensor order will be denoted by Υ_Q. To simplify the discussion, we assume $M_1 = M_2 = \cdots = M_d = M$ for the rest of the thesis.

Another task that is typically important in the presentation of the following results is the ordering of the multi-indices under tensor order truncation scheme. This task is accomplished by using the rank of $\boldsymbol{\alpha}$, which is denoted by $|\boldsymbol{\alpha}|$ and defined by

$$|\boldsymbol{\alpha}| = \sum_{i=1}^{d} \alpha_i (M+1)^{d-i} \tag{2.1}$$

to order elements in Υ_Q.

The mathematical manipulation in this thesis will also treat matrices. For this purpose, we will use the notation $[\boldsymbol{A}]_{p,q}$ to denote the scalar entry in a matrix $\boldsymbol{A} \in \mathbb{N}^{m\times m}$ located at the p^{th} row and q^{th} column. Furthermore, $\{\boldsymbol{A}\}_{p,q}^{n}$ is used to identify a block of size $n \times n$ in the matrix $\boldsymbol{A} \in \mathbb{N}^{m\times m}$ that occupies rows p through $p+n-1$ and columns q through $q+n-1$.

2.2 Mathematical Formulation

This section presents the basic ideas used to represent general circuits in the mathematical domain. We start first by considering the mathematical formulation of linear circuits, then follow that by the mathematical formulation of nonlinear circuits.

2.2.1 Mathematical Formulation of Linear Circuits

Linear circuits can be described either in the frequency-domain (FD) or in the time-domain (TD). The general approach used to provide the mathematical formulation is based on the idea

of Modified Nodal Analysis (MNA) which was first presented in [16].

The MNA formulation for a linear circuit in the frequency-domain takes the following form:

$$(\boldsymbol{G} + s\boldsymbol{C})\boldsymbol{X}(s) = \boldsymbol{U}(s) \tag{2.2}$$

where $\boldsymbol{G}$ and $\boldsymbol{C} \in \mathbb{R}^{N\times N}$ are matrices describing the memoryless and memory elements in the circuit, respectively, $\boldsymbol{X}(s) \in \mathbb{C}^N$ is a vector of circuit response (e.g., nodes voltages and inductors currents), and $\boldsymbol{U}(s) \in \mathbb{C}^N$ is a vector representing the independent stimulus of the circuit, all given in the Laplace-domain, with N representing the number of the variables in the circuit response and $s = j\omega$ representing the frequency variable.

Example

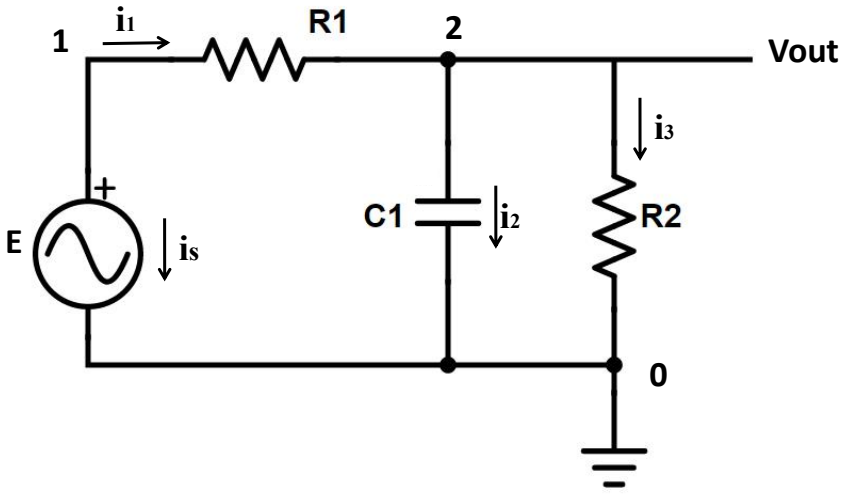

Figure 2.1: A simple linear circuit example.

Figure 2.1 shows a simple linear circuit that is used as an example to illustrate the MNA

formulation for linear circuits. The matrices $\boldsymbol{G}$ and $\boldsymbol{C}$ in this example take the following form:

$$\boldsymbol{G} = \begin{bmatrix} \frac{1}{R_1} & -\frac{1}{R_1} & 1 \\ -\frac{1}{R_1} & \frac{1}{R_1} + \frac{1}{R_2} & 0 \\ 1 & 0 & 0 \end{bmatrix}$$

$$\boldsymbol{C} = \begin{bmatrix} 0 & 0 & 0 \\ 0 & C_1 & 0 \\ 0 & 0 & 0 \end{bmatrix}$$

which the vector of circuit responses and independent stimulus take the form:

$$\boldsymbol{X}(s) = [v_1(s), v_2(s), i_s(s)]^T$$

$$\boldsymbol{U}(s) = [0, 0, E(s)]^T$$

2.2.2 Mathematical Formulation of Nonlinear Circuits

While linear circuits allow both time-domain and frequency-domain formulations, nonlinear circuits allow only the time-domain formulation. This is because the Laplace transform is defined for only linear circuits.

The time-domain representation for nonlinear circuits takes the following form:

$$\boldsymbol{C}\frac{d\boldsymbol{x}(t)}{dt} + \boldsymbol{G}\boldsymbol{x}(t) + \boldsymbol{f}(\boldsymbol{x}(t)) = \boldsymbol{b}(t) \tag{2.3}$$

where $\boldsymbol{G}$ and $\boldsymbol{C}$ are matrices that have already been defined in (2.2) for the linear circuits. $\boldsymbol{b}(t) \in \mathbb{R}^N$ and $\boldsymbol{x}(t) \in \mathbb{R}^N$ in the above formulation represents the time-domain vector of independent sources and circuit responds. $\boldsymbol{f}(\boldsymbol{x}(t))$ is the vector of nonlinear algebraic function that capture the nonlinear elements in the circuit.

The following example illustrate the mathematical formulation of nonlinear circuits.

Example

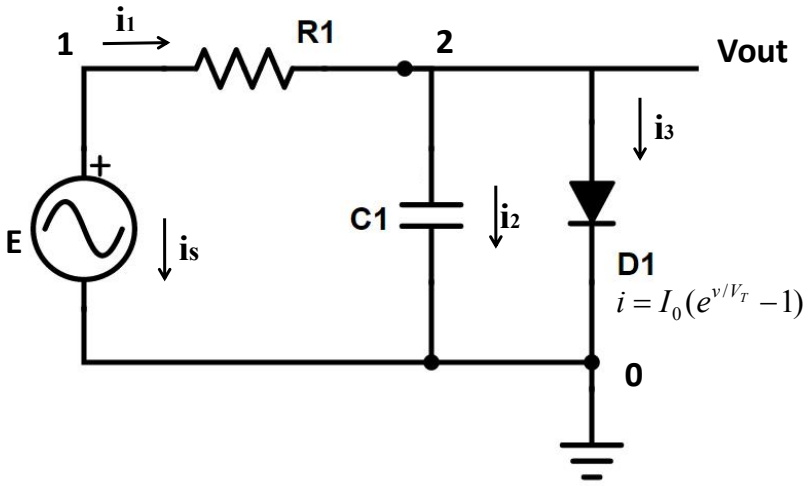

Figure 2.2: A simple nonlinear circuit example.

Considering Figure 2.2, the mathematical formulation for this circuit involves the matrices $\boldsymbol{G}$ and $\boldsymbol{C}$ which are given by:

$$\boldsymbol{G} = \begin{bmatrix} \frac{1}{R_1} & -\frac{1}{R_1} & 1 \\ -\frac{1}{R_1} & \frac{1}{R_1} & 0 \\ 1 & 0 & 0 \end{bmatrix}$$

$$\boldsymbol{C} = \begin{bmatrix} 0 & 0 & 0 \\ 0 & C_1 & 0 \\ 0 & 0 & 0 \end{bmatrix}$$

The additional nonlinear element added to this circuit is the diode. Representing this nonlinearity requires adding a vector of nonlinear functions $\boldsymbol{f}(\boldsymbol{x}(t))$, which in this example would be given by:

$$\boldsymbol{f}(\boldsymbol{x}(t)) = [0, I_0(e^{v_2(t)/V_T} - 1), 0]^T$$

The set of circuit sources is represented by the vector $\boldsymbol{b}(t)$, which is given by

$$\boldsymbol{b}(t) = [0, 0, E(t)]^T$$

2.3 Mathematical Formulation with Uncertainty

This section describes a more general circuit formulation, one in which one or more value of circuit components, e.g. the capacitance of a given capacitor or the geometrical dimensions of a given transistor, is subject to manufacturing uncertainty due to process or environmental variability.

To capture this uncertainty, we use a vector of random variables and denoted by:

$$\boldsymbol{\xi} = [\xi_1, \xi_2, \cdots, \xi_d]^T$$

Here, the RVs ξ_1,ξ_2,$\cdots$, ξ_d are taken to be of the standard types, e.g. Gaussian or Uniform, RV. More on the exact definition of RVs will be given in the next chapter.

The presence of the design uncertainty is captured by making the matrices describing the circuit formulation ($\boldsymbol{G}$ and $\boldsymbol{C}$) as well as the vector of nonlinear function of $\boldsymbol{f}(\boldsymbol{x}(t))$ dependent

on the RVs $\boldsymbol{\xi}$ as well. Thus (2.2) and (2.3) are modified as follows:

$$\boldsymbol{Y}(\boldsymbol{\xi}, s)\boldsymbol{X}(\boldsymbol{\xi}, s) = \boldsymbol{U}(s) \tag{2.4}$$

where $\boldsymbol{Y}(\boldsymbol{\xi}, s) = \boldsymbol{G}(\boldsymbol{\xi}) + s\boldsymbol{C}(\boldsymbol{\xi})$, and

$$\boldsymbol{C}(\boldsymbol{\xi})\frac{d\boldsymbol{x}(\boldsymbol{\xi}, t)}{dt} + \boldsymbol{G}(\boldsymbol{\xi})\boldsymbol{x}(\boldsymbol{\xi}, t) + \boldsymbol{f}(\boldsymbol{x}(\boldsymbol{\xi}, t), \boldsymbol{\xi}) = \boldsymbol{b}(t) \tag{2.5}$$

respectively. The response we are looking for, $\boldsymbol{X}(\boldsymbol{\xi}, s)$ and $\boldsymbol{x}(\boldsymbol{\xi}, t)$, is a random variable at each frequency or time points.

2.4 Statistical Analysis of Circuit Performance

The set of RVs ξ_1,ξ_2,$\cdots$,ξ_d in the circuit formulation acts as a source of uncertainty in the circuit performance, which in represented by the response of the circuit, whether it is a frequency-domain, i.e., $\boldsymbol{X}(\boldsymbol{\xi}, s)$ or in the time-domain, i.e., $\boldsymbol{x}(\boldsymbol{\xi}, t)$. In both cases, $\boldsymbol{X}(\boldsymbol{\xi}, s)$ and $\boldsymbol{x}(\boldsymbol{\xi}, t)$ are functions of RVs that can have one of the standard distributions, e.g. Gaussian or Uniform distribution. This fact of having the circuit response dependent on RVs makes the response itself a random entity that needs to be regarded as a stochastic process, whose characterization should be best carried out through characterizing its so-called probability density function (pdf).

The next chapter presents a basic background on the subject of statistical analysis highlighting the main aspects that are relevant to the proposed approach.

Chapter 3

Background on Statistical Analysis

The goal of this chapter is to summarize the fundamental ideas in statistical analysis which are relevant to the proposed approach in this thesis. Section 3.1 and Section 3.2 outline the foundational concepts of probability theory, such as the notion of random variables, the Probability Density Function (pdf) and the concept of the function of RVs. Following this presentation, Section 3.3 describes the main approaches used in the statistical analysis. Particular emphasis in this section is placed on the common or traditional approaches used in the circuit domains, such as the Monte Carlo (MC) approach. Another approach for statistical analysis, and perhaps a more recent one than the MC, is the approach based on the concept of generalized Polynomial Chaos (gPC) is also highlighted in this section. It should be stressed that the gPC approach serves as the foundational basis upon which the proposed approach is developed.

3.1 Background on Probability Theory and Random Variable

In discussing a certain random phenomenon, one typically speaks of a set of all possible experiment outcomes, which is termed the sample space typically denoted by S. An event space, denoted by $\tilde{F}$, is a set of events, where each event is a subset in S. The probability of an event is then a value (a real number) assigned to the event by a probability measure (a mapping from the event space to the real line with certain properties) denoted by P. The three entities of the sample space, the event space and the probability measure together constitute what is known as the probability space (S,$\tilde{F}$,P)[17].

The case of tossing a fair coin can serve as an example to illustrate the idea of probability space. In this example, the possible outcomes include heads (H) and tails (T), thus, the sample space for this is $S = \{H, T\}$. The event space is $\tilde{F} = \{\emptyset, H, T, S\}$, where $\emptyset$ is the null event and in this case means neither heads nor tails, and $S = \{H, T\}$ means either heads or tails. Here, the probability measure would be $P(\emptyset) = 0$, $P(H) = P(T) = \frac{1}{2}$ and $P(S) = 1$.

Next, quantifying a random phenomenon is typically handled through the notion of random variable (RV). A real random variable X over a probability space (S,$\tilde{F}$,P) is a function mapping S to $\mathbb{R}$ so that the inverse image of any interval $(-\infty, y]$ is an event, i.e., for all $y \in \mathbb{R}$, $\{s|X(s) \leq y, s \in S\} \in \tilde{F}$[17].

Furthermore, probabilistic characterization of an RV is carried out using the concept of the probability distribution, probability distribution function (PDF) and the probability density function (pdf). The probability distribution refers to the relationship between all the potential values

of an RV with its probability of occurrence, i.e.,

$$P_{X_i} = P(X = X_i), \forall i, \tag{3.1}$$

while the probability distribution function ($F_X(x)$) and the probability density function ($f_X(x)$) are defined as:

$$F_X(x) = P(X \leq x), x \in \mathbb{R} \tag{3.2}$$

$$f_X(x) = \frac{d}{dx} F_X(x), x \in \mathbb{R} \tag{3.3}$$

respectively.

Using the pervious example of tossing a fair coin, if we define an RV X by assuming $X(T) = -1$ and $X(H) = 1$, then the probability distribution, probability distribution function and probability density function will be,

$$P(X = -1) = P(X = 1) = \frac{1}{2} \tag{3.4}$$

$$F_X(x) = P(X \leq x) = \begin{cases} 0 & , \quad x < -1 \\ \frac{1}{2} & , \quad -1 \leq x < 1 \\ 1 & , \quad x \geq 1 \end{cases} \tag{3.5}$$

and

$$f_X(x) = \frac{d}{dx} F_X(x) = \frac{1}{2}\delta(x+1) + \frac{1}{2}\delta(x-1) \tag{3.6}$$

respectively, where $\delta(x)$ is the Dirac delta function.

Characterizing an RV is often done through two parameters, which are the expectation (or mean value) and variance (in many situations, however, the latter parameter is replaced by its

square root which is known as the standard derivation donated by σ.). Expectation refers, generally speaking, to the average value of an RV and the variance provides the information of how far the values will spread out around its expectation. Both of the expectation and the variance can be computed using a specific formula that depends on the type of RVs. Two types of RVs are distinguished in the following text along with the formulas used to compute their expectation and variances.

Discrete Random Variables

A discrete RV is an RV whose potential values can only be chosen from a finite or countable infinite set of discrete values. Let X be a discrete RV with a selection from possible values $X_1, X_2, \cdots$ and its probability distribution is given by

$$P_i = P(X = X_i) \tag{3.7}$$

The expectation and variance of X are defined as,

$$E\{X\} = \sum_i P_i X_i = \mu_X \tag{3.8}$$

$$\sigma_X^2 = var(X) = \sum_i P_i (X_i - \mu_X)^2 = E\{X^2\} - E^2\{X\} \tag{3.9}$$

respectively.

Some classical discrete RVs are Binomial RV, Hypergeometric RV and Poisson RV [17] where each of them has a unique probability distribution. For example, the Binomial distribution with the positive integer indices n and p describes the probability of the number of successes k ($0 \leq k \leq n$) from n independent experiments, where each experiment is either considered to be

success with a probability of p, or failure with a probability of $1-p$. The probability distribution of the Binomial distribution is given by:

$$P(X=k) = \binom{n}{k} p^k (1-p)^{n-k} \tag{3.10}$$

where $\binom{n}{k} = \frac{n!}{k!(n-k)!}$. In fact, tossing a fair coin once is a special case of Binomial distribution with $n=1$ and $p=0.5$.

The probability distribution of the Hypergeometric distribution and Poisson distribution take the form of:

$$P(X=k) = \frac{\binom{A}{k}\binom{A-B}{n-k}}{\binom{B}{n}} \tag{3.11}$$

and

$$P(X=k) = \frac{\mu^k}{k!} e^{-\mu} \tag{3.12}$$

respectively, where A, B and n are positive integer indices for Hypergeometric distribution and μ is the parameter for Poisson distribution. (3.11) holds when k is positive integer and satisfies $max(0, n+A-B) \leq k \leq min(A, n)$, being zero otherwise, where the function of $max(\cdot)$ and $min(\cdot)$ are used to pick out the maximum and minimum value. On the other hand, (3.12) holds when k is a non-negative integer, otherwise, the probability is zero.

Continuous Random Variables

A continuous RV, on the other hand, can assume any value in its range. In other words, if the probability distribution function of a given RV is continuous everywhere, and differentiable everywhere except possibly at some set of points with a finite number of points in every finite interval, then the RV is a continuous RV. It should be stressed that for a continuous RV, Y, it

follows that $P(Y = a) = 0$ for all a, due to the fact that its probability distribution function $F_Y(y)$ is continuous at a. A continuous RV then describes situations where only events including intervals of real numbers can have non-zero probability; in these situations, the probability density function is the rate at which the probability accumulates and therefore can be interpreted as describing the relative likelihood of the outcomes [17].

Assuming the range of Y on the real line is limited between two values Y_1 and Y_2. The expressions of expectation and variance have the form of:

$$E\{Y\} = \int_{-\infty}^{\infty} y f_Y(y) dy = \int_{Y_1}^{Y_2} y f_Y(y) dy = \mu_Y, y \in \mathbb{R} \tag{3.13}$$

$$\sigma_Y^2 = var(Y) = E\left\{(Y - E\{Y\})^2\right\} = E\{Y^2\} - E^2\{Y\} \tag{3.14}$$

Some well-known continuous distribution are Uniform, Gaussian, Gamma and Beta Distributions and their pdf are as follows:

- The Uniform Distribution: The pdf of an RV Y with an Uniform distribution on the interval $[a, b]$, denoted as $U(a, b)$, is given by:

$$f_Y(y) = \begin{cases} \frac{1}{b-a} & , \quad a \leq y \leq b \\ 0 & , \quad \text{otherwise} \end{cases} \tag{3.15}$$

- The Gaussian Distribution: The pdf of an RV Y with a Gaussian distribution, denoted as $N(\mu, \sigma^2)$, is given by:

$$f_Y(y) = \frac{1}{\sqrt{2\pi}\sigma} e^{-\frac{(y-\mu)^2}{2\sigma^2}} \tag{3.16}$$

  where the mean μ and variance σ^2 of Gaussian distribution can be obtained directly from its pdf.

- The Gamma Distribution: An RV Y is said to be a Gamma distribution if its pdf satisfy the form of:

$$f_Y(y) = \begin{cases} \frac{\beta^\alpha}{\Gamma(\alpha)} y^{\alpha-1} e^{-y\beta} & , \quad y \geq 0 \ \ and \ \ \alpha, \beta > 0 \\ 0 & , \quad \text{otherwise} \end{cases} \tag{3.17}$$

where α and β here are the indices for Gamma distribution and $\Gamma(\cdot)$ is the Gamma function with the definition below:

$$\Gamma(\alpha) = \int_0^\infty x^{\alpha-1} e^{-x} dx \tag{3.18}$$

An example of Gamma distributions is shown in Fig. 3.1.

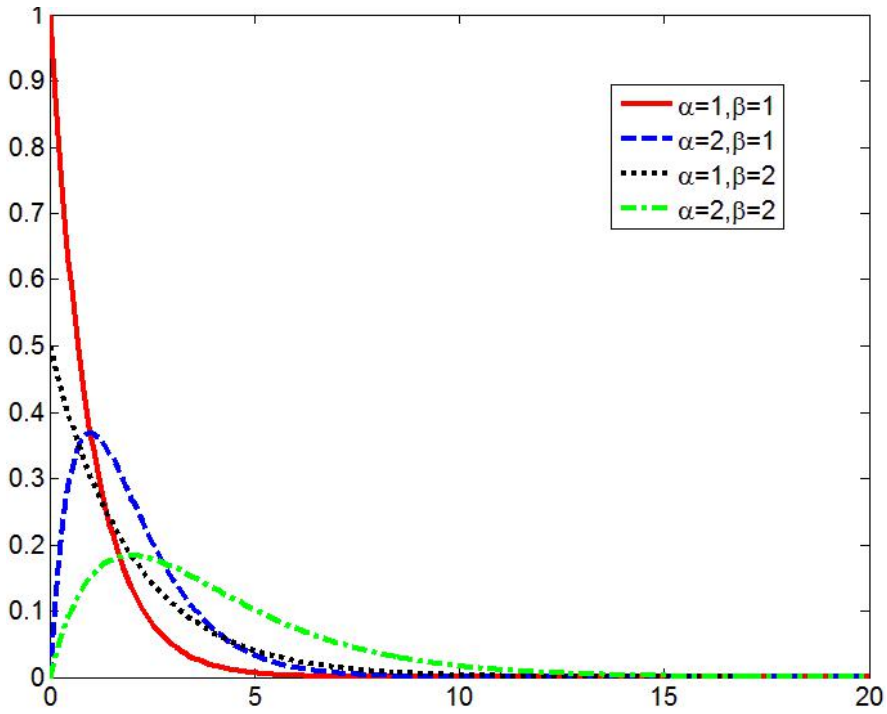

Figure 3.1: Examples of the pdf of Gamma Distribution.

- The Beta Distribution: An RV Y is said to have a beta distribution if its pdf satisfy the

form of:

$$f_Y(y) = \begin{cases} \frac{1}{B(\alpha,\beta)} y^{\alpha-1}(1-y)^{\beta-1} & , \quad 0 \leq y \leq 1 \ \ and \ \ \alpha, \beta > 0 \\ 0 & , \quad \text{otherwise} \end{cases} \tag{3.19}$$

where α and β here are the indices of Beta distribution and $B(\cdot,\cdot)$ is the Beta function defined as $B(\alpha,\beta) = \frac{\Gamma(\alpha)\Gamma(\beta)}{\Gamma\alpha+\beta}$ An example of Beta distributions is shown in Fig. 3.2.

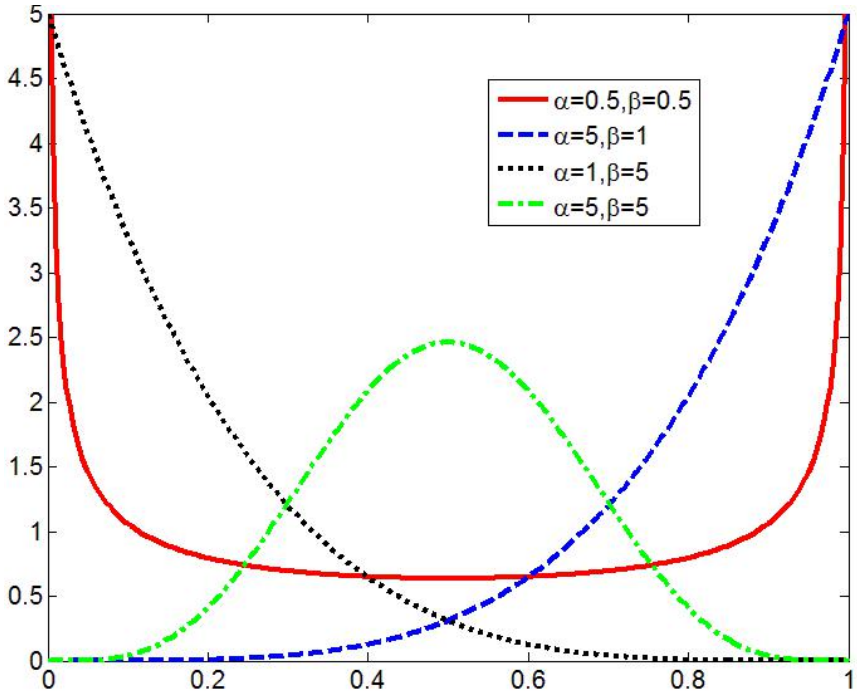

Figure 3.2: Examples of the pdf of Beta Distribution.

3.2 Functions of Random Variables

In the context of this work, one often deals with the function of RVs. For example, the frequency-domain response of a linear circuit in the presence of uncertainty is given by (2.4) which can be

rewritten in the following form:

$$\boldsymbol{X}(\boldsymbol{\xi}, s) = (\boldsymbol{G}(\boldsymbol{\xi}) + s\boldsymbol{C}(\boldsymbol{\xi}))^{-1}\boldsymbol{U}(s) \tag{3.20}$$

It is obvious here that the response, for a given frequency value, e.g. $s = jw$, is a function of the random variable.

Although, it is often the case that the pdf of any random variable is known by being a standard one, e.g. Gaussian, the pdf of the function of RV is unknown and needs to be computed. For example, one need to compute the pdf of $\boldsymbol{X}(\boldsymbol{\xi}, s)$ at a given value for s.

To address this need, we let $\boldsymbol{W} = \boldsymbol{g}(\boldsymbol{\xi})$ stand for a set of functions of the RVs $\boldsymbol{\xi}$. Here, $\boldsymbol{W}$ is a vector of m functions, that is:

$$W_1 = g_1(\xi_1, \xi_2, \cdots, \xi_d)$$

$$W_2 = g_2(\xi_1, \xi_2, \cdots, \xi_d)$$

$$\vdots$$

$$W_m = g_m(\xi_1, \xi_2, \cdots, \xi_d)$$

The probability density function for the RVs $\boldsymbol{W}$, in the case of $m = d$, at given vector of value, $\boldsymbol{w}$, is given by:

$$f_{\boldsymbol{W}}(\boldsymbol{w}) = \frac{f_{\boldsymbol{\xi}}(\check{\boldsymbol{\xi}}_{\boldsymbol{1}})}{(|J(\check{\boldsymbol{\xi}}_{\boldsymbol{1}})|)} + \frac{f_{\boldsymbol{\xi}}(\check{\boldsymbol{\xi}}_{\boldsymbol{2}})}{(|J(\check{\boldsymbol{\xi}}_{\boldsymbol{2}})|)} + \cdots + \frac{f_{\boldsymbol{\xi}}(\check{\boldsymbol{\xi}}_{\boldsymbol{l}})}{(|J(\check{\boldsymbol{\xi}}_{\boldsymbol{l}})|)} \tag{3.21}$$

where $\check{\boldsymbol{\xi}}_{\boldsymbol{1}}$,$\check{\boldsymbol{\xi}}_{\boldsymbol{2}}$,$\cdots$,$\check{\boldsymbol{\xi}}_{\boldsymbol{l}}$ are the vector-valued solutions for the vector equation

$$\boldsymbol{w} = \boldsymbol{g}(\boldsymbol{\xi})$$

and where $J(\boldsymbol{\xi})$ is the Jacobian determinant of $\boldsymbol{g}(\cdot)$ with respects to $\boldsymbol{\xi}$, i.e.,

$$J(\boldsymbol{\xi}) = det \begin{bmatrix} \frac{\partial g_1}{\partial \xi_1} & \frac{\partial g_1}{\partial \xi_2} & \dots & \frac{\partial g_1}{\partial \xi_d} \\ \frac{\partial g_2}{\partial \xi_1} & \frac{\partial g_2}{\partial \xi_2} & \dots & \frac{\partial g_2}{\partial \xi_d} \\ \vdots & \vdots & \ddots & \vdots \\ \frac{\partial g_d}{\partial \xi_1} & \frac{\partial g_d}{\partial \xi_2} & \dots & \frac{\partial g_d}{\partial \xi_d} \end{bmatrix}$$

Of course, we assume $J(\check{\xi}_i) \neq 0$ for all i. [17]

Although the above formula appears to be charting a simple way to calculate the pdf of the circuit response, it remains highly unpractical due to the fact that it is not possible to obtain analytical expressions for $\boldsymbol{g}(\boldsymbol{\xi})$ or for its inverse in the domain of circuit simulations. The following section presents the common alternative approaches that enable performing the statistical analysis on circuit response to identifying its pdf.

3.3 Background on Statistical Analysis methods

With the circuit response , either in the frequency-domain or in the time-domain, being dependent on a set of random parameters, represented by a vector $\boldsymbol{\xi}$ of d random parameters, it becomes imperative that one should treat it as a function of random variables. Similar to the characterization of a given RVs, where a probability density function is typically and ideally to provide a picture of its statistical variability, the characterization of the function of RVs can be ideally accomplished through computing its pdf.

The goal in this section is to provide a background on the methods most commonly used to achieve this goal.

The emphasis in the presented background in this section is placed on two main approaches, namely, the Monte-Carlo approach and the generalized Polynomial Chaos.

3.3.1 The Monte Carlo Methods

The Monte Carlo Method is one of the oldest and most commonly used techniques in commercial circuit simulators to carry out statistical analysis for general circuits. In addition to the statistical analysis, MC methods are also used in optimization and numerical integration [1].

Typically, MC-based methods are attractive in large part due to the simplicity in implementation. In the MC framework, one generates, say K, random independent realizations of the random parameters $\boldsymbol{\xi}_i$, $i = 1, 2, \cdots, K$. At each value of the random parameter, the problem is considered a deterministic problem. For example, considering the frequency-domain response $\boldsymbol{X}(\boldsymbol{\xi}, s)$, the problem of computing $\boldsymbol{X}(\boldsymbol{\xi}, s)$ is by solving the system of equations

$$\boldsymbol{X}(\boldsymbol{\xi}_i, s) = (\boldsymbol{G}(\boldsymbol{\xi}_i) + s\boldsymbol{C}(\boldsymbol{\xi}_i))^{-1}\boldsymbol{U}(s)$$

at a given value $\boldsymbol{\xi}_i$ of $\boldsymbol{\xi}$.

Upon solving the above problem for $i = 1, 2, \cdots, K$, the solutions are collected in an ensemble of solutions. From this ensemble of solutions, statistical information such as mean and variance can be extracted by the following estimators

$$\mu_{\boldsymbol{X}} = E\{\boldsymbol{X}\} \approx \hat{\mu}_{\boldsymbol{X}} = \frac{1}{K}\sum_{i=1}^{K}\boldsymbol{X}_i \tag{3.22}$$

$$\sigma^2_{\boldsymbol{X}} = var(\boldsymbol{X}) \approx \hat{\sigma}^2_{\boldsymbol{X}} = \frac{1}{K-1}\sum_{i=1}^{K}(\boldsymbol{X}_i - \hat{\mu}_{\boldsymbol{X}})^2 \tag{3.23}$$

respectively. One can also construct the pdf from the ensemble of solutions by using some commonly used software, for example, the Distribution fitting tools of MATLAB.

As can be observed from the above description, MC-based methods require only repetitive solutions for the circuit equations. Moreover, the accuracy of the result can be increased by simply increasing the number of realizations, i.e., K, as the Law of Large Number [18] guarantees that the Monte-Carlo simulation result, for example, mean value $\hat{\mu}_{\boldsymbol{X}}$, converges almost surely to the exact mean value $\mu_{\boldsymbol{X}}$ with the increasing of K, that is,

$$P(\lim_{K\to\infty} \hat{\mu}_{\boldsymbol{X}} = \mu_{\boldsymbol{X}}) = 1$$

In fact, this simplicity is the main reason for its popularity in the commercial circuit simulations.

However, the main drawback in the MC-methods is the slow convergence rate, which means they require a large number of those solutions to converge. For example, the mean value typically converges as $\frac{1}{\sqrt{K}}$) [19],[20], where K is the number of realizations, that is the number of solutions of the system. For large systems, with a large computational cost at each realization point, this slow convergence of MC becomes a significant drawback that is hard to ignore.

3.3.2 The Generalized Polynomial Chaos

The generalized Polynomial Chaos (gPC) forms the basis of the proposed approach presented in the next chapter. This method is a generalize to the pervious approach call Polynomial Chaos, which is first forward by N. Wiener in 1938 [21], using Hermite polynomial to model statistical problem with RV of Gaussian distribution. However, for the problem with non-Gaussian distribution, the standard PC start to face several problems, especially in terms of convergence and

probability approximation[22][23]. The generalization of PC is down by D.Xiu in his work [2] in 2002 to alleviate the difficulty of standard PC.

The basic idea in the gPC starts by expanding $\boldsymbol{X}(\boldsymbol{\xi}, s)$ in a set of orthogonal polynomials. To facilitate presenting the core idea of the gPC, we assume first that the underlying random space is uni-dimensional, i.e., that $d = 1$, where $\boldsymbol{\xi}$, the vector of random variable is replaced by the scalar RV, ξ. In this case, the expansion of $\boldsymbol{X}(\xi, s)$ in the orthogonal polynomial takes the following form

$$\boldsymbol{X}(\xi, s) = \sum_{i=0}^{\infty} \hat{\boldsymbol{X}}_i(s)\phi_i(\xi) \tag{3.24}$$

where $\phi_i(\xi)$ is an i-th degree polynomial in ξ, and $\hat{\boldsymbol{X}}_i(s)$ is an s-dependent coefficients vectors with dimension N that need to be computed.

The set of polynomials $\phi_i(\xi)$ are orthogonal polynomials with respect to a certain weighting function, $w(\xi)$, over the domain of the RV, ξ, i.e.

$$< \phi_i(\xi), \phi_j(\xi) >= \int_{\Omega} \phi_i(\xi)\phi_j(\xi)w(\xi)d\xi = \delta_{i,j}\theta_i \tag{3.25}$$

where Ω is the support of the polynomial, θ_i is the so-called inter-product, which is a constant whose value depends on the degree i and type of the polynomials and $\delta_{i,j}$ is the Kronecker delta function defined by:

$$\delta_{i,j} = \begin{cases} 1 \quad , & i = j \\ 0 \quad , & \text{otherwise} \end{cases} \tag{3.26}$$

The key principle in the gPC is that basic statistical information of $\boldsymbol{X}(\xi, s)$ can be extracted from the coefficients, $\hat{\boldsymbol{X}}_i(\xi, s)$, directly.

To explain this principle, assume that ξ is standard Gaussian RV, where its probability density

function is given by

$$p(\xi) = \frac{1}{\sqrt{2\pi}} e^{-\frac{\xi^2}{2}} \tag{3.27}$$

and let $\phi_i(\xi)$ be given by the probabilistic Hermite polynomial of the i^{th} degree, i.e.

$$\phi_i(\xi) \equiv H_i(\xi) = (-1)^i e^{\frac{\xi^2}{2}} \frac{d^i}{d\xi^i} e^{-\frac{\xi^2}{2}} \tag{3.28}$$

It is well-known [24] that the Hermite polynomials are orthogonal with respect to the weighting function $w(\xi)$ that is given by

$$w(\xi) = e^{-\frac{\xi^2}{2}} = \sqrt{2\pi} p(\xi) \tag{3.29}$$

As probability theory states, the mean value of $\boldsymbol{X}(\xi, s)$ is obtained from

$$E\{\boldsymbol{X}(\xi, s)\} = \int_\Omega \boldsymbol{X}(\xi, s) p(\xi) d(\xi) \tag{3.30}$$

Now substituting from the expansion in (3.24) and (3.29) into (3.30) and manipulating, using the fact that $H_0(\xi) \equiv 1$, shows that the mean value is given by

$$\begin{aligned} E\{\boldsymbol{X}(\xi, s)\} &= \int_\Omega \sum_{i=0}^{\infty} \hat{\boldsymbol{X}}_i(s) \phi_i(\xi) \frac{1}{\sqrt{2\pi}} w(\xi) \mathrm{d}\xi \\ &= \frac{1}{\sqrt{2\pi}} \sum_{i=0}^{\infty} \hat{\boldsymbol{X}}_i(s) < \phi_i(\xi), \phi_0(\xi) > \\ &= \frac{\theta_0}{\sqrt{2\pi}} \sum_{i=0}^{\infty} \hat{\boldsymbol{X}}_i(s) \delta_{0,i} \\ &= \frac{\theta_0}{\sqrt{2\pi}} \hat{\boldsymbol{X}}_0(s) \end{aligned} \tag{3.31}$$

where the orthogonality of the Hermite polynomial, with respect to the weigh $e^{-\frac{\xi^2}{2}}$ has been used to obtain the last equality. In a similar manner, the variance of $\boldsymbol{X}(\xi, s)$ is extracted from the

coefficients $\hat{\boldsymbol{X}}_i(s)$ as can be seen from the following manipulation

$$
\begin{aligned}
var\{\boldsymbol{X}(\xi,s)\} &= E\{\boldsymbol{X}^2(\xi,s)\} - E^2\{\boldsymbol{X}(\xi,s)\} \\
&= E\left\{\left(\sum_{i=0}^{\infty}\hat{\boldsymbol{X}}(s)\phi_i(\xi)\right)^2\right\} - \mu^2 \\
&= \frac{1}{\sqrt{2\pi}}\int_{\Omega}\left(\sum_{i=0}^{\infty}\sum_{j=0}^{\infty}\hat{\boldsymbol{X}}_i(s)\hat{\boldsymbol{X}}_j(s)\phi_i(\xi)\phi_j(\xi)w(\xi)d\xi\right) - \mu^2 \\
&= \frac{1}{\sqrt{2\pi}}\sum_{i=0}^{\infty}\sum_{j=0}^{\infty}\hat{\boldsymbol{X}}_i(s)\hat{\boldsymbol{X}}_j(s) < \phi_i(\xi),\phi_j(\xi) > -\mu^2 \\
&= \frac{1}{\sqrt{2\pi}}\sum_{i=0}^{\infty}\sum_{j=0}^{\infty}\hat{\boldsymbol{X}}_i(s)\hat{\boldsymbol{X}}_j(s)\delta_{i,j}\theta_i - \mu^2 \\
&= \frac{1}{\sqrt{2\pi}}\sum_{i=0}^{\infty}\hat{\boldsymbol{X}}_i^2(s)\theta_i - \mu^2 \\
&\approx \frac{1}{\sqrt{2\pi}}\sum_{i=0}^{k}\hat{\boldsymbol{X}}_i^2(s)\theta_i - \mu^2
\end{aligned}
\tag{3.32}
$$

The main point to take out from the above discussion is that the coefficients $\hat{\boldsymbol{X}}(s)$ are the key to computing the statistical properties of $\boldsymbol{X}(\xi,s)$.

There are three main questions that need to be answered to fully describe the gPC approach.

- How can one deal with other standard RVs which are not Gaussian in their pdf?
- How can the gPC be generalized to multi-random parameter, i.e., for the case where $d > 1$?
- How can we compute the coefficients $\hat{\boldsymbol{X}}(s)$ in a computationally efficient manner?

The remainder of this section addresses the above questions.

Generalization to other types of RVs

It should be stressed that the key that enabled extracting the statistical information from the coefficients of the expansion was the fact the weight of the orthogonal polynomial takes the same

form of the pdf of the RV except a constant scale. This important point is easily seen from equation (3.29). This fact suggests that in order to carry the same principle beyond the Gaussian distribution to other standard RVs with other distributions, one has to search for orthogonal polynomials whose weight is identical to the pdf of those RVs. Fortunately, orthogonal polynomials whose weighting functions are identical to many standard distributions do exist. To illustrate further this idea, table 3.1 lists the distribution of common discrete and continuous RVs in the second column, indicating in the third column the polynomial to the distribution. The fourth column in table 3.1 shows the support of the polynomial, that is the domain of its orthogonality. Also, from (3.31) and (3.32), one also need to know the inner-product of the polynomial base used for gPC in order to calculate the statistical information. Some commonly used polynomial base for gPC as well as their weighting function and inner-product are provided in table 3.2.

Treatment of multi-random parameters $d > 1$

Handling of the multi-random parameters is done by adopting the multi-dimensional version of the orthogonal polynomials of the Askey-Wiener type. A multi-dimensional Askey-Wiener polynomial for d independent RVs, ξ_i $i = 1, 2, \cdots, d$ is expressed in the following form

$$\phi_{\boldsymbol{\alpha}}(\boldsymbol{\xi}) = \prod_{i=1}^{d} \phi_{\alpha_i}(\xi_i) \tag{3.33}$$

where $\phi_{\alpha_i}(\xi_i)$ is a single-dimensional polynomial in ξ_i and of a degree α_i. The single-dimensional expansion is also generalized to the multi-dimensional expansion, as follows

$$\boldsymbol{X}(\boldsymbol{\xi}, s) = \sum_{\boldsymbol{\alpha} \in \Upsilon_Q} \hat{\boldsymbol{X}}_{\boldsymbol{\alpha}}(s) \phi_{\boldsymbol{\alpha}}(\boldsymbol{\xi}) \tag{3.34}$$

[1] Chenyshev is not a gPC basis, however, it has less decoupling error which means a better result can be achieved when proposed algorithm applied, detail information can be found in next chapter.

Table 3.1: gPC polynomial basis for different probability distribution

	Distribution	gPC basis polynomial	Support
Continuous	Gaussian	Hermitee	$(-\infty, \infty)$
	Uniform	Legendre	$[a, b]$
	Gamma	Laguerre	$[0, \infty)$
	Beta	Jacobi	$[a, b]$
Discrete	Poisson	Charlier	$\{0, 1, 2, \cdots\}$
	Binomial	Krawtchouk	$\{0, 1, \cdots, N\}$
	Negative Binomial	Merxner	$\{0, 1, 2, \cdots\}$
	Hypergeometric	Hahn	$\{0, 1, \cdots, N\}$

The coefficients in the above expansion, similar to the expansion in (3.24), are vectors of size N whereas the subscripts $\boldsymbol{\alpha}$ are integer-valued vectors of dimension d, whose components, α_i, represent the various degrees of the polynomials $\phi_{\alpha_i}(\xi_i)$. The subscript $\boldsymbol{\alpha}$ in the above expansion many be thought of as an integer-vector-valued label that generalizes the single-integer value label of the uni-dimensional expansion in (3.24).

Similar to (3.25), the orthogonality and corresponding inner-product of a multi-dimensional

Table 3.2: Orthogonality of commonly used gPC polynomial basis

Polynomial Basis	Notation	Weighting Function	Inner-Product
Hermite Polynomial	$H_n(\xi)$	$e^{-\frac{\xi^2}{2}}$	$\sqrt{2\pi}n!$
Legendre Polynomial	$P_n(\xi)$	1	$\frac{2}{2n+1}$
Generalized Laguerre Polynomial	$L_n^{(\alpha)}(\xi)$	$\frac{\xi^\alpha e^{-\xi}}{\Gamma(\alpha+1)}$	$\binom{n+\alpha}{n}$
Jacobi Polynomial	$J_n^{\alpha,\beta}(\xi)$	$(1-\xi)^\alpha(1+\xi)^\beta$	$\frac{2^{\alpha+\beta+1}}{2n+\alpha+\beta+1}\frac{\Gamma(n+\alpha+1)\Gamma(n+\beta+1)}{\Gamma(n+\alpha+\beta+1)n!}$
Chebyshev[1]	$T_n(\xi)$	$\frac{1}{\sqrt{1-\xi^2}}$	$\frac{\pi}{2}+\frac{\pi}{2}\delta_{0,n}$

polynomial is given by

$$\langle\phi_{\boldsymbol{\alpha}}(\boldsymbol{\xi}),\phi_{\boldsymbol{\beta}}(\boldsymbol{\xi})\rangle=\int_{\boldsymbol{\Omega}}\phi_{\boldsymbol{\alpha}}(\boldsymbol{\xi})\phi_{\boldsymbol{\beta}}(\boldsymbol{\xi})\boldsymbol{w}(\boldsymbol{\xi})\mathrm{d}\boldsymbol{\xi}=\prod_{i=1}^{d}\int_{\Omega_i}\phi_{\alpha_i}(\xi_i)\phi_{\beta_i}(\xi_i)w_i(\xi_i)\mathrm{d}\xi_i=\Theta_{\boldsymbol{\alpha}}\delta_{\boldsymbol{\alpha},\boldsymbol{\beta}} \quad (3.35)$$

where $\delta_{\boldsymbol{\alpha},\boldsymbol{\beta}}=\prod_{i=1}^{d}\delta_{\alpha_i\beta_i}$ and $\Theta_{\boldsymbol{\alpha}}=\prod_{i=1}^{d}\theta_{\alpha_i}$ with $\theta_{\alpha_i}=\int_{\Omega_i}\phi_{\alpha_i}(\xi_i)\phi_{\alpha_i}(\xi_i)w(\xi_i)d\xi_i$.

The main attractive feature in the gPC based on the Askey-Wiener polynomials is that it allows performing statistical analysis of the system with multiple RVs, which may have different pdfs. For example, assume that a given circuit has a random space with dimensionality $d=2$, where the first RV, ξ_1 is Gaussian RV, whereas the second RV ξ_2 is uniform RV with pdf given by

$$p(\xi_2)=\begin{cases}\frac{1}{2} & , \quad -1\leq\xi_2\leq 1\\ 0 & , \quad \text{otherwise}\end{cases} \quad (3.36)$$

In a situation like that, the orthogonal polynomial basis function $\phi_{\boldsymbol{\xi}}(\boldsymbol{\xi})$ would be in the following form

$$\phi_{\boldsymbol{\alpha}}(\boldsymbol{\xi})=H_{\alpha_1}(\xi_1)P_{\alpha_2}(\xi_2) \quad (3.37)$$

Table 3.3 lists the exact form for each polynomial for different values of α_1 and α_2.

Table 3.3: Example of multi-index and multi-dimensional OP when $d = 2$, $M_1 = M_2 = 2$ (the distribution of two random variables are Gaussian and Uniform respectively

α_1	α_2	$\lvert\boldsymbol{\alpha}\rvert$	$\phi_{\boldsymbol{\alpha}}$	Polynomials
0	0	0	$H_0(\xi_1)P_0(\xi_2)$	1
0	1	1	$H_0(\xi_1)P_1(\xi_2)$	ξ_2
0	2	2	$H_0(\xi_1)P_2(\xi_2)$	$\frac{1}{2}(3\xi_2^2 - 1)$
1	0	3	$H_1(\xi_1)P_0(\xi_2)$	ξ_1
1	1	4	$H_1(\xi_1)P_1(\xi_2)$	$\xi_1\xi_2$
1	2	5	$H_1(\xi_1)P_2(\xi_2)$	$\xi_1\frac{1}{2}(3\xi_2^2 - 1)$
2	0	6	$H_2(\xi_1)P_0(\xi_2)$	$\xi_1^2 - 1$
2	1	7	$H_2(\xi_1)P_1(\xi_2)$	$(\xi_1^2 - 1)\xi_2$
2	2	8	$H_2(\xi_1)P_2(\xi_2)$	$(\xi_1^2 - 1)\frac{1}{2}(3\xi_2^2 - 1)$

Computing the expansion coefficients

The last question that still needs to be addressed is the methodology of computing the coefficients of the expansion, or $\hat{\boldsymbol{X}}_{\boldsymbol{\alpha}}(s)$. To this end, the available literature shows that there are several methods that could be used to obtain the expansion coefficients, which will be illustrated next.

- **Numerical integration via quadrature**

The mathematical expression of the expansion coefficients can be obtained by simply using the projection theorem, i.e.

$$\hat{\boldsymbol{X}}_{\boldsymbol{\alpha}}(s) = \frac{\langle \boldsymbol{X}(\boldsymbol{\xi}, s), \phi_{\boldsymbol{\alpha}}(\boldsymbol{\xi}) \rangle}{\langle \phi_{\boldsymbol{\alpha}}(\boldsymbol{\xi}), \phi_{\boldsymbol{\alpha}}(\boldsymbol{\xi}) \rangle} = \frac{\int_{\boldsymbol{\Omega}} \boldsymbol{X}(\boldsymbol{\xi}, s) \phi_{\boldsymbol{\alpha}}(\boldsymbol{\xi}) \boldsymbol{w}(\boldsymbol{\xi}) \mathrm{d}\boldsymbol{\xi}}{\Theta_{\boldsymbol{\alpha}}} \tag{3.38}$$

Although the above integral can not be solved analytically as it involves the unknown response $\boldsymbol{X}(\boldsymbol{\xi}, s)$, it could be approximated through some numerical integral methods such as Gaussian Quadratures. The Gaussian Quadrature provides an approximation of a weighted integral of a function $f(\xi)$ and is tightly related to orthogonal polynomials [25]. The Gaussian Quadrature can be classified into different types with respect to the weighting function involved in the integral. For example, if the weighting function happened to be the weight of Hermite polynomial, the Quadrature is named Gauss-Hermite quadrature. Some other types of quadratures are Gauss-Legendre, Gauss-Laguerre, etc. The Gaussian Quadratures approximate the integral in terms of a weighted summation of the function values computed at specific points (nodes) within the domain of integration. The general form is

$$\int_{\Omega} f(\xi) w(\xi) d\xi \approx \sum_{i=0}^{k} f(\xi_i) w_i \tag{3.39}$$

where $w(\xi)$ is the weighting function and w_i are corresponding discrete weights. With a direct analogy to the Askey-Wiener scheme, the nodes ξ_i are the roots of the $(k+1)th$ polynomial corresponding to the weighting function $w(\xi)$[26]. For example, if $w(\xi)$ is chosen to be the weighting function of Hermite polynomials, the nodes are the roots of the equation $H_{k+1}(\xi) = 0$. The weights, on the other hand, are available through many literatures, for example, the weights for Gauss-Legendre Quadrature is given by [27]

$$w_i = \frac{1}{(1-\xi_i^2)(P'_{k+1}(\xi_i))^2}$$

where P'_{k+1} is the derivative of the $(k+1)th$ Legendre polynomial.

For the case of multi-RVs, i.e. $d > 1$, the Gaussian quadrature can be generalized via tensor product summations along each dimension[28], i.e.

$$\int_{\boldsymbol{\Omega}} f(\boldsymbol{\xi})\boldsymbol{w}(\boldsymbol{\xi})d\boldsymbol{\xi} \approx \sum_{i_1=0}^{k_1} \cdots \sum_{i_d=0}^{k_d} f(\xi_{1,i_1}, \cdots, \xi_{d,i_d}) \prod_{j=1}^{d} w_{j,i_j} \tag{3.40}$$

- **Stochastic collocation**

The stochastic collocation manage to find an approximation, $\boldsymbol{Z}(\boldsymbol{\xi})$, to approximate the actual response, $\boldsymbol{X}(\boldsymbol{\xi})$, of the circuit, where the approximation is exactly the same as $\boldsymbol{X}(\boldsymbol{\xi})$ at a discrete set of P nodes (collocation points) $\boldsymbol{\xi}_i$ $i = 1, 2, \cdots, P$, i.e.,

$$\boldsymbol{Z}(\boldsymbol{\xi}_i) \equiv \boldsymbol{X}(\boldsymbol{\xi}_i) \tag{3.41}$$

The $\boldsymbol{Z}(\boldsymbol{\xi})$ can be constructed either using Lagrange interpolation approach [29],[30] or a matrix inversion approach [31], and the second approach can be used to approximate the expansion coefficient $\hat{\boldsymbol{X}}_\alpha$.

The matrix inversion approach start by prescribing a polynomial interpolating basis, such as,

$$\boldsymbol{Z}(\boldsymbol{\xi}) = \sum_{\boldsymbol{\alpha} \in \Upsilon_Q} \hat{\boldsymbol{Z}}_{\boldsymbol{\alpha}} \phi_{\boldsymbol{\alpha}}(\boldsymbol{\xi}), \tag{3.42}$$

which the expansion coefficients $\hat{\boldsymbol{Z}}_{\boldsymbol{\alpha}}$ can be used to approximate the coefficients $\hat{\boldsymbol{X}}_\alpha$ one is looking for. Next, by substituting (3.42) into (3.41), one can obtain a set of P equations,

$$\sum_{\boldsymbol{\alpha} \in \Upsilon_Q} \hat{\boldsymbol{Z}}_{\boldsymbol{\alpha}} \phi_{\boldsymbol{\alpha}}(\boldsymbol{\xi}_i) = \boldsymbol{X}(\boldsymbol{\xi}_i), \tag{3.43}$$

which can be written into a matrix form of,

$$(\boldsymbol{A} \otimes I_N)\bar{\boldsymbol{Z}} = \check{\boldsymbol{X}}, \tag{3.44}$$

where $\bar{\boldsymbol{Z}}$ is a vector constructed from the vector coefficients $\hat{\boldsymbol{Z}}_{\boldsymbol{\alpha}}$ ordered by the rank of $\boldsymbol{\alpha}$, $|\boldsymbol{\alpha}|$, and $\boldsymbol{A}$ is a $P \times Q$ matrix with the following form,

$$[\boldsymbol{A}]_{i,j} = \phi_{\boldsymbol{\alpha}}(\boldsymbol{\xi}_i), \quad |\boldsymbol{\alpha}| = j - 1, \tag{3.45}$$

and $\check{\boldsymbol{X}}$ is a vector with the form of

$$\check{\boldsymbol{X}} = [\boldsymbol{X}(\boldsymbol{\xi}_1), \boldsymbol{X}(\boldsymbol{\xi}_1), \cdots, \boldsymbol{X}(\boldsymbol{\xi}_P)]^T \tag{3.46}$$

To prevent the problem from becoming underdetermined, we require the number of collocation points not to be smaller than the number of gPC expansion terms, i.e.,$P \leq Q$.

The section of nodes is the key ingredient in all stochastic collocation methods [19]. Practically there are several rules available in the literature, such as the tensor product and sparse grids [32]. The detailed information of the points selection rule can be found in [31].

The advantage of the matrix inversion approach is that the interpolating polynomials are prescribed and well defined. Once the nodal set is given, the existence of the interpolation can always be determined in the spirit of determining whether the determinant of $\boldsymbol{A}$ is zero. However, an important and very practical concern is the accuracy of the interpolation. Even though the interpolation has no error at the nodal points, error can become wild between the nodes. This is particularly true in high-dimensional spaces[31].

- **Galerkin projection**

Unlike the above two methods, where calculating the expansion coefficients by first computing several deterministic results at certain nodes in the random space, followed by a

weighted summation to obtain the expansion coefficients, the Galerkin projection computes the expansion coefficients by expanding the circuit equations into a larger but deterministic system of equations whose solution directly yields the values for those PC coefficients. As the proposed approach is based on this stream, the detail about Galerkin projection will be provided next.

Generalized Polynomial Chaos approach based on Galerkin Projection

The GP process proceeds by substituting from (3.34) into (2.4), multiplying both sides by $\phi_{\boldsymbol{\gamma}}(\boldsymbol{\xi})w(\boldsymbol{\xi})$ and integrating over $\boldsymbol{\Omega}$, dividing by the inner product $\Theta_{\boldsymbol{\gamma}}$ and finally repeating this process for all multi-indices $\boldsymbol{\gamma} \in \Upsilon_Q$. This process results in a larger (augmented) system of equations,

$$\bar{\boldsymbol{Y}}(s)\bar{\boldsymbol{X}}(s) = \bar{\boldsymbol{U}}(s) \tag{3.47}$$

where $\bar{\boldsymbol{X}}(s) \in \mathbb{R}^{NQ}$ is a vector constructed from the vector coefficients of $\hat{\boldsymbol{X}}_{\boldsymbol{\alpha}}(s)$ ordered by the rank of $\boldsymbol{\alpha}$, $|\boldsymbol{\alpha}|$, and $\bar{\boldsymbol{U}}(s) = [\boldsymbol{U}(s)^T, 0, \cdots, 0]^T$. The matrix $\bar{\boldsymbol{Y}}(s)$ is a matrix of size $QN \times QN$. This matrix can be described as a block structured matrix, where each block has a unique relationship with multi-indices $\boldsymbol{\alpha}$ and $\boldsymbol{\gamma}$ and is given by

$$\left\{\bar{\boldsymbol{Y}}(s)\right\}_{|\boldsymbol{\gamma}|N+1,|\boldsymbol{\alpha}|N+1}^{N} = \frac{\int_{\boldsymbol{\Omega}} \boldsymbol{Y}(\boldsymbol{\xi}, s)\phi_{\boldsymbol{\alpha}}(\boldsymbol{\xi}, s)\phi_{\boldsymbol{\gamma}}(\boldsymbol{\xi}, s)\boldsymbol{w}(\boldsymbol{\xi})\mathrm{d}\boldsymbol{\xi}}{\Theta_{\boldsymbol{\gamma}}} \tag{3.48}$$

and $\bar{\boldsymbol{Y}}(s)$ is constructed by populating it with the above blocks for $\boldsymbol{\alpha}, \boldsymbol{\gamma} \in \Upsilon_Q$. In order to calculate the block in (3.48), we need to expand $\boldsymbol{Y}(\boldsymbol{\xi}, s)$ by the corresponding gPC basis, which yields:

$$\boldsymbol{Y}(\boldsymbol{\xi}, s) = \sum_{\boldsymbol{\beta} \in \Upsilon_Q} \hat{\boldsymbol{Y}}_{\boldsymbol{\beta}}(s)\phi_{\boldsymbol{\beta}}(\boldsymbol{\xi}) \tag{3.49}$$

Substituting (3.34) back into (3.48), provides,

$$\left\{\bar{\boldsymbol{Y}}(s)\right\}_{|\boldsymbol{\gamma}|N+1,|\boldsymbol{\alpha}|N+1}^{N}=\frac{\int_{\boldsymbol{\Omega}}\sum_{\boldsymbol{\beta}\in\Upsilon_Q}\hat{\boldsymbol{Y}}_{\boldsymbol{\beta}}(s)\phi_{\boldsymbol{\beta}}(\boldsymbol{\xi})\phi_{\boldsymbol{\alpha}}(\boldsymbol{\xi},s)\phi_{\boldsymbol{\gamma}}(\boldsymbol{\xi},s)\boldsymbol{w}(\boldsymbol{\xi})\mathrm{d}\boldsymbol{\xi}}{\Theta_{\boldsymbol{\gamma}}} \tag{3.50}$$

We use $\boldsymbol{\Psi}_{\boldsymbol{\beta},\boldsymbol{\alpha},\boldsymbol{\gamma}}$ as the notation of the triple product integral,

$$\boldsymbol{\Psi}_{\boldsymbol{\beta},\boldsymbol{\alpha},\boldsymbol{\gamma}}=\int_{\boldsymbol{\Omega}}\phi_{\boldsymbol{\beta}}(\boldsymbol{\xi})\phi_{\boldsymbol{\alpha}}(\boldsymbol{\xi})\phi_{\boldsymbol{\gamma}}(\boldsymbol{\xi})\boldsymbol{w}(\boldsymbol{\xi})d\boldsymbol{\xi}=\prod_{i=1}^{d}\Psi_{\beta_i,\alpha_i,\gamma_i} \tag{3.51}$$

where the $\Psi_{\beta_i,\alpha_i,\gamma_i}=\int_{\Omega_i}\phi_{\beta_i}(\xi_i)\phi_{\alpha_i}(\xi_i)\phi_{\gamma_i}(\xi_i)w_i(\xi_i)d\xi_i$ represents the triple product integral for each RV. The above equation can be simplified as:

$$\left\{\bar{\boldsymbol{Y}}(s)\right\}_{|\boldsymbol{\gamma}|N+1,|\boldsymbol{\alpha}|N+1}^{N}=\frac{\sum_{\boldsymbol{\beta}\in\Upsilon_Q}\hat{\boldsymbol{Y}}_{\boldsymbol{\beta}}(s)\boldsymbol{\Psi}_{\boldsymbol{\beta},\boldsymbol{\alpha},\boldsymbol{\gamma}}}{\Theta_{\boldsymbol{\gamma}}} \tag{3.52}$$

To facilitate describing the structure of $\bar{\boldsymbol{Y}}$, a single RV is first considered. In a single RV setting the structure of the block is given by,

$$\left\{\bar{\boldsymbol{Y}}\right\}_{\gamma N+1,\alpha N+1}^{N}=\frac{\sum_{\beta=0}^{M}\hat{\boldsymbol{Y}}_{\beta}(s)\Psi_{\beta,\alpha,\gamma}}{\theta_{\gamma}} \tag{3.53}$$

where $\gamma=0,1,2,\cdots,M$. Now using the above expression for the block, (3.47) can be rewritten in the following block matrix format,

$$\begin{bmatrix}\sum_{\beta=0}^{M}\hat{\boldsymbol{Y}}_{\beta}\frac{\Psi_{\beta00}}{\theta_0} & \sum_{\beta=0}^{M}\hat{\boldsymbol{Y}}_{\beta}\frac{\Psi_{\beta10}}{\theta_0} & \cdots & \sum_{\beta=0}^{M}\hat{\boldsymbol{Y}}_{\beta}\frac{\Psi_{\beta M0}}{\theta_0}\\ \sum_{\beta=0}^{M}\hat{\boldsymbol{Y}}_{\beta}\frac{\Psi_{\beta01}}{\theta_1} & \sum_{\beta=0}^{M}\hat{\boldsymbol{Y}}_{\beta}\frac{\Psi_{\beta11}}{\theta_1} & \cdots & \sum_{\beta=0}^{M}\hat{\boldsymbol{Y}}_{\beta}\frac{\Psi_{\beta M1}}{\theta_1}\\ \vdots & \vdots & \ddots & \vdots\\ \sum_{\beta=0}^{M}\hat{\boldsymbol{Y}}_{\beta}\frac{\Psi_{\beta0M}}{\theta_M} & \sum_{\beta=0}^{M}\hat{\boldsymbol{Y}}_{\beta}\frac{\Psi_{\beta1M}}{\theta_M} & \cdots & \sum_{\beta=0}^{M}\hat{\boldsymbol{Y}}_{\beta}\frac{\Psi_{\beta MM}}{\theta_M}\end{bmatrix}\times\begin{bmatrix}\hat{\boldsymbol{X}}_0\\ \hat{\boldsymbol{X}}_1\\ \vdots\\ \hat{\boldsymbol{X}}_M\end{bmatrix}=\begin{bmatrix}U\\ 0\\ \vdots\\ 0\end{bmatrix}$$

The dependence of each block on the frequency variable, s, has been suppressed. By factorizing the above matrix, the system in (3.47) is solved for the desired coefficients of expansion, i.e., $\hat{\boldsymbol{X}}_{\boldsymbol{\alpha}}(s)$, at a given frequency $s=jw$. As the expansion coefficients of $\hat{\boldsymbol{Y}}(\boldsymbol{\xi},s)$ should be known

to us, the only problem left is how to calculate the triple product $\Phi_{\beta,\alpha,\gamma}$. Luckily, there are closed form expressions for this if the expansion basis is Hermite or Legendre polynomials, which are presented next.

- Triple product for Hermite polynomials. [33]

$$\int_{-\infty}^{\infty} H_\beta(\xi)H_\alpha(\xi)H_\gamma(\xi)w(\xi)d\xi = \frac{\beta!\alpha!\gamma!}{(m-\beta)!(m-\alpha)!(m-\gamma)!}, \tag{3.54}$$

  where $m = \frac{\alpha+\beta+\gamma}{2}$; the above equation holds when m and all the arguments of factorial are non-negative integers, otherwise, the results of triple products are typically zero.

- Triple product for Legendre polynomials, [34]

$$\begin{aligned}&\int_{-1}^{1} P_\beta(\xi)P_\alpha(\xi)P_\gamma(\xi)w(\xi)d\xi \\ &= (-1)^{m-\alpha}\frac{\gamma!(2m-2\gamma)!m!}{(m-\beta)!(m-\alpha)!(m-\gamma)!(2m+1)!}\sum_{t=p}^{q}(-1)^t\frac{(\beta+t)!(\alpha+\gamma-t)!}{t!(\beta-t)!(\alpha-\gamma+t)!(\gamma-t)!}\end{aligned} \tag{3.55}$$

  where $m = \frac{\alpha+\beta+\gamma}{2}$, $p = max(0, \gamma-\alpha)$ and $q = min(\alpha+\gamma, \beta, \gamma)$. The above equation holds when m and and all the arguments of factorials are non-negative integers, otherwise, the result of triple products are zero.

Drawbacks of the Galerkin Projection

While the main advantage of gPC approach based on the Galerkin Projection is that only one factorization (LU factorization in this case) of the matrix $\bar{\boldsymbol{Y}}$ is needed to compute the coefficients $\hat{\boldsymbol{X}}_{\boldsymbol{\alpha}}(s)$ and deduce the statistical properties of $\boldsymbol{X}(\boldsymbol{\xi}, s)$, this advantage quickly disappears if the number of RVs is more than few random variables (for example 4 RVs). The reason for that is the size of this matrix grows quickly with the number of RVs. To illustrate the growth in size of the

augmented matrix $\bar{\boldsymbol{Y}}$, first note that the size of this matrix is $QN \times QN$, where Q is the number of coefficients in the expansion, which depends on the way of defining the set of multi-indices included in the expansion. For example, for a set of multi-indices truncated according to tensor order, then Q is given by,

$$Q = \prod_{i=1}^{d} (M_i + 1)$$

where M_i is the truncation order for random parameter ξ_i.

Moreover, it is not only the growth in size that presents the most challenging problem, but also the structure of this matrix makes factorization a cumbersome task that easily overwhelms any computing platform. Far from being the sparse structure of the block $\hat{\boldsymbol{Y}}$, which rises from the sparsity of the circuit connection, the structure of $\bar{\boldsymbol{Y}}$ is significantly dense, which makes the utilization of sparse matrix factorization largely ineffective.

3.4 Discussion

The goal of the proposed approach in the next chapter is to allow replacing the matrix $\bar{\boldsymbol{Y}}$ with a sparse matrix of the block diagonal form. In fact, this idea was developed earlier for the special case where the orthogonal polynomials were of the Hermite type. The core contribution of this thesis is to generalize this idea to arbitrary polynomials.

Chapter 4

Proposed Decoupling Approach

4.1 Introduction

From the discussion of the gPC method based on the Galerkin projection, it was demonstrated that the main drawback of this approach is having to factorize a huge matrix with non-sparse structure. This drawback effectively limits the number of design parameters d to a very few (below 3) RVs.

The main objective of this chapter is to introduce a new approach that aims to address this drawback and allow the gPC method based on the Galerkin projection to handle problems with higher multi-dimensional random space d. This basic idea in the proposed approach relies on developing an alternative formulation for the Galerkin projection that enables replacing the matrix $\bar{\boldsymbol{Y}}$ with another matrix, which will be denoted by $\tilde{\boldsymbol{Y}}$, that has a block-diagonal structure. It is well known that factorization of block diagonal matrix can be performed by factorizing the diagonal blocks individually and independently of each other. This means that the alternative

formulation of the Galerkin projection method can be viewed as some kind of decoupling the original matrix into the individual blocks that appear on the diagonal of the alternative matrix $\tilde{\boldsymbol{Y}}$.

It should be stressed that a similar objective underlies the work proposed in[35]. However, that work was only limited to the special case where the orthogonal polynomials used in the expansion are the Hermite probabilistic polynomials, i.e., $\phi_{\boldsymbol{\alpha}}(\boldsymbol{\xi}) = \prod_{i=1}^{d} H_{\alpha_i}(\xi_i)$. The goal of the approach presented in this chapter is to carry this technique to a general system of orthogonal polynomials. One also needs to highlight one important fact that enabled the success of the approach present in [35] for the Hermite polynomials, namely that the triple product integral of the Hermite polynomials has a closed-form analytical expression as shown by (3.54). Unfortunately, such a closed-form expression does not necessarily exist in the literature for other systems of polynomials. This lack of closed-form expressions adds another level of difficulty in seeking a generalization of the approach in [35] to a general system of orthogonal polynomials.

In order to overcome such problems, the generalized decoupling approach is developed. Basically, the decoupling approach manages to decouple the augmented matrix, i.e. $\bar{\boldsymbol{Y}}$, into block diagonal form which can be factorized in parallel. Each block has the same size and sparse pattern as the original circuit. Thus, its computational cost is linearly increasing with the number of expansion coefficients. The proposed approach does not require a closed-form expression for the integral of triple product. It rather uses the three three-term recurrence relation, which is satisfied by all orthogonal polynomials, to derive the alternative formulation leading the decoupling paradigm. This chapter will provide the details of the theoretical basis of generalized decoupling approach in the first section, which includes the closed-form formula for the augmented matrix $\bar{\boldsymbol{Y}}(s)$. This will be followed by three more detailed discussions (first two is for FD analysis for s-

ingle RV and multi-random variables cases and the third one is an TD analysis for multi-random variables problem) to show how the augmented matrices can be decoupled into blocks of size $N \times N$.

One additional advantage of the proposed approach, which arises from being applicable to any system of orthogonal polynomials, is that allows considering orthogonal polynomials of the non-Askey-Wiener. This study of non-Askey-Wiener polynomials is presented in section 4.3. Finally, section 4.4 presents a characterization of the error arising from the decoupling procedure.

4.2 The Generalized Decoupling Approach

4.2.1 Theoretical Basis

The underlying theory of the proposed approach requires first expanding the matrix $\boldsymbol{Y}(\boldsymbol{\xi}, s)$ in a multi-dimensional Taylor series expansion in $\boldsymbol{\xi}$ as follows,

$$\boldsymbol{Y}(\boldsymbol{\xi}, s) = \sum_{\boldsymbol{\beta}} \breve{\boldsymbol{Y}}_{\boldsymbol{\beta}}(s) \prod_{i=1}^{d} {\xi_i}^{\beta_i} \tag{4.1}$$

It is important to stress here that the proposed algorithm does not require a Taylor series expansion, and the Taylor expansion is only used in providing the theoretical foundation. The proposed approach is based on a fundamental theoretical result that is described by the following theorems.

Theorem 1. *Let* $\boldsymbol{K}_{i,\beta_i} \in \mathbb{R}^{(M+1)\times(M+1)}$ *be defined from*

$$\left[\boldsymbol{K}_{i,\beta_i}\right]_{\gamma_i+1,\alpha_i+1} = \Phi_{\beta_i,\alpha_i,\gamma_i} \tag{4.2}$$

where

$$\Phi_{\beta_i,\alpha_i,\gamma_i} = \frac{\int_{\Omega_i} \xi_i^{\beta_i} \phi_{\alpha_i}(\xi_i)\phi_{\gamma_i}(\xi_i) w(\xi_i) d\xi_i}{\Theta_{\gamma_i}} \tag{4.3}$$

Then the augmented matrix $\bar{\boldsymbol{Y}}(s)$ is given by the following closed-form expression,

$$\bar{\boldsymbol{Y}}(s) = \sum_{\boldsymbol{\beta}} \boldsymbol{K}_{1,\beta_1} \otimes \boldsymbol{K}_{2,\beta_2} \otimes \cdots \otimes \boldsymbol{K}_{d,\beta_d} \otimes \breve{\boldsymbol{Y}}_{\boldsymbol{\beta}}(s) \tag{4.4}$$

where $\otimes$ is the Kronecker product operator.

The proof of theorem 1 is based on the following lemma 1.

Lemma 1. *Let $\boldsymbol{p}, \boldsymbol{q} \in \mathbb{N}^d$ be a multi-indices with d components p_i, q_i, respectively, with $p_i, q_i = 0, \cdots, M$ and $i = 1, \cdots, d$, and assume that there is a sequence of d matrices denoted by $\boldsymbol{A}_i \in \mathbb{R}^{(M+1)\times(M+1)}$. Furthermore, let $\boldsymbol{B}$ be a matrix in $\mathbb{C}^{N\times N}$ and define the matrix $\boldsymbol{D}$ such that*

$$\boldsymbol{D} = \boldsymbol{A}_1 \otimes \cdots \otimes \boldsymbol{A}_d \tag{4.5}$$

It then follows that,

$$[\boldsymbol{D}]_{|\boldsymbol{p}|+1,|\boldsymbol{q}|+1} = \prod_{i=1}^{d} [\boldsymbol{A}_i]_{p_i+1,q_i+1} \tag{4.6}$$

$$\{\boldsymbol{D} \otimes \boldsymbol{B}\}^{N}_{|\boldsymbol{p}|N+1,|\boldsymbol{q}|N+1} = \prod_{i=1}^{d} [\boldsymbol{A}_i]_{p_i+1,q_i+1}\, \boldsymbol{B} \tag{4.7}$$

Proof. The proof of the above lemma follows directly from the properties of the Kronecker product and can be verified by considering a simple case such as $d = 2$. □

With the above lemma, the proof of theorem 1 is as follows:

Proof. The proof of theorem 1 is given by first substituting (4.1) into (3.50), which yields

$$\begin{aligned}
&\{\bar{\boldsymbol{Y}}\}^{N}_{|\boldsymbol{\gamma}|N+1,|\boldsymbol{\alpha}|N+1} \\
&\quad= \frac{\int_{\boldsymbol{\Omega}}(\sum_{\boldsymbol{\beta}} \hat{\boldsymbol{Y}}_{\boldsymbol{\beta}} \prod_{i=1}^{d} \xi_i^{\beta_i})\phi_{\boldsymbol{\alpha}}(\boldsymbol{\xi}, s)\phi_{\boldsymbol{\gamma}}(\boldsymbol{\xi}, s)w(\boldsymbol{\xi})\mathrm{d}\boldsymbol{\xi}}{\Theta_{\boldsymbol{\gamma}}} \\
&\quad= \sum_{\boldsymbol{\beta}} \hat{\boldsymbol{Y}}_{\boldsymbol{\beta}} \prod_{i=1}^{d} \frac{\int_{\Omega_i} \xi_i^{\beta_i}\phi_{\alpha_i}(\xi_i, s)\phi_{\gamma_i}(\xi_i, s)w(\xi_i)\mathrm{d}\xi_i}{\Theta_{\gamma_i}} \\
&\quad= \sum_{\boldsymbol{\beta}} \hat{\boldsymbol{Y}}_{\boldsymbol{\beta}}(s) \prod_{i=1}^{d} \Phi_{\beta_i,\alpha_i,\gamma_i}
\end{aligned} \tag{4.8}$$

Using (4.2) simplifies the above to,

$$\{\bar{\boldsymbol{Y}}\}^{N}_{|\boldsymbol{\gamma}|N+1,|\boldsymbol{\alpha}|N+1} = \sum_{\boldsymbol{\beta}} \hat{\boldsymbol{Y}}_{\boldsymbol{\beta}}(s) \prod_{i=1}^{d} [\boldsymbol{K}_{i,\beta_i}]_{\gamma_i+1,\alpha_i+1} \tag{4.9}$$

It is easy to see that, using Lemma 1 in (4.9) yields (4.4), thereby proving theorem 1. □

Theorem 2. *The matrix $\boldsymbol{K}_{i,\beta_i}$ defined in (4.2) can be also represented as:*

$$\boldsymbol{K}_{i,\beta_i} = \tilde{\boldsymbol{K}}_{i,\beta_i} + \boldsymbol{\Delta}_{i,\beta_i} \tag{4.10}$$

with

$$\tilde{\boldsymbol{K}}_{i,\beta_i} = \boldsymbol{T}_i^{\beta_i} \tag{4.11}$$

where $\boldsymbol{T}_i$ is a tridiagonal matrix of the form

$$\boldsymbol{T}_i = \begin{bmatrix}
e_{i,0} & d_{i,1} & & & & \\
c_{i,0} & e_{i,1} & d_{i,2} & & & \\
 & c_{i,1} & e_{i,2} & \ddots & & \\
 & & c_{i,2} & \ddots & d_{i,M-1} & \\
 & & & \ddots & e_{i,M-1} & d_{i,M} \\
 & & & & c_{i,M-1} & e_{i,M}
\end{bmatrix} \tag{4.12}$$

and $\boldsymbol{\Delta}_{i,\beta_i}$

$$\boldsymbol{\Delta}_{i,\beta_i} = \begin{cases} 0 & (\beta_i = 0) \\ \sum_{j=0}^{\beta_i - 1} \boldsymbol{\Gamma}_{i,\beta_i - j} \boldsymbol{T}_i^j & (\beta_i \geq 1) \end{cases} \tag{4.13}$$

with $\boldsymbol{\Gamma}_{i,\beta_i} \in \mathbb{R}^{(M+1)\times(M+1)}$ *(*$\beta_i \geq 1$*) being a matrix whose* (p, q) *entry is represent through:*

$$[\boldsymbol{\Gamma}_{i,\beta_i}]_{p,q} = \begin{cases} 0 & (q < M+1) \\ c_{i,M} \Phi_{\beta_i - 1, q, p-1} & (q = M+1) \end{cases} \tag{4.14}$$

The proof of the theorem 2 is based on a fundamental property of any orthogonal polynomials system, the three term recurrence relationship, summarized by Lemma 2 as follows:

Lemma 2. *Given any sequence of orthogonal polynomials* $\phi_n(\xi)$*, there exists a sequence of constants* a_n, b_n *and* g_n *such that*

$$\phi_0(\xi) = 1 \tag{4.15}$$

$$\phi_1(\xi) = (a_0 \xi - g_0)\phi_0(\xi) \tag{4.16}$$

$$\phi_{n+1}(\xi) = (a_n \xi - g_n)\phi_n(\xi) - b_n \phi_{n-1}(\xi) \quad (n \geq 1) \tag{4.17}$$

Proof. A proof of the above lemma can be found in many standard texts on the subject of orthogonal polynomials [36] □

With this lemma, the results of Theorem 2 are developed as follows.

Proof. Recall the three term recurrence relationship given by Lemma 2: the relationship can be rewritten in another form by separating the term with and without ξ. In addition, a subscript i will

be added to highlight the fact that different RVs ξ_i may be represented by different polynomials. Thus, (4.15)-(4.17) take the following form,

$$\xi_i \phi_{i,0}(\xi_i) = c_{i,0}\phi_{i,1}(\xi_i) + d_{i,0}\phi_{i,0}(\xi_i) \tag{4.18}$$

$$\xi_i \phi_{i,n}(\xi_i) = c_{i,n}\phi_{i,n+1}(\xi_i) + d_{i,n}\phi_{i,n}(\xi_i) + e_{i,n}\phi_{i,n-1}(\xi_i) \ (n \geq 1) \tag{4.19}$$

where $c_{i,n} = \frac{1}{a_{i,n}}$, $d_{i,n} = \frac{g_{i,n}}{a_{i,n}}$ and $e_n = \frac{b_{i,n}}{a_{i,n}}$.

We remark that when $\beta_i = 0$, we have $\boldsymbol{K}_{i,0}$ is just an identity matrix since by the orthogonality of $\phi_i(\xi_i)$, we have

$$[\boldsymbol{K}_{i,0}]_{\gamma_i+1,\alpha_i+1} = \frac{\int_{\Omega_i} \phi_{\alpha_i}(\xi_i)\phi_{\gamma_i}(\xi_i)w(\xi_i)d\xi_i}{\Theta_{\gamma_i}} = \delta_{\alpha_i,\gamma_i}$$

so the statements in theorem 2 are satisfied automatically when $\beta_i = 0$.

For $\beta_i \geq 1$, the entries in the first column in $\boldsymbol{K}_{i,\beta_i}$ can be obtained by setting $\alpha_i = 0$ in (4.2), yielding

$$[\boldsymbol{K}_{i,\beta_i}]_{\gamma_i+1,1} = \frac{\int_{\Omega_i} \xi_i^{\beta_i}\phi_0(\xi_i)\phi_{\gamma_i}(\xi_i)w(\xi_i)d\xi_i}{\Theta_{\gamma_i}}$$

and (4.18) can be applied onto above equation , which is

$$\begin{aligned}
&[\boldsymbol{K}_{i,\beta_i}]_{\gamma_i+1,1} \\
&= \frac{\int_{\Omega_i} \xi_i^{\beta_i-1}[\xi_i\phi_0(\xi_i)]\phi_{\gamma_i}(\xi_i)w(\xi_i)d\xi_i}{\Theta_{\gamma_i}} \\
&= \frac{\int_{\Omega_i} \xi_i^{\beta_i-1}(c_0\phi_1(\xi_i) + d_0\phi_0(\xi_i))\phi_{\gamma_i}(\xi_i)w(\xi_i)d\xi_i}{\Theta_{\gamma_i}} \\
&= c_0[\boldsymbol{K}_{i,\beta_i-1}]_{\gamma_i+1,2} + d_0[\boldsymbol{K}_{i,\beta_i-1}]_{\gamma_i+1,1}
\end{aligned} \tag{4.20}$$

$$
\begin{aligned}
&[\boldsymbol{K}_{i,\beta_i-1}\boldsymbol{T}_i]_{\gamma_i+1,\alpha_i+1} \\
&= \begin{cases}
c_{i,0}[\boldsymbol{K}_{i,\beta_i-1}]_{\gamma_i+1,2} + d_{i,0}[\boldsymbol{K}_{i,\beta_i-1}]_{\gamma_i+1,1} & (\alpha_i = 0) \\
c_{i,\alpha_i}[\boldsymbol{K}_{i,\beta_i-1}]_{\gamma_i+1,\alpha_i+2} + d_{i,\alpha_i}[\boldsymbol{K}_{i,\beta_i-1}]_{\gamma_i+1,\alpha_i+1} + e_{i,\alpha_i}[\boldsymbol{K}_{i,\beta_i-1}]_{\gamma_i+1,\alpha_i} & (0 < \alpha_i < M) \\
d_{i,M}[\boldsymbol{K}_{i,\beta_i-1}]_{\gamma_i+1,M+1} + e_{i,M}[\boldsymbol{K}_{i,\beta_i-1}]_{\gamma_i+1,M} & (\alpha_i = M)
\end{cases}
\end{aligned} \tag{4.22}
$$

Entries in other columns in $\boldsymbol{K}_{i,\beta_i}$ are given by $\alpha_i \geq 1$, which are given by

$$
\begin{aligned}
&[\boldsymbol{K}_{i,\beta_i}]_{\gamma_i+1,\alpha_i+1} \\
&= \frac{\int_{\Omega_i} \xi_i^{\beta_i} \phi_{\alpha_i}(\xi_i)\phi_{\gamma_i}(\xi_i)w(\xi_i)d\xi_i}{\Theta_{\gamma_i}} \\
&= c_{\alpha_i}[\boldsymbol{K}_{i,\beta_i-1}]_{\gamma_i+1,\alpha_i+2} + d_{\alpha_i}[\boldsymbol{K}_{i,\beta_i-1}]_{\gamma_i+1,\alpha_i+1} \\
&+ e_{\alpha_i}[\boldsymbol{K}_{i,\beta_i-1}]_{\gamma_i+1,\alpha_i}
\end{aligned} \tag{4.21}
$$

for $\alpha_i \geq 1$.

On the other hand, due to the tridiagonal structure of matrix $\boldsymbol{T}_i$, it is easy to show that the entries in the matrix product $\boldsymbol{K}_{i,\beta_i-1}\boldsymbol{T}_i$ satisfy the expression in (4.22), shown at the top of the next page.

Comparing (4.20), (4.21) and (4.22), reveals that the two matrices $\boldsymbol{K}_{i,\beta_i}$ and $\boldsymbol{K}_{i,\beta_i-1}\boldsymbol{T}_i$ are equivalent except for the last column, i.e. for $\alpha_i = M$. Thus if we use $\boldsymbol{\Gamma}_{i,\beta_i}$, given by (4.14), to represent this difference between $\boldsymbol{K}_{i,\beta_i}$ and $\boldsymbol{K}_{i,\beta_i-1}\boldsymbol{T}_i$, we may be able to write

$$
\boldsymbol{K}_{i,\beta_i} = \boldsymbol{K}_{i,\beta_i-1}\boldsymbol{T}_i + \boldsymbol{\Gamma}_{i,\beta_i} \quad (\beta_i \geq 1) \tag{4.23}
$$

Then by recursively substituting (4.23) into itself for β_i times, one obtains

$$\boldsymbol{K}_{i,\beta_i} = \boldsymbol{K}_{i,0}\boldsymbol{T}_i^{\beta_i} + \sum_{j=0}^{\beta_i-1} \boldsymbol{\Gamma}_{\beta_i-j}\boldsymbol{T}_i^{j} \tag{4.24}$$

Since $\boldsymbol{K}_{i,0}$ is an identity matrix, then (4.10) follows from (4.24) proving Theorem 2. □

Some examples of the three term recurrence relationship and matrix $\boldsymbol{T}$ for different polynomials:

- Hermite Polynomials

$$H_0(\xi) = 1 \quad H_1(\xi) = \xi \quad H_{n+1}(\xi) = \xi H_n(\xi) - nH_{n-1}(\xi)$$

$$\Rightarrow c_0 = 1 \quad e_0 = 0 \quad c_n = 1 \quad e_n = 0 \quad d_n = n$$

$$\boldsymbol{T} = \begin{bmatrix} 0 & 1 & 0 & \cdots & 0 & 0 \\ 1 & 0 & 2 & \cdots & 0 & 0 \\ 0 & 1 & 0 & \cdots & 0 & 0 \\ \vdots & \vdots & \vdots & \ddots & \vdots & \vdots \\ 0 & 0 & 0 & \cdots & 0 & M \\ 0 & 0 & 0 & \cdots & 1 & 0 \end{bmatrix}$$

- Legendre Polynomials

$$P_0(\xi) = 1 \quad P_1(\xi) = \xi$$

$$P_{n+1}(\xi) = \frac{2n+1}{n+1}\xi T_n(\xi) - \frac{n}{n+1}T_{n-1}(\xi)$$

$$\Rightarrow c_0 = 1 \quad e_0 = 0 \quad c_n = \frac{n+1}{2n+1} \quad e_n = 0 \quad d_n = \frac{n}{n+1}$$

$$\boldsymbol{T} = \begin{bmatrix} 0 & \frac{1}{3} & 0 & \cdots & 0 & 0 \\ 1 & 0 & \frac{2}{5} & \cdots & 0 & 0 \\ 0 & \frac{2}{3} & 0 & \cdots & 0 & 0 \\ \vdots & \vdots & \vdots & \ddots & \vdots & \vdots \\ 0 & 0 & 0 & \cdots & 0 & \frac{M}{2M+1} \\ 0 & 0 & 0 & \cdots & \frac{M}{2M-1} & 0 \end{bmatrix}$$

- Generalized Laguerre polynomials

$$L_0^\alpha(\xi) = 1 \quad L_1^\alpha(\xi) = 1 + \alpha - \xi$$

$$L_{n+1}^\alpha(\xi) = \frac{(2n+1+\alpha-\xi)L_n^\alpha(\xi) - (n+\alpha)L_{n-1}^\alpha(\xi)}{n+1}$$

$$\Rightarrow c_0 = -1 \quad e_0 = 1+\alpha$$

$$\Rightarrow c_n = -(n+1) \quad e_n = 2n+1+\alpha \quad d_n = -(n+\alpha)$$

$$\boldsymbol{T} = \begin{bmatrix} 1+\alpha & -(1+\alpha) & 0 & \cdots & 0 & 0 \\ -1 & 3+\alpha & -(2+\alpha) & \cdots & 0 & 0 \\ 0 & -2 & 5+\alpha & \cdots & 0 & 0 \\ \vdots & \vdots & \vdots & \ddots & \vdots & \vdots \\ 0 & 0 & 0 & \cdots & 2M-1+\alpha & -(M+\alpha) \\ 0 & 0 & 0 & \cdots & -M & 2M+1+\alpha \end{bmatrix}$$

The basic idea of the decoupling approach is based on developing an alternative formulation for the augmented matrix that enables transforming it into a block-diagonal matrix whose diagonal blocks can be factorized independently. To simplify the presentation, this idea will

be first explained for the frequency-domain analysis of linear circuits from the perspective of a single-dimensional random space in section 4.2.2, followed by the general case of multi-random parameters in 4.2.3 and a time-domain analysis of nonlinear circuits in section 4.2.4.

4.2.2 Decoupling Approach: FD Analysis for Single Random Case

In the case of a problem with a single random variable, except all the multi-index, i.e. $\boldsymbol{\alpha}$, $\boldsymbol{\beta}$ and $\boldsymbol{\gamma}$, will be simplified as α, β and γ, some equations such as (4.1) and (3.48) would also take the simplified form:

$$\boldsymbol{Y}(\xi, s) = \sum_{\beta=0}^{\infty} \breve{\boldsymbol{Y}}_{\beta}(s)\xi^{\beta} \tag{4.25}$$

$$\{\bar{\boldsymbol{Y}}\}_{\gamma N+1,\alpha N+1}^{N} = \frac{\int_{\Omega} \boldsymbol{Y}(\xi, s)\phi_{\alpha}(\xi, s)\phi_{\gamma}(\xi, s)w(\xi)\mathrm{d}\xi}{\Theta_{\gamma}} \tag{4.26}$$

By substituting (4.25) into (4.26), the closed form expression of any blocks in $\bar{\boldsymbol{Y}}$ can be given by:

$$\{\bar{\boldsymbol{Y}}\}_{\gamma N+1,\alpha N+1}^{N} = \frac{\int_{\Omega} \sum_{\beta=0}^{\infty} \breve{\boldsymbol{Y}}_{\beta}(s)\xi^{\beta}\phi_{\alpha}(\xi)\phi_{\gamma}(\xi)w(\xi)d\xi}{\Theta_{\gamma}} = \sum_{\beta=0}^{\infty} \breve{\boldsymbol{Y}}_{\beta}(s)\Phi_{\beta,\alpha,\gamma} \tag{4.27}$$

Thus the augmented matrix equation will have the form of:

$$\begin{bmatrix} \sum_{\beta=0}^{\infty} \breve{\boldsymbol{Y}}_{\beta}\Phi_{\beta 00} & \sum_{\beta=0}^{\infty} \breve{\boldsymbol{Y}}_{\beta}\Phi_{\beta 10} & \cdots & \sum_{\beta=0}^{\infty} \breve{\boldsymbol{Y}}_{\beta}\Phi_{\beta M0} \\ \sum_{\beta=0}^{\infty} \breve{\boldsymbol{Y}}_{\beta}\Phi_{\beta 01} & \sum_{\beta=0}^{\infty} \breve{\boldsymbol{Y}}_{\beta}\Phi_{\beta 11} & \cdots & \sum_{\beta=0}^{\infty} \breve{\boldsymbol{Y}}_{\beta}\Phi_{\beta M1} \\ \vdots & \vdots & \ddots & \vdots \\ \sum_{\beta=0}^{\infty} \breve{\boldsymbol{Y}}_{\beta}\Phi_{\beta 0M} & \sum_{\beta=0}^{\infty} \breve{\boldsymbol{Y}}_{\beta}\Phi_{\beta 1M} & \cdots & \sum_{\beta=0}^{\infty} \breve{\boldsymbol{Y}}_{\beta}\Phi_{\beta MM} \end{bmatrix} \times \begin{bmatrix} \hat{\boldsymbol{X}}_0 \\ \hat{\boldsymbol{X}}_1 \\ \vdots \\ \hat{\boldsymbol{X}}_M \end{bmatrix} = \begin{bmatrix} U \\ 0 \\ \vdots \\ 0 \end{bmatrix}$$

and it is easy to find the following expression of augmented matrix $\bar{\boldsymbol{Y}}(s)$ just by observing the above equation;

$$\bar{\boldsymbol{Y}}(s) = \sum_{\beta=0}^{\infty} \boldsymbol{K}_{\beta} \otimes \breve{\boldsymbol{Y}}_{\beta}(s) \tag{4.28}$$

which satisfy the expression in theorem 1.

The decoupling approach is based on using the matrix $\tilde{\boldsymbol{K}}_\beta$ instead of $\boldsymbol{K}_\beta$ in constructing the augmented matrix. The augmented matrix obtained from this approach is denoted $\tilde{\boldsymbol{Y}}(s)$ to distinguish it from the original matrix $\bar{\boldsymbol{Y}}(s)$. Thus,

$$\tilde{\boldsymbol{Y}}(s) = \sum_{\beta=0}^{\infty} \tilde{\boldsymbol{K}}_\beta \otimes \breve{\boldsymbol{Y}}_\beta(s). \tag{4.29}$$

In a similar manner, the solution obtained from factorizing this matrix is denoted $\tilde{\boldsymbol{X}}(s)$, i.e,

$$\tilde{\boldsymbol{Y}}(s)\tilde{\boldsymbol{X}}(s) = \bar{\boldsymbol{U}}(s) \tag{4.30}$$

to highlight that it is an approximation of the exact solution $\bar{\boldsymbol{X}}(s)$.

In order to show the key advantage of using $\tilde{\boldsymbol{Y}}(s)$ instead of $\bar{\boldsymbol{Y}}(s)$, we express $\tilde{\boldsymbol{K}}_\beta$ by its eigen-decomposition,

$$\tilde{\boldsymbol{K}}_\beta = \boldsymbol{V}\boldsymbol{D}^\beta\boldsymbol{V}^{-1} \tag{4.31}$$

where $\boldsymbol{V}$ is the matrix of eigenvectors of the matrix $\boldsymbol{T}$ (obtained from (4.12)) and $\boldsymbol{D}$ is a diagonal matrix whose diagonal elements are the eigenvalues of $\boldsymbol{T}$. One needs to stress here that the matrix of eigenvectors $\boldsymbol{V}$ is independent of the index β. This fact will come into focus in the decoupling process presented next.

Substituting (4.31) into (4.29) and using basic properties of the Kronecker product operator [37] which allows us to factor the matrix $\boldsymbol{V}$ out of the summation over β, enables casting $\tilde{\boldsymbol{Y}}(s)$ in the following form,

$$\tilde{\boldsymbol{Y}}(s) = (\boldsymbol{V} \otimes \boldsymbol{I}_N)\left(\sum_{\beta=0}^{\infty} \boldsymbol{D}^\beta \otimes \breve{\boldsymbol{Y}}_\beta(s)\right)\left(\boldsymbol{V}^{-1} \otimes \boldsymbol{I}_N\right) \tag{4.32}$$

where $\boldsymbol{I}_N$ is an identity matrix of size N. Note that the matrix in the middle $\sum_{\beta=0}^{\infty} \boldsymbol{D}^{\beta} \otimes \breve{\boldsymbol{Y}}_{\beta}(s)$ is block-diagonal,

$$\sum_{\beta=0}^{\infty} \boldsymbol{D}^{\beta} \otimes \boldsymbol{Y}_{\beta} = \begin{bmatrix} \sum_{\beta=0}^{\infty} \breve{\boldsymbol{Y}}_{\beta} \lambda_0^{\beta} & & & \\ & \sum_{\beta=0}^{\infty} \breve{\boldsymbol{Y}}_{\beta} \lambda_1^{\beta} & & \\ & & \ddots & \\ & & & \sum_{\beta=0}^{\infty} \breve{\boldsymbol{Y}}_{\beta} \lambda_M^{\beta} \end{bmatrix} \tag{4.33}$$

where λ_k, $k = 0, 1, \cdots, M$ are the eigenvalues of $\boldsymbol{T}$. Comparing the diagonal blocks in (4.33) with the Taylor expansions in (4.25) for a single random parameter ($d = 1$), leads to the following conclusion,

$$\sum_{\beta=0}^{\infty} \boldsymbol{D}^{\beta} \otimes \boldsymbol{Y}_{\beta} = \begin{bmatrix} \boldsymbol{Y}(\lambda_0, s) & & & \\ & \boldsymbol{Y}(\lambda_1, s) & & \\ & & \ddots & \\ & & & \boldsymbol{Y}(\lambda_M, s) \end{bmatrix} \tag{4.34}$$

Solving the system (4.30) proceeds by first factorizing the above matrix, via factorizing its diagonal blocks $\boldsymbol{Y}(\lambda_i, s)$ independently or in parallel, then running a Forward/Backward substitution with the vector $\boldsymbol{V}^{-1} \otimes \boldsymbol{I}_N \bar{\boldsymbol{U}}(s)$. $\tilde{\boldsymbol{X}}(s)$ is then obtained by mapping the result from those steps using the transformation operator $\boldsymbol{V} \otimes \boldsymbol{I}_N$.

The key computational advantage in the above approach stems from having to factorize only the individual blocks $\boldsymbol{Y}(\xi, s)$ at $\xi = \lambda_i$ as opposed to factorizing the augmented matrix $\bar{\boldsymbol{Y}}(s)$.

4.2.3 Decoupling Approach: FD Analysis for Multi-random Case

Generalizing the decoupling method to the general case of d-dimensional random space is performed in analogous manner, where $\boldsymbol{K}_{i,\beta_i}$ in (4.4) is replaced with $\tilde{\boldsymbol{K}}_{i,\beta_i}$

$$\tilde{\boldsymbol{Y}} = \sum_{\boldsymbol{\beta}} \tilde{\boldsymbol{K}}_{1,\beta_1} \otimes \cdots \otimes \tilde{\boldsymbol{K}}_{d,\beta_d} \otimes \breve{\boldsymbol{Y}}_{\boldsymbol{\beta}} \tag{4.35}$$

Similarly, by substituting $\tilde{\boldsymbol{K}}_{\beta_i} = \boldsymbol{V}_i \boldsymbol{D}_i^{\beta_i} \boldsymbol{V}_i^{-1}$ into (4.35), where $\boldsymbol{V}_i$ and $\boldsymbol{D}_i$ are the eigenvector and eigenvalue matrices of $\boldsymbol{T}_i$, we obtain

$$\begin{aligned}\tilde{\boldsymbol{Y}}(s) = (\boldsymbol{V}_1 \otimes \boldsymbol{V}_2 \otimes \cdots \otimes \boldsymbol{V}_d \otimes \boldsymbol{I}_N) \\ \left(\sum_{\boldsymbol{\beta}} \boldsymbol{D}_1^{\beta_1} \otimes \boldsymbol{D}_2^{\beta_2} \otimes \cdots \otimes \boldsymbol{D}_d^{\beta_d} \otimes \breve{\boldsymbol{Y}}_{\boldsymbol{\beta}} \right) \\ \left(\boldsymbol{V}_1^{-1} \otimes \boldsymbol{V}_2^{-1} \otimes \cdots \otimes \boldsymbol{V}_d^{-1} \otimes \boldsymbol{I}_N \right)\end{aligned} \tag{4.36}$$

Examining the matrix in the middle of the above formulation reveals that it has a block diagonal structure with Q blocks, and whose p^{th} block is given by,

$$\left\{ \sum_{\boldsymbol{\beta}} \boldsymbol{D}_1^{\beta_1} \otimes \boldsymbol{D}_2^{\beta_2} \otimes \cdots \otimes \boldsymbol{D}_d^{\beta_d} \otimes \breve{\boldsymbol{Y}}_{\boldsymbol{\beta}}(s) \right\}_{pN+1,pN+1}^{N} = \sum_{\boldsymbol{\beta}} \left(\prod_{j=1}^{d} \lambda_{\sigma_{i,j}}^{\beta_j} \right) \breve{\boldsymbol{Y}}_{\beta_j}(s) \tag{4.37}$$

where $\lambda_{\sigma_{i,j}}$ is the i^{th} eigenvalue of $\boldsymbol{T}_j$. Comparing (4.37) with (4.1) leads to

$$\left\{ \sum_{\boldsymbol{\beta}} \boldsymbol{D}_1^{\beta_1} \otimes \boldsymbol{D}_2^{\beta_2} \otimes \cdots \otimes \boldsymbol{D}_d^{\beta_d} \otimes \breve{\boldsymbol{Y}}_{\boldsymbol{\beta}}(s) \right\}_{pN+1,pN+1}^{N} = \boldsymbol{Y}(\bar{\boldsymbol{\lambda}}, s) \tag{4.38}$$

where,

$$\bar{\boldsymbol{\lambda}} = \begin{bmatrix} \lambda_{\sigma_{i,1}} & \lambda_{\sigma_{i,2}} & \cdots & \lambda_{\sigma_{i,d}} \end{bmatrix}^T \tag{4.39}$$

Here is an example of the diagonally block matrix for the case of $d = 2$ and $M = 2$,

$$\begin{bmatrix} Y(\lambda_{\sigma_1,1}, \lambda_{\sigma_1,2}, s) & & & & & \\ & Y(\lambda_{\sigma_1,1}, \lambda_{\sigma_2,2}, s) & & & & \\ & & Y(\lambda_{\sigma_1,1}, \lambda_{\sigma_3,2}, s) & & & \\ & & & Y(\lambda_{\sigma_2,1}, \lambda_{\sigma_1,2}, s) & & \\ & & & & \ddots & \\ & & & & & Y(\lambda_{\sigma_3,1}, \lambda_{\sigma_3,2}, s) \end{bmatrix}$$

4.2.4 Decoupling Approach: TD Analysis for Multi-random Case

The generalization of the above proposed decoupling procedure to time-domain analysis for non-linear circuits is pursued by first stating the generalized MNA formulation of nonlinear circuits in the time-domain, which is given by (2.5).

$$\boldsymbol{C}(\boldsymbol{\xi})\frac{d\boldsymbol{x}(\boldsymbol{\xi},t)}{dt} + \boldsymbol{G}(\boldsymbol{\xi})\boldsymbol{x}(\boldsymbol{\xi},t) + \boldsymbol{f}(\boldsymbol{x}(\boldsymbol{\xi},t),\boldsymbol{\xi}) = \boldsymbol{b}(t)$$

The development of the proposed approach proceeds by expanding both $\boldsymbol{x}(\boldsymbol{\xi},t)$ and $\boldsymbol{f}(\boldsymbol{x}(\boldsymbol{\xi},t),\boldsymbol{\xi})$ in the gPC base,

$$\boldsymbol{f}(\boldsymbol{x}(\boldsymbol{\xi},t),\boldsymbol{\xi}) = \sum_{\boldsymbol{\alpha}\in\Upsilon_Q} \hat{\boldsymbol{f}}_{\boldsymbol{\alpha}}(t)\phi_{\boldsymbol{\alpha}}(\boldsymbol{\xi}) \tag{4.40}$$

$$\boldsymbol{x}(\boldsymbol{\xi},t) = \sum_{\boldsymbol{\alpha}\in\Upsilon_Q} \hat{\boldsymbol{x}}_{\boldsymbol{\alpha}}(t)\phi_{\boldsymbol{\alpha}}(\boldsymbol{\xi}) \tag{4.41}$$

Next, by a substitution from (4.41) and (4.40) into (2.5) and performing the GP, one obtains the following,

$$\bar{\boldsymbol{C}}\frac{d\bar{\boldsymbol{x}}(t)}{dt} + \bar{\boldsymbol{G}}\bar{\boldsymbol{x}}(t) + \bar{\boldsymbol{f}}(t) = \bar{\boldsymbol{b}}(t) \tag{4.42}$$

where $\bar{\boldsymbol{G}}$ and $\bar{\boldsymbol{C}}$ are constructed in an analogous manner to $\bar{\boldsymbol{Y}}$, i.e., using their Taylor series,

$$\bar{\boldsymbol{G}} = \sum_{\boldsymbol{\beta}} \boldsymbol{K}_{1,\beta_1} \otimes \boldsymbol{K}_{2,\beta_2} \otimes \cdots \otimes \boldsymbol{K}_{d,\beta_d} \otimes \hat{\boldsymbol{G}}_{\boldsymbol{\beta}} \tag{4.43}$$

$$\bar{\boldsymbol{C}} = \sum_{\boldsymbol{\beta}} \boldsymbol{K}_{1,\beta_1} \otimes \boldsymbol{K}_{2,\beta_2} \otimes \cdots \otimes \boldsymbol{K}_{d,\beta_d} \otimes \hat{\boldsymbol{C}}_{\boldsymbol{\beta}}, \tag{4.44}$$

while $\bar{\boldsymbol{f}}(t)$ is a vector that is comprised of the coefficients $\hat{\boldsymbol{f}}_{\boldsymbol{\alpha}}(t)$, $\boldsymbol{\alpha} \in \Upsilon_Q$. In addition, $\bar{\boldsymbol{b}}(t)$ is given by $[\boldsymbol{b}(t), 0, \cdots, 0]^T$.

The system of (4.42) is a set of deterministic nonlinear differential equations that can be solved through any of the classical time-stepping methods. For simplicity, we adopt the Backward Euler (BE). Discretization using BE at a set of discrete time points, t_n $n = 0, 1, 2, \cdots$, yields

$$(\bar{\boldsymbol{G}} + \frac{1}{h}\bar{\boldsymbol{C}})\bar{\boldsymbol{x}}_n + \bar{\boldsymbol{f}}_n = \bar{\boldsymbol{b}}_n + \frac{1}{h}\bar{\boldsymbol{C}}\bar{\boldsymbol{x}}_{n-1} \tag{4.45}$$

where $\bar{\boldsymbol{x}}_n$, $\bar{\boldsymbol{f}}_n$, $\bar{\boldsymbol{b}}_n$ represent $\bar{\boldsymbol{x}}(t_n)$, $\bar{\boldsymbol{f}}(\bar{\boldsymbol{x}}_n)$, $\bar{\boldsymbol{b}}(t_n)$, respectively, and h is the step size. The above equation is a nonlinear algebraic system that can be solved using iterative technique such as Newton-Raphson method with an initial guess $\bar{\boldsymbol{x}}_n^{(0)}$, as follows,

$$\bar{\boldsymbol{x}}_n^{(i)} = \bar{\boldsymbol{x}}_n^{(i-1)} - \eta_x^{(i)} \tag{4.46}$$

where

$$\eta_x^{(i)} = \boldsymbol{\jmath}^{-1}(\bar{\boldsymbol{x}}_n^{(i-1)})\boldsymbol{\Phi}(\bar{\boldsymbol{x}}_n^{(i-1)}) \tag{4.47}$$

$$\boldsymbol{\Phi}(\bar{\boldsymbol{x}}_n^{(i-1)}) = (\bar{\boldsymbol{G}} + \frac{1}{h}\bar{\boldsymbol{C}})\bar{\boldsymbol{x}}_n^{(i-1)} + \bar{\boldsymbol{f}}(\bar{\boldsymbol{x}}_n^{(i-1)}) - \bar{\boldsymbol{b}}_n - \frac{1}{h}\bar{\boldsymbol{C}}\bar{\boldsymbol{x}}_{n-1} \tag{4.48}$$

$$\boldsymbol{\jmath}(\bar{\boldsymbol{x}}_n^{(i-1)}) = \frac{1}{h}\bar{\boldsymbol{C}} + \bar{\boldsymbol{G}} + \frac{\partial \bar{\boldsymbol{f}}(\bar{\boldsymbol{x}}_n)}{\partial \bar{\boldsymbol{x}}_n}|_{\bar{\boldsymbol{x}}_n = \bar{\boldsymbol{x}}_n^{(i-1)}} \tag{4.49}$$

To present the main theoretical result needed in the decoupling procedure for nonlinear circuits, we define first the Jacobian matrix $\boldsymbol{J}(\boldsymbol{\xi})$

$$\boldsymbol{J}(\boldsymbol{\xi}) = \frac{\partial \boldsymbol{f}(\boldsymbol{x}(\boldsymbol{\xi}, t), \boldsymbol{\xi})}{\partial \boldsymbol{x}(\boldsymbol{\xi}, t)} \tag{4.50}$$

and represent it by its Taylor series expansion in $\boldsymbol{\xi}$,

$$\boldsymbol{J}(\boldsymbol{\xi}) = \sum_{\boldsymbol{\beta}} \hat{\boldsymbol{J}}_{\boldsymbol{\beta}} \prod_{i=1}^{d} {\xi_i}^{\beta_i} \tag{4.51}$$

Theorem 3. *The nonlinear part of the augmented Jacobian matrix $\mathfrak{J}$, i.e. $\frac{\partial \bar{\boldsymbol{f}}(\bar{\boldsymbol{x}})}{\partial \bar{\boldsymbol{x}}}$, can be represented by*

$$\bar{\boldsymbol{J}}(\bar{\boldsymbol{x}}) = \frac{\partial \bar{\boldsymbol{f}}(\bar{\boldsymbol{x}})}{\partial \bar{\boldsymbol{x}}} = \sum_{\boldsymbol{\beta}} \boldsymbol{K}_{1,\beta_1} \otimes \boldsymbol{K}_{2,\beta_2} \otimes \cdots \otimes \boldsymbol{K}_{d,\beta_d} \otimes \hat{\boldsymbol{J}}_{\boldsymbol{\beta}} \tag{4.52}$$

The theorem 3 can be proven as follows:

Proof. Obviously $\bar{\boldsymbol{J}}$ is a matrix of size $QN \times QN$, which can be represented in the block formats with blocks

$$\{\bar{\boldsymbol{J}}\}_{|\boldsymbol{\gamma}|N+1,|\boldsymbol{\alpha}|N+1}^{N} = \frac{\partial \boldsymbol{f}_{\boldsymbol{\gamma}}(t)}{\partial \boldsymbol{x}_{\boldsymbol{\alpha}}} \tag{4.53}$$

where $\frac{\partial \boldsymbol{f}_{\boldsymbol{\gamma}}(t)}{\partial \boldsymbol{x}_{\boldsymbol{\alpha}}}$ is a $N \times N$ matrix. Next, recall the orthogonality property of the polynomials, which results in the following:

$$\boldsymbol{f}_{\boldsymbol{\gamma}}(t) = \frac{1}{\boldsymbol{\Theta}_{\boldsymbol{\gamma}}} \int_{\Omega} \boldsymbol{f}(\boldsymbol{x}(\boldsymbol{\xi}, t), \boldsymbol{\xi}) \phi_{\boldsymbol{\gamma}}(\boldsymbol{\xi}) w(\boldsymbol{\xi}) d\boldsymbol{\xi} \tag{4.54}$$

Substituting (4.54) into (4.53) one obtains,

$$\begin{aligned} \frac{\partial \boldsymbol{f}_{\boldsymbol{\gamma}}(t)}{\partial \boldsymbol{x}_{\boldsymbol{\alpha}}} &= \frac{1}{\boldsymbol{\Theta}_{\boldsymbol{\gamma}}} \int_{\Omega} \frac{\partial \boldsymbol{f}(\boldsymbol{x}(\boldsymbol{\xi},t),\boldsymbol{\xi})}{\partial \boldsymbol{x}_{\boldsymbol{\alpha}}} \phi_{\boldsymbol{\gamma}}(\boldsymbol{\xi}) w(\boldsymbol{\xi}) d\boldsymbol{\xi} \\ &= \frac{1}{\boldsymbol{\Theta}_{\boldsymbol{\gamma}}} \int_{\Omega} \frac{\partial \boldsymbol{f}(\boldsymbol{x}(\boldsymbol{\xi},t),\boldsymbol{\xi})}{\partial \boldsymbol{x}(\boldsymbol{\xi},t)} \frac{\partial \boldsymbol{x}(\boldsymbol{\xi},t)}{\partial \boldsymbol{x}_{\boldsymbol{\alpha}}} \phi_{\boldsymbol{\gamma}}(\boldsymbol{\xi}) w(\boldsymbol{\xi}) d\boldsymbol{\xi} \end{aligned} \tag{4.55}$$

From (4.41),(4.51), (4.50) and (4.3), (4.55) can be rewritten as:

$$\begin{aligned} \frac{\partial \boldsymbol{f}_{\boldsymbol{\gamma}}(t)}{\partial \boldsymbol{x}_{\boldsymbol{\alpha}}} &= \frac{1}{\boldsymbol{\Theta}_{\boldsymbol{\gamma}}} \int_{\Omega} \sum_{\boldsymbol{\beta}} \hat{\boldsymbol{J}}_{\boldsymbol{\beta}} \prod_{i=1}^{d} \xi_i^{\beta_i} \phi_{\boldsymbol{\alpha}}(\boldsymbol{\xi}) \phi_{\boldsymbol{\gamma}}(\boldsymbol{\xi}) w(\boldsymbol{\xi}) d\boldsymbol{\xi} \\ &= \sum_{\boldsymbol{\beta}} \hat{\boldsymbol{J}}_{\boldsymbol{\beta}} \prod_{i=1}^{d} \Phi_{\beta_i, \alpha_i, \mathcal{N}\gamma_i} \end{aligned} \tag{4.56}$$

A comparison between the above expression and (4.8) proves theorem 3. □

Substituting (4.43), (4.44) and (4.52) into (4.49) and using the corresponding $\tilde{\boldsymbol{K}}_{i,\beta_i}$ instead of $\boldsymbol{K}_{i,\beta_i}$, the alternate augmented Jacobian matrix, $\tilde{\boldsymbol{j}}$, is given by

$$\tilde{\boldsymbol{j}} = \sum_{\boldsymbol{\beta}} \tilde{\boldsymbol{K}}_{1,\beta_1} \otimes \tilde{\boldsymbol{K}}_{2,\beta_2} \otimes \cdots \otimes \tilde{\boldsymbol{K}}_{d,\beta_d} \otimes (\frac{1}{h}\hat{\boldsymbol{C}}_{\boldsymbol{\beta}} + \hat{\boldsymbol{G}}_{\boldsymbol{\beta}} + \hat{\boldsymbol{J}}_{\boldsymbol{\beta}}) \tag{4.57}$$

Again, by substituting $\tilde{\boldsymbol{K}}_{\beta_i}$ in above equation with their eigen-decomposition, we obtain

$$\begin{aligned}\tilde{\boldsymbol{j}} = (\boldsymbol{V}_1 \otimes \boldsymbol{V}_2 \otimes \cdots \otimes \boldsymbol{V}_d \otimes \boldsymbol{I}_N) \\ \left(\sum_{\boldsymbol{\beta}} \boldsymbol{D}_1^{\beta_1} \otimes \boldsymbol{D}_2^{\beta_2} \otimes \cdots \otimes \boldsymbol{D}_d^{\beta_d} \otimes (\frac{1}{h}\hat{\boldsymbol{C}}_{\boldsymbol{\beta}} + \hat{\boldsymbol{G}}_{\boldsymbol{\beta}} + \hat{\boldsymbol{J}}_{\boldsymbol{\beta}}) \right) \\ \left(\boldsymbol{V}_1^{-1} \otimes \boldsymbol{V}_2^{-1} \otimes \cdots \otimes \boldsymbol{V}_d^{-1} \otimes \boldsymbol{I}_N\right)\end{aligned} \tag{4.58}$$

It is obviously that the middle of the above formulation has a block diagonal structure with Q blocks, and whose p^{th} diagonal block is given by,

$$\begin{aligned}\left\{ \sum_{\boldsymbol{\beta}} \boldsymbol{D}_1^{\beta_1} \otimes \boldsymbol{D}_2^{\beta_2} \otimes \cdots \otimes \boldsymbol{D}_d^{\beta_d} \otimes \hat{\boldsymbol{Y}}_{\boldsymbol{\beta}}(s) \right\}_{pN+1,pN+1}^{N} \\ = \sum_{\boldsymbol{\beta}} (\prod_{j=1}^{d} \lambda_{\sigma_{i,j}}^{\beta_j})(\frac{1}{h}\hat{\boldsymbol{C}}_{\beta} + \hat{\boldsymbol{G}}_{\beta} + \hat{\boldsymbol{J}}_{\beta}) \\ = \frac{1}{h}\boldsymbol{C}(\bar{\boldsymbol{\lambda}}) + \boldsymbol{G}(\bar{\boldsymbol{\lambda}}) + \boldsymbol{J}(\bar{\boldsymbol{\lambda}})\end{aligned} \tag{4.59}$$

4.2.5 Summary

The derivations in the previous sections basically suggest that the augmented matrix $\bar{\boldsymbol{Y}}(s)$ be replaced by $\tilde{\boldsymbol{Y}}(s)$, with the latter being a similarity transformation of a block diagonal matrix, whose diagonal blocks are matrices computed at the eigenvalues of the matrix $\boldsymbol{T}_i$, and where the similarity transformation operator is given by $\boldsymbol{V}_1 \otimes \cdots \otimes \boldsymbol{V}_d \otimes \boldsymbol{I}_N$ that is problem-independent.

Factorizing matrix $\tilde{\boldsymbol{Y}}(s)$ can then be carried out by factorizing the diagonal blocks (independently or in parallel) and using the similarity transformation to transform the solution from the decoupled domain into the coupled domain. Moreover, it is easy to notice that the system that decoupled approach need to solve is just the original system when random parameters equal to some specific value (the eigenvalue of $\boldsymbol{K}$ matrices). Notice that the MC method is to repetitive solving the system after assigning the random parameters to a certain value from the random samples generated according to their distribution. So the program for MC methods can be used directly for this methods. Also, for most of the situation, the number of coefficients is far less than the times of MC simulation, which means this approach can be used as a more efficient way of doing statistical analysis.

4.3 Non-Askey-Wiener Polynomials

The theoretical basis for the decoupling approach presented in the previous chapter motivates considering other types of orthogonal polynomials in the course of SG-based decoupled approach. Indeed, the basic theorem in this section provides the necessary tools to explore systems of orthogonal polynomials other than the Askey-Wiener type polynomials commonly used in the area of generalized polynomial chaos.

It should be emphasized that by adopting a non-Askey-Wiener type of polynomials in the course of decoupled gPC, one would be merely seeking to construct a polynomial-based model for the circuit performance in terms of the uncertain design parameters. This should be contrasted with classical gPC based on the Askey-Wiener type of polynomials where the computed polynomial coefficients are sufficient to characterize the statistical moments (e.g., mean and s-

tandard deviation) of the circuit performance. Nevertheless, it should be stressed that having a polynomial-based model (even one based on non-Askey-Wiener type of polynomials) still serves as a valuable and effective vehicle to carry out full statistical characterization of the circuit response, where this is typically done by running a full MC-based evaluation on the polynomial-based models. The pdf often provides a more comprehensive picture of the variability of a certain RV or a function of RV; more than the mean or the variance.

A case is point here is two RVs both having zero mean and unity variance, yet with too different pdf, as shown in Fig 4.1. This figure depicts the pdf of those two variables, namely,

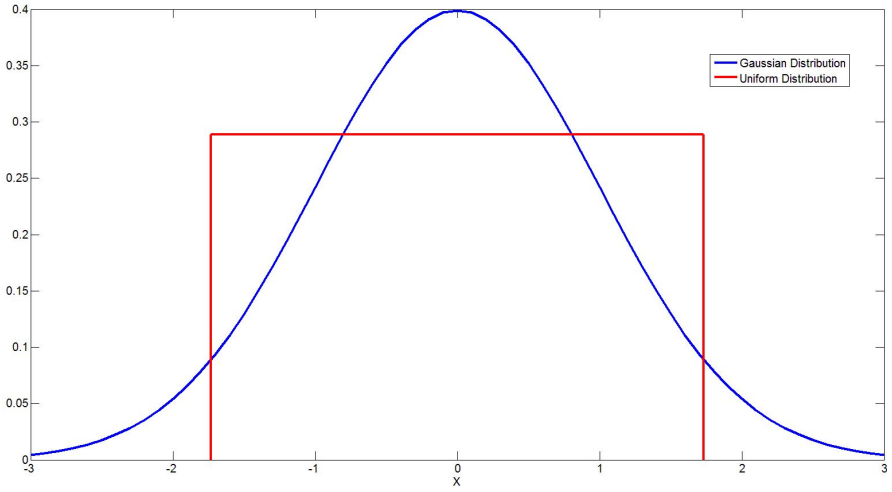

Figure 4.1: Gaussian and Uniform distributions with same mean and variance

the uniform distribution $U(-\sqrt{3}, \sqrt{3})$ and the Gaussian distribution $N(0, 1)$. As can be seen from the figure, much can be gleaned from the pdf than the simple knowledge if the mean and variance.

Nevertheless, there are situations where the mean and variance suffice to characterize the variability, such as the case where the circuit designer is interested in getting the variance of the

time-domain response as a function of time. For such situation, instead of running a full MC on the generated polynomials to generate the pdf, one can also obtain the statistical moments (e.g. mean and variance) from the coefficients of a Non-Askey-Wiener polynomials. This is typically done by converting the coefficients of a Non-Askey-Wiener polynomials to one of the Askey-Wiener types through a conversion matrix $\boldsymbol{L}$. Appendix A shows how to construct this matrix.

Another key factor that motivates exploring the notion of non-Askey-Wiener polynomials in the context of decoupled gPC is that the decoupling approach proposed in the previous section offers a quantifiable measure of the error that arises from the decoupling process. This aspect of the proposed approach, which will be presented in the next section, enables examining the behavior of the different systems of polynomials in the decoupling approach in terms of their accuracy of the approximation.

The idea of using a non-Askey-Wiener stems from the observation that the core of the decoupling approach relies on the eigenvalues and eigenvectors of the tridiagonal matrix $\boldsymbol{T}_i$. As shown in the appendix, this matrix results from the so-called three term recurrence relation which is satisfied by any system of orthogonal polynomials. Indeed, as the proof presented in the appendix demonstrates, the main difference between the various systems lies in the coefficients $c_{i,k}, d_{i,k}$ and $e_{i,k}$, $k = 0, \cdots, M_i$.

For example, when using the system of Chebyshev polynomials in the proposed decoupling

approach, then the matrix $\boldsymbol{T}_i$ takes the following form,

$$\boldsymbol{T}_i = \begin{bmatrix} 0 & \frac{1}{2} & & & & \\ 1 & 0 & \frac{1}{2} & & & \\ & \frac{1}{2} & 0 & \ddots & & \\ & & \frac{1}{2} & \ddots & \frac{1}{2} & \\ & & & \ddots & 0 & \frac{1}{2} \\ & & & & \frac{1}{2} & 0 \end{bmatrix} \tag{4.60}$$

The next section investigates the impact of the polynomial system on the decoupling error.

4.4 Study of the Decoupling Error

Characterizing the error arising from the proposed decoupling procedure can be carried out by considering the matrix $\boldsymbol{E} = \bar{\boldsymbol{Y}}(s) - \tilde{\boldsymbol{Y}}(s)$, which represents the deviation of the decoupled matrix from the original non-decoupled matrix. Taking the norm of $\boldsymbol{E}$, $\|\boldsymbol{E}\|$, as a measure for this deviation, it then follows (using properties of the Kronecker product $\|\boldsymbol{A}\otimes\boldsymbol{B}\| = \|\boldsymbol{A}\|\cdot\|\boldsymbol{B}\|$) that,

$$\|\boldsymbol{E}\| \leq \sum_{\boldsymbol{\beta}} \prod_{i=1}^{d} \|\boldsymbol{\Delta}_{i,\beta_i}\| \cdot \|\hat{\boldsymbol{Y}}(s)\|$$

The above expression shows that the deviation matrix $\boldsymbol{E}$ is influenced by $\boldsymbol{\Delta}_{i,\beta_i}$, which is problem independent, and only depends on the system of polynomials adopted in the approach. More precisely, $\boldsymbol{\Delta}_{i,\beta_i}$ depends on the constants c_{i,β_i}, d_{i,β_i} and e_{i,β_i} for $i = 0, \cdots, M$ which characterize the system of orthogonal polynomials. In addition, those coefficients also depend on the truncation index M and the i^{th} mutli-index component β_i

To further illustrate this point, Table 4.1 compares the ratio of $\|\boldsymbol{\Delta}_{i,\beta_i}\|/\|\boldsymbol{K}_{i,\beta_i}\|$ for several systems of polynomials, and for different values of β_i and M. Where α here is an index for Laguerre polynomials.

As can be seen in the table, the Chebyshev polynomials appear to produce deviation matrices with smaller norms. This fact suggests that Chebyshev polynomials can provide better approximation in the decoupling approach. In fact, this observation will also be highlighted in the numerical simulation of the next section. Moreover, it also needs to be stressed here that the decoupling error matrix $\boldsymbol{\Delta}_1 \equiv 0$, which can be easily obtained from the (**??**). This means if the system has a linear relationship with the random parameter, such as a random value capacitor or inductor, the decoupling approach will provide the exact results as there is no decoupling error anymore.

Table 4.1: ratio between the Frobenius norm of $\boldsymbol{\Delta}_\beta$ and $\boldsymbol{K}_\beta$ for the case of single random variable problem (d=1), $\beta = 2, 3, 4$ and $M = 2, 3, 4$ for different gPC basis

	Hermite	Legendre	Laguerre ($\alpha = 1$)	Chebyshev
$\beta = 2\ M = 2$	0.4704	0.2340	0.1689	0.2132
$\beta = 2\ M = 3$	0.3563	0.1972	0.1438	0.1890
$\beta = 2\ M = 4$	0.2665	0.1756	0.1271	0.1715
$\beta = 3\ M = 2$	0.4767	0.2176	0.3574	0.1612
$\beta = 3\ M = 3$	0.3913	0.1620	0.3023	0.1414
$\beta = 3\ M = 4$	0.3231	0.1402	0.2657	0.1291
$\beta = 4\ M = 2$	0.7776	0.3792	0.5387	0.2881
$\beta = 4\ M = 3$	0.6205	0.2714	0.4593	0.2327
$\beta = 4\ M = 4$	0.4854	0.2298	0.4047	0.2117
$\beta = 5\ M = 2$	0.7871	0.3978	0.6927	0.2847
$\beta = 5\ M = 3$	0.6745	0.2706	0.6023	0.2080
$\beta = 5\ M = 4$	0.5670	0.2142	0.5357	0.1843

Chapter 5

Numerical Examples

In this chapter, numerical examples are provided to validate the proposed decoupling approach. In all of the three examples presented in this section, the polynomial coefficients obtained through the proposed approach are used to construct a polynomial-based model in the uncertain circuit design parameters. Subsequently, MC-based evaluations of the polynomial-model using 30,000 values of the design parameters randomly selected in the random design space is carried out to generate the Probability Density Function (pdf) of the circuit output. The pdf obtained in this manner is also compared in each of the examples against the traditional MC simulations of the original circuit and with the same number of simulation points.

In presenting the following simulations, the results obtained from the traditional MC are referred to simply as "Monte-Carlo", while those computed based the gPC are referred to by the type of polynomials (e.g., Hermite) used in the gPC technique for single random problems and gPC basis for multi-random problems. In addition, we adopted a truncation order of 3 for all the example. And all the MC simulation adopt a 30000 realization except for those mentioned in the

figures.

5.1 Examples for Decoupling approach

5.1.1 Example 1

This example provides mainly a proof of concept for the proposed approach and serves as a vehicle to compare the performance of the different polynomials systems used under the decoupling framework.

The circuit used in this example is the RLC circuit shown in Fig. 5.1, where the source is sinusoidal with frequency 159.16MHz and 1V amplitude. The objective in this example is to perform the statistical characterization of the voltage at the "output node" shown on the circuit.

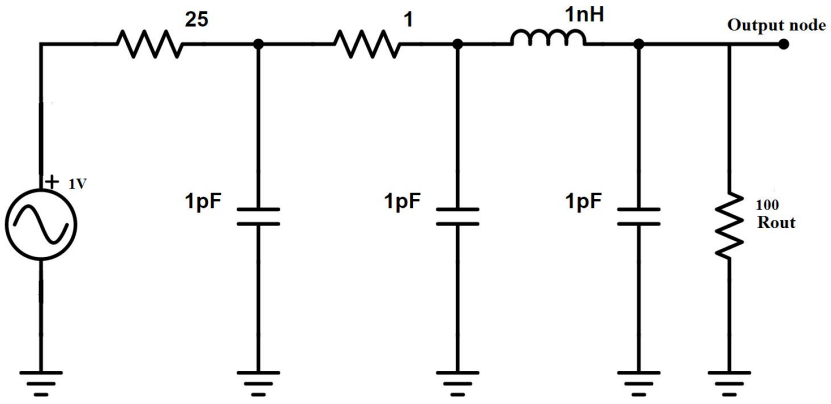

Figure 5.1: Schematic of RLC circuit used in Example 1.

The design uncertainty in this circuit has been introduced by allowing that R_{out} in the circuit be modeled by a random variable ξ. Three sets of experiments were conducted by assuming that

ξ is an RV with three possible pdfs, namely the Gaussian (ξ ~$N(0,1)$), Uniform (ξ ~$U(-1,1)$) and the Gamma (ξ ~$\Gamma(\alpha+1,1), \alpha=1$) distributions, respectively. More specifically, R_{out} in the three experiments will be respectively, given by,

$$\begin{aligned}
\text{experiment 1:} \quad R_{\text{out}} &= 100 \times (1 + 0.15\xi)\,\Omega \\
\text{experiment 2:} \quad R_{\text{out}} &= 100 \times (1 + 0.5\xi)\,\Omega \\
\text{experiment 3:} \quad R_{\text{out}} &= 100 \times (1 + 0.15\xi)\,\Omega
\end{aligned}$$

Figs. 5.2 through 5.4 show the pdf obtained in each of the three experiments using the traditional MC and compare them against those obtained from the proposed decoupled gPC approach through utilizing the so-called conventional polynomials, namely, Hermite, Legendre and Laguerre polynomials, respectively. Figs. 5.2-5.4 also contrasts the accuracy of a decoupled gPC using the conventional type of polynomials against the one based on the Chebyshev-based polynomials. Worthy of note here is the fact that the decoupled-based Chebyshev polynomials outperform the Legendre and Hermite polynomials in terms of the accuracy when compared to the traditional MC. This observation is in line with the error characterization discussed in Section 4.4.

5.1.2 Example 2

This example considers the statistical analysis of an active low-pass filter is shown in Fig.5.5, where the OpAmp equivalent circuit model is shown in Fig. 5.6. The design uncertainty in this circuit was introduced by creating a $d = 3$ random space with RVs (ξ_1, ξ_2, ξ_3) and letting the

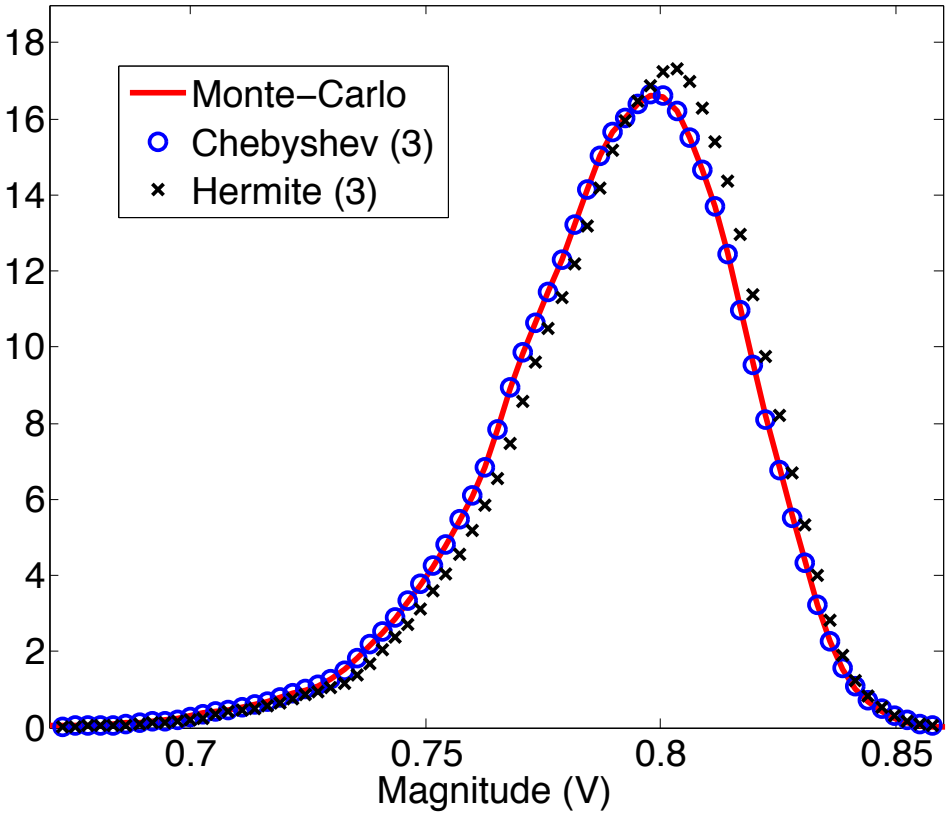

Figure 5.2: pdf Comparison between Hermite and Chebyshev expansion for Gaussian distribution.

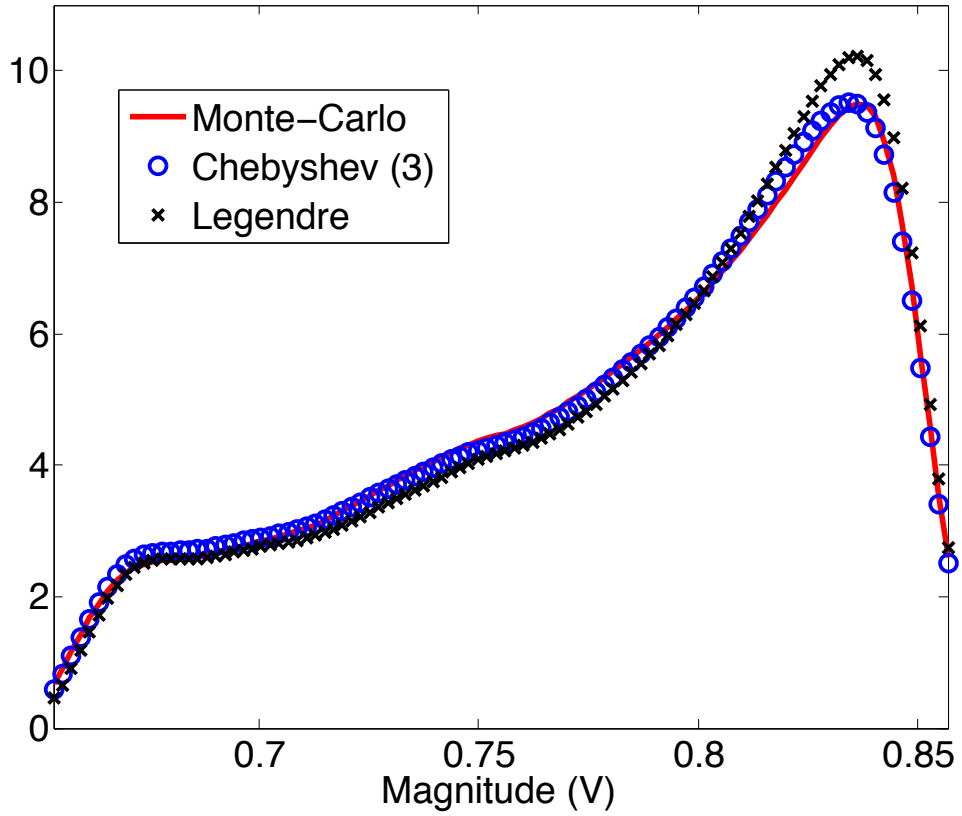

Figure 5.3: pdf Comparison between Legendre and Chebyshev expansion for Uniform distribution.

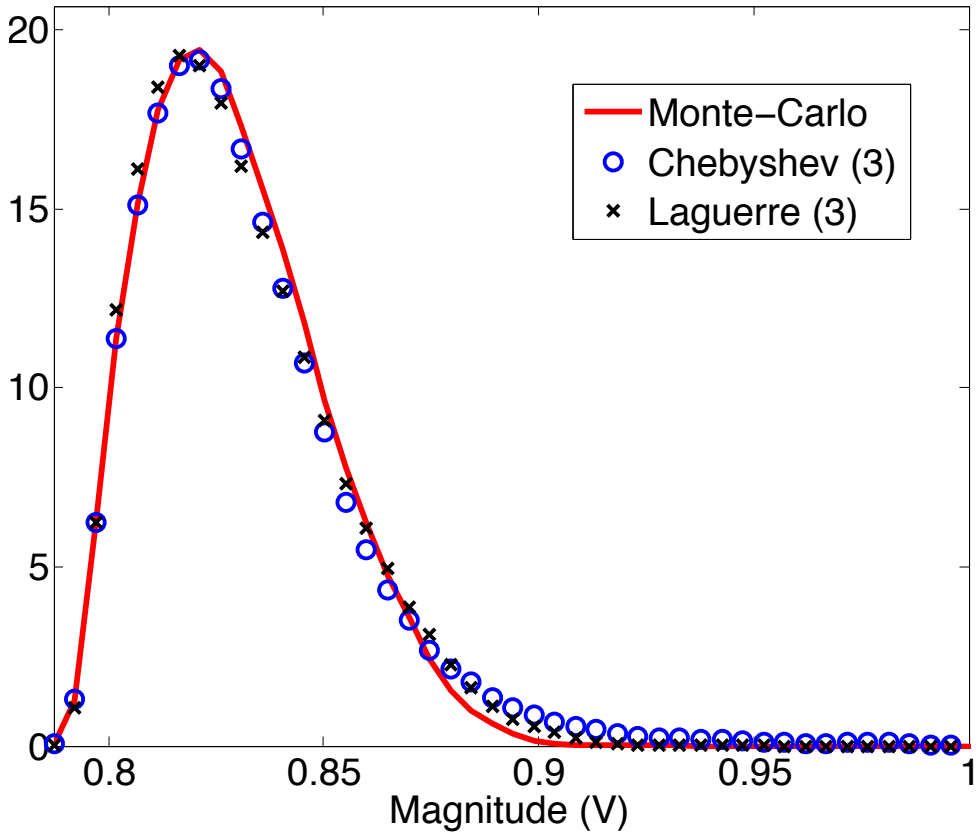

Figure 5.4: pdf Comparison between Laguerre and Chebyshev expansion for Uniform distribution.

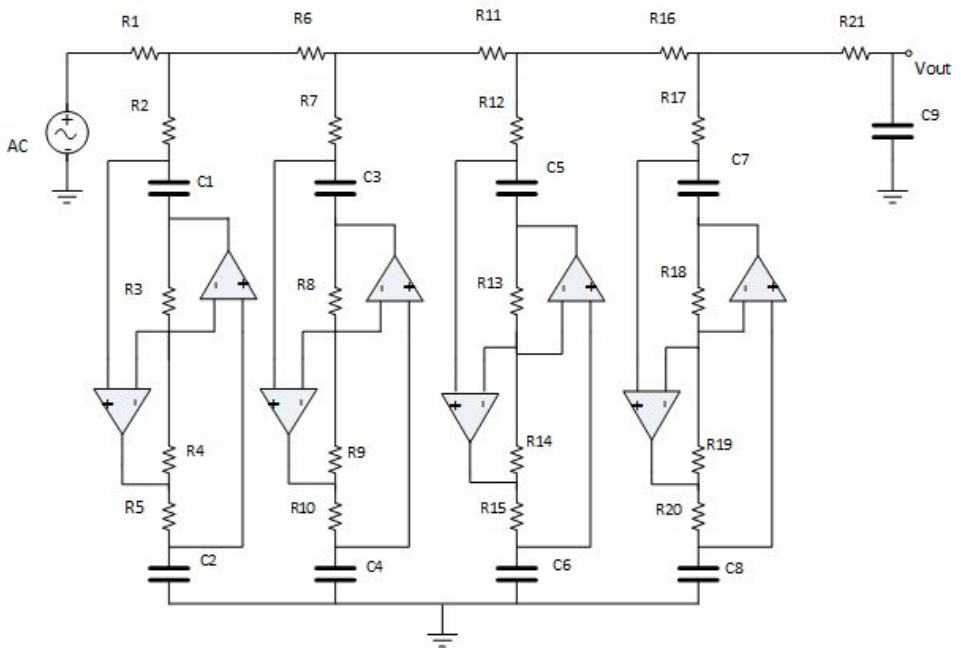

$R1 = 5.4779k\Omega \quad R2 = 2.0076k\Omega \quad R3 = R4 = R8 = R9 = R13 = R14 = R18 = R19 = 3.3k\Omega \quad R5 = 4.5898k\Omega$
$R6 = 4.44k\Omega \quad R7 = 5.9999k\Omega \quad R10 = 4.2573k\Omega \quad R11 = 3.2201k\Omega \quad R12 = 5.88327k\Omega \quad R15 = 5.62599k\Omega$
$R16 = 3.63687k\Omega \quad R17 = 1.0301k\Omega \quad R20 = 2.808498k\Omega \quad R21 = 1.2201k\Omega \quad C1 = 12nF \quad C3 = 6.8nF$
$C5 = 4.7nF \quad C7 = 6.8nF \quad C2 = C4 = C6 = C8 = C9 = 10nF$

Figure 5.5: Schematic of low-pass filter for example 2.

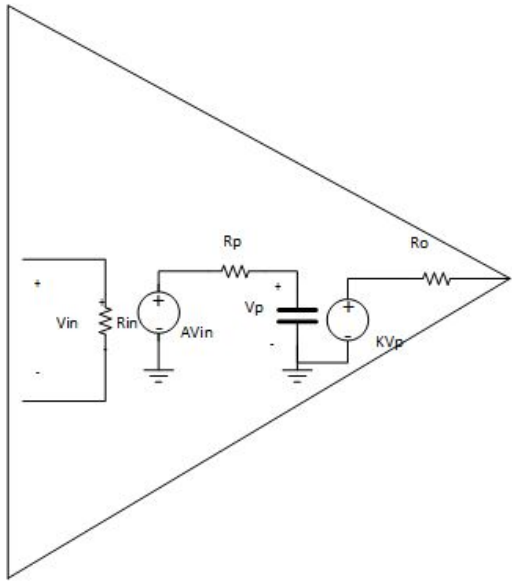

$R_{in} = 10M\Omega \quad R_P = 1k\Omega \quad C_P = 1.59\mu F \quad A = 100000 \quad R_O = 75\Omega \quad K = 1$

Figure 5.6: OpAmp subsircuit model.

circuit parameters R1, R21 and C9 be given in terms of those parameters as follow

$$\begin{aligned} R1 &= \bar{R}1(1 + 0.5 \times \xi_1) \\ R21 &= \bar{R}21(1 + 0.15 \times \xi_2) \\ C9 &= \bar{C}9(1 + 0.15 \times \xi_3) \end{aligned}$$

where $\bar{R}1$, $\bar{R}21$ and $\bar{C}9$ are the nominal design values given in Fig.5.5. In this example the RVs ξ_1, ξ_2 and ξ_3 are assumed to be distributed as Uniform, Normal, and Gamma distributions, respectively.

Fig.5.7 presents the pdf of the output voltage at node V_{out} at a frequency of 1600 MHz obtained from three different approaches, as follows,

- traditional MC with 30,000 simulations,
- the proposed gPC decoupling technique using the a hybrid polynomial expansion from the Legendre (in ξ_1), Hermite (in ξ_2) and Laguerre (in ξ_3), and
- the proposed gPC decoupling technique using Chebyshev polynomial in ξ_1, ξ_2 and ξ_3.

In the latter two approaches, the gPC polynomials ware implemented with degree 3 polynomials in all of ξ_1, ξ_2 and ξ_3.

To generate time-domain simulation for this example, the circuit was simulated with sinusoidal voltage source at the input, and the time-domain voltage response at the output node was then considered for statistical analysis. Fig. 5.8 shows distribution of the time-domain response indicating the mean value. Fig. 5.9 presents the variance in the time-domain response.

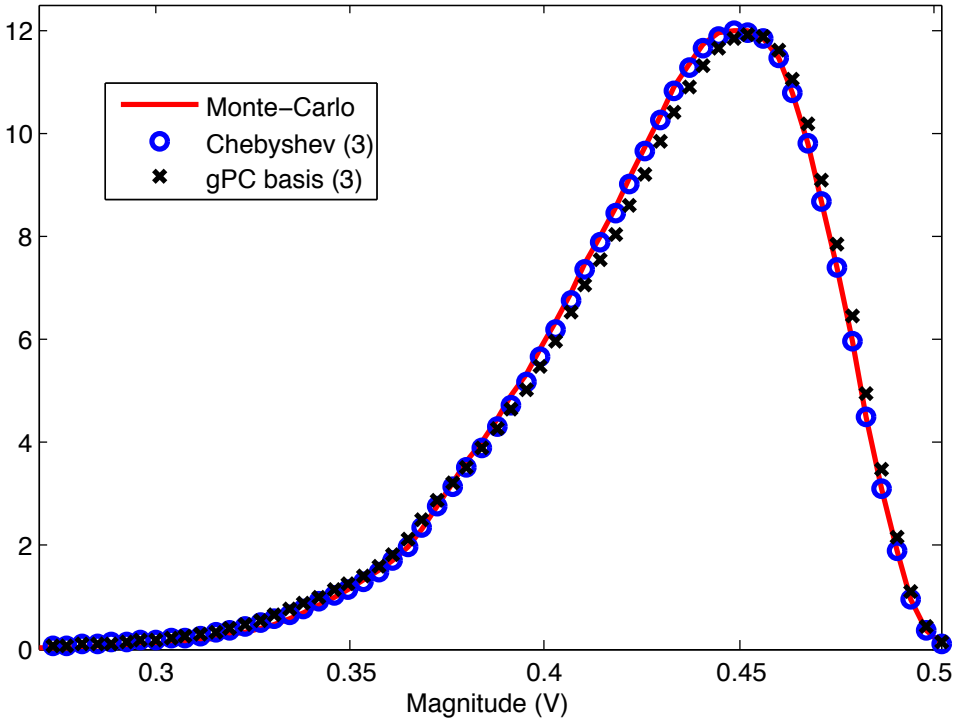

Figure 5.7: pdf Comparison between multi-dimensional Chebyshev expansion and gPC basis expansion.

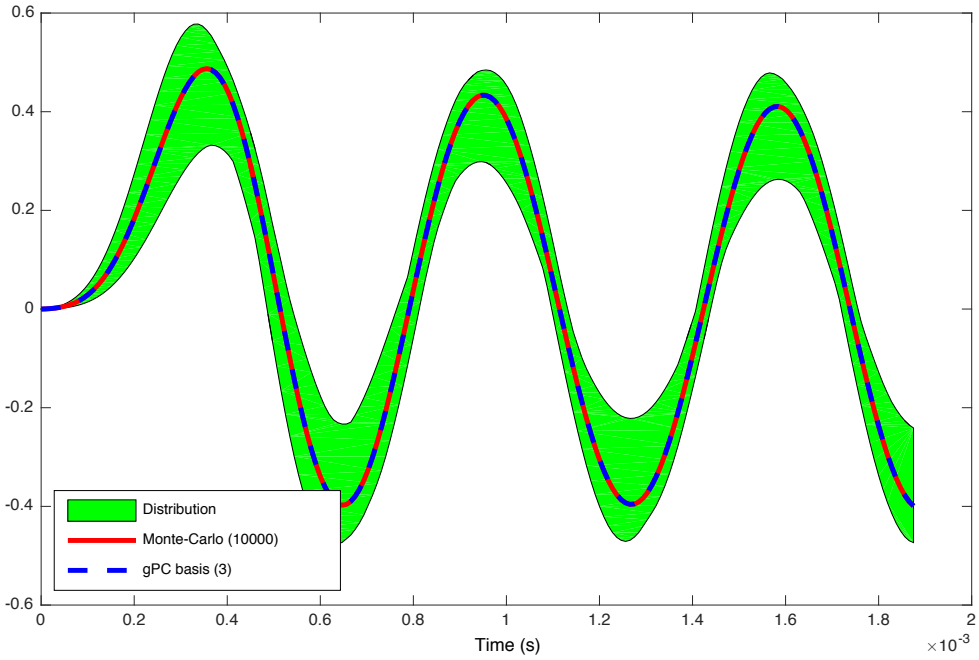

Figure 5.8: Distribution and the mean value of the output voltage.

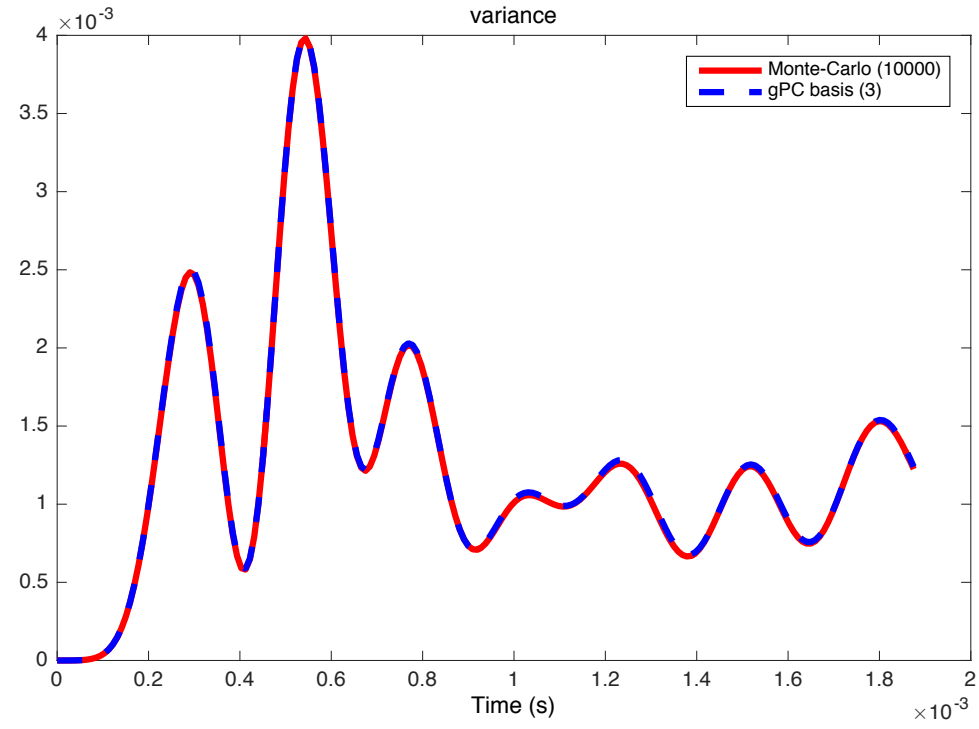

Figure 5.9: Variance of the output voltage.

5.1.3 Example 3

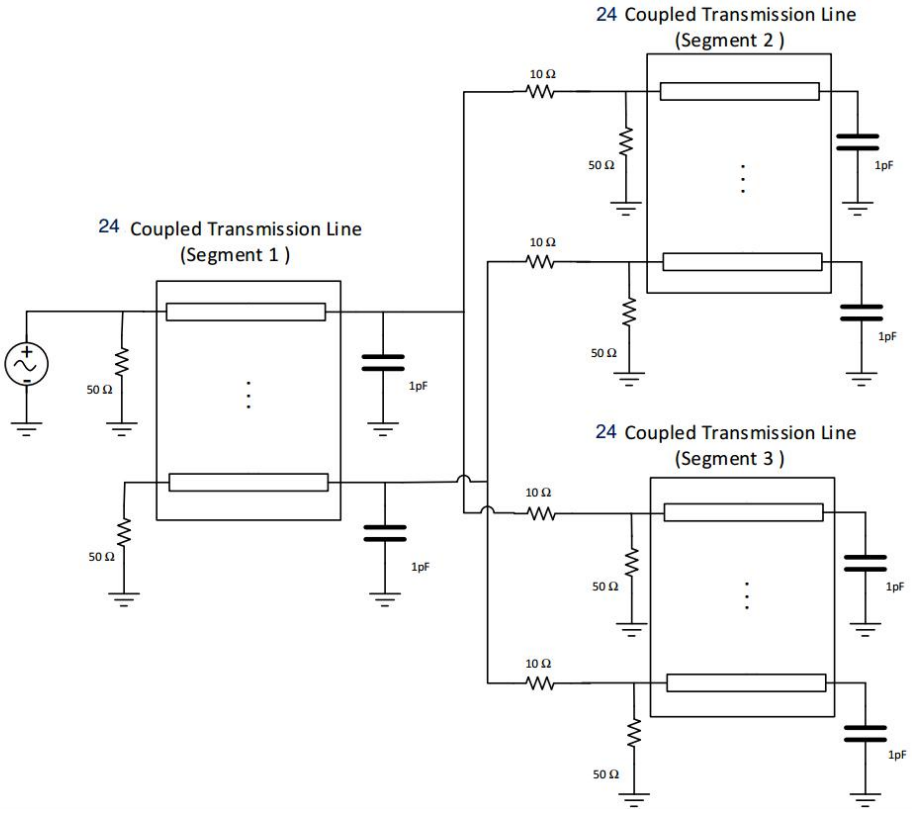

Figure 5.10: Schematic of low-pass filter for example 3.

This example was carried out using the circuit shown in Fig. 5.10. The circuit consists of 3 segments of coupled Multi-conductor Transmission Lines (MTLs) with 24 conductors. Input sources were attached to conductors 1, 7, 13, 19 of the first segment. Design uncertainty in this circuit was introduced by modeling five discrete components connecting the MTLs networks using five independent random variables. Four of the RVs are attached to the resistor in parallel with the sources and have been assumed to be uniformly distributed with values given by $50 \times (1 + 0.3\xi_i)\Omega$, $i = 1, \cdots, 4$. The fifth RV is given by a Gaussian distribution and is attached to the capacitor connected to the output node, at the far end of conductor 3 of the segment 2, and modeled by $1 \times (1 + 0.15 \times \xi_5)pF$. The pdf is shown in Figs.5.11, 5.12 and 5.13 are for

the output responses at 4GHz, 6GHz and 8GHz, respectively. Similar to the previous example,

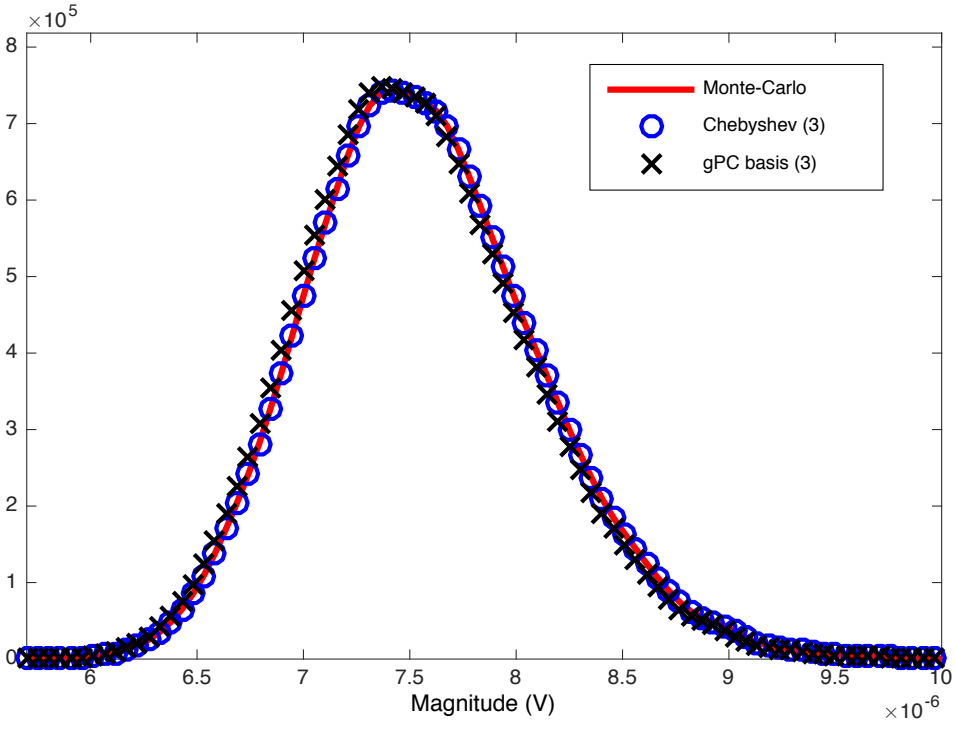

Figure 5.11: pdf Comparison between multi-dimensional Chebyshev expansion and gPC basis expansion at 4 GHz.

the pdf has been obtained through the same three different approaches which are compared in Fig. 5.11-5.13. One also needs to highlight in this figure that the Chebyshev-based decoupling fares better than the ones based on the more conventional polynomials, which in this case are the Legendre and Hermite polynomials. Also, a frequency sweep from DC to 10 GHz is shown in Fig. 5.14 and Fig. 5.15.

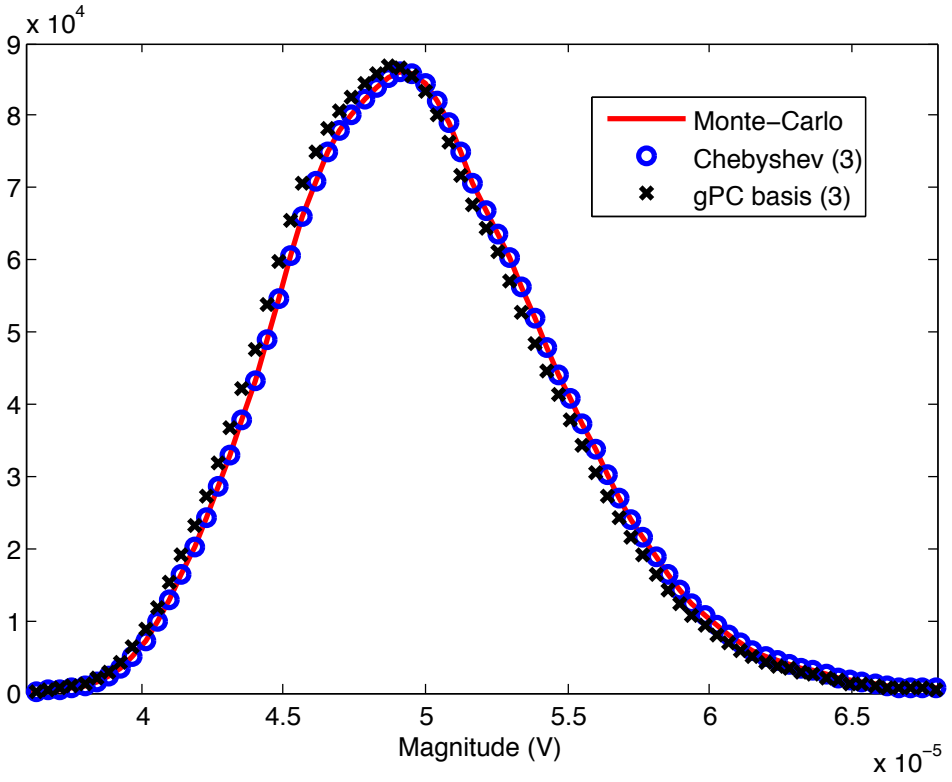

Figure 5.12: pdf Comparison between multi-dimensional Chebyshev expansion and gPC basis expansion at 6 GHz.

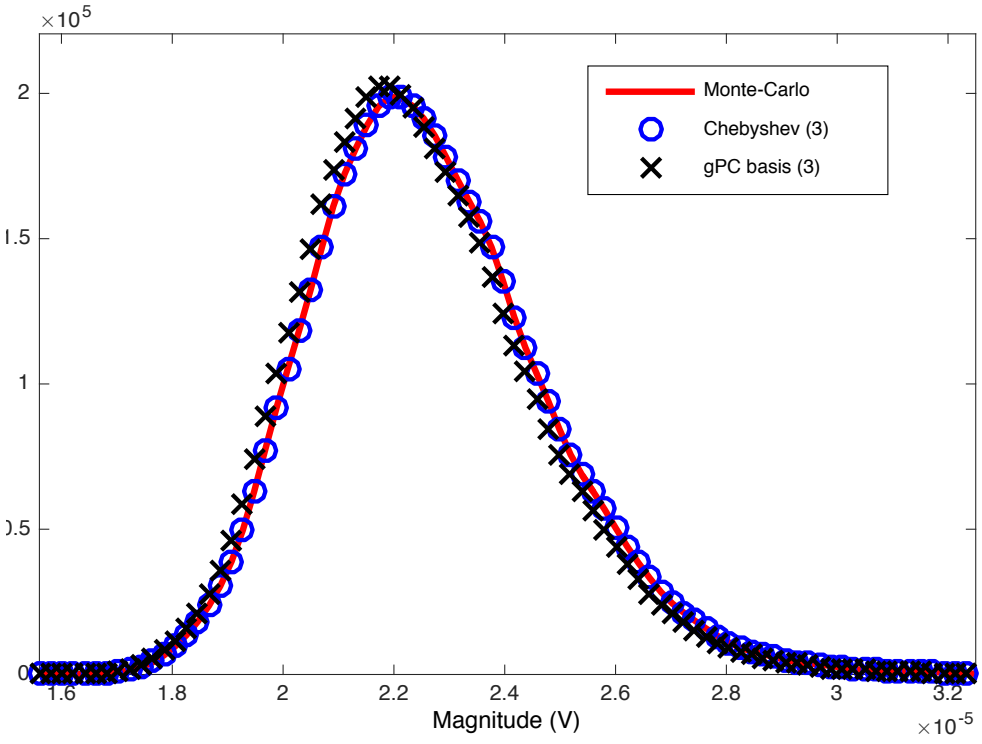

Figure 5.13: pdf Comparison between multi-dimensional Chebyshev expansion and gPC basis expansion at 8 GHz.

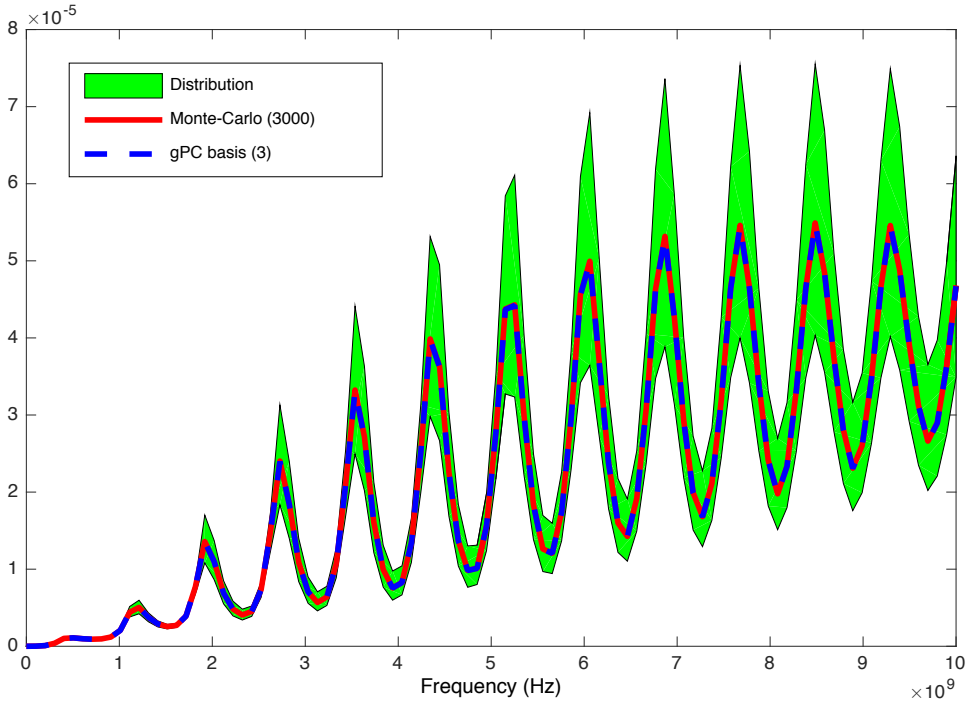

Figure 5.14: Distribution and mean value of the output voltage.

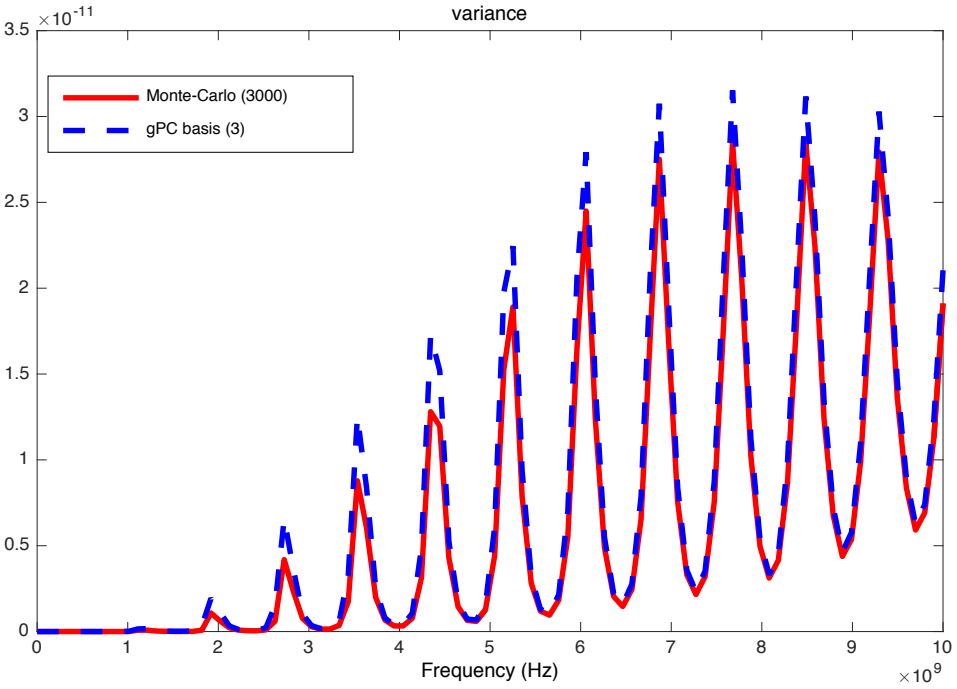

Figure 5.15: Variance of the output voltage.

5.2 CPU Time Comparison

This section provides the theoretical computational cost and CPU time comparison for all three examples. The CPU time was measured using MATLAB R2013a. In the case of circuit simulation, the most time consuming part during the simulation should be the LU decomposition as the computational cost is proportional to the cubic of the matrix size, which will dominate if the system is large enough. From chapters 4, it shows that the computational cost of decoupling gPC is directly related with the number of expansion coefficients, which related to the truncation order and number of random parameters. If we use K to represent the number of simulations needed for a Monte Carlo simulation, the computational cost can be summarized in Table 5.1. where Noc means the number of coefficients. Due to the slow convergence rate of MC, a few

Table 5.1: Computational complexity comparison of three methods

	matrix multiply with vector $\propto O(N^2)$	LU decomposition $\propto O(N^3)$	Forward/Backward substitution $\propto O(N^2)$
Monte Carlo	0	K	2K
Decoupled gPC	Noc^2	Noc	$2Noc$

thousands of simulation are normally required for an accurate result, which means the decoupled gPC is more efficient than MC methods if the expansion coefficients are less than K. Especially when N is large, as the time cost in LU decomposition will become more dominate than other types of calculation. Table 5.2 shows the basic information as well as CPU time for all three examples in this thesis, all the MC simulations adopt 30000 as the times of realization. From

Table 5.1, notice that with the increasing of the problem size, the speed up is more and more close to the ratio of $\frac{K}{Noc}$ because the time cost for LU decomposition will increasingly dominate, the results of example 3 in Table 5.2 satisfy the theoretical prediction quite well as the ratio is $\frac{30000}{1024} = 29.29$, which is quite close to the real measured result.

Table 5.2: CPU time comparison

Example	Problem Size			CPU (seconds)		Speed-up
	N	d	Noc	MC	Decoupled gPC	
Example 1	8	1	4	88.16	0.0281	3137
Example 2	67	3	64	202.05	0.3384	597
Example 3	4490	5	1024	28820	1050.3	27.4

Chapter 6

Conclusion and Future Work

6.1 Conclusion

This paper presented a generalization of the decoupled gPC approach to the problem of statistical analysis of high-speed interconnects. While previous decoupling approach has been limited to GP-PC with only Hermite polynomials. The mathematical derivation in this paper shown the decoupling method in a general way for all type of orthogonal polynomials with the analysis of error mechanism. The study of decoupling error not only help us understand the approach better, but also provide us a tool of considering non-Askey-Wiener polynomials with less decoupling error.

Numerical examples have been presented to validate the proposed technique by comparing the result from MC simulation with the decoupled approach and moment equations methods. And the CPU time comparison at the end provides us how efficiency this two approach is when compare with traditional Monte Carlo methods.

6.2 Future Work

Several possible future work based on the results of this thesis are including but not limited to:

- Improvements of the decoupling approach: The decoupled gPC achieve a better efficiency than traditional gPC by managing to decouple the augmented matrix into block diagonally form. However, there may still some potential ways for a faster simulation based on decoupled gPC. The improvements of the decoupling approach could be achieved by reducing the number of diagonal blocks that needs to be factorized after the decoupling of the augmented matrix. Which may be carried out by either adopting a better truncation scheme or by finding and excluding the blocks which only make little contribution to the results. For example, considering the case in 4.2.2, the response of the circuit, i.e. $\tilde{\boldsymbol{X}}(s) = [\tilde{\boldsymbol{X}}_0(s), \tilde{\boldsymbol{X}}_1(s), \cdots, \tilde{\boldsymbol{X}}_M(s)]^T$ can be calculate through,

$$\begin{bmatrix} \tilde{\boldsymbol{X}}_0(s) \\ \tilde{\boldsymbol{X}}_1(s) \\ \vdots \\ \tilde{\boldsymbol{X}}_M(s) \end{bmatrix} = (\boldsymbol{V}^{-1} \otimes \boldsymbol{I}_N) \begin{bmatrix} \boldsymbol{Y}^{-1}(\lambda_0, s) & & & \\ & \boldsymbol{Y}^{-1}(\lambda_1, s) & & \\ & & \ddots & \\ & & & \boldsymbol{Y}^{-1}(\lambda_M, s) \end{bmatrix} (\boldsymbol{V} \otimes \boldsymbol{I}_N) \begin{bmatrix} \boldsymbol{U}(s) \\ 0 \\ \vdots \\ 0 \end{bmatrix} \tag{6.1}$$

  One can obtain the expression for a given block in $\tilde{\boldsymbol{X}}(s)$, i.e. $\tilde{\boldsymbol{X}}_i(s)$, with the expression,

$$\tilde{\boldsymbol{X}}_i(s) = \sum_{j=0}^{M} [\boldsymbol{V}]_{i+1,j+1} [\boldsymbol{V}^{-1}]_{j+1,1} \boldsymbol{Y}^{-1}(\lambda_{j+1}, s) \boldsymbol{U}(s) \tag{6.2}$$

  In above equation, the inversion of matrix $\boldsymbol{Y}(\lambda_{j+1}, s)$ can be excluded if $[\boldsymbol{V}^{-1}]_{j+1,1}$ is small enough, which could further reduce the computational cost of the decoupling approach.

- Sensitivity analysis: In the example part of this thesis, all the truncation scheme we adopt is

the tensor order truncation scheme with the order of 3 for each random variables. However, the uncertainty for different circuit components has a different effect on the circuit response even with the same statistical property. So sensitivity analysis will allow us to obtain the best simulation results with a minimum CPU time cost by adjusting the truncation order due to the effect of corresponding components to the results.

- Applying the generalized decoupled approach to other problems: In this thesis, we use the circuit as an example to demonstrate the idea of this approach. However, there are not evidence limits this approach to other types of statistical problems. For example, the polynomial chaos also applied to handle the problem of variability due to uncertainty in physical parameters of Carbon Nanotube interconnects [38].

APPENDICES

Appendix A

Coefficients Conversion

The conversion of expansion coefficients of non-Askey-Wiener polynomials to the corresponding gPC polynomials basis can be achieved by using a converting matrix $\boldsymbol{L}$. The function of this converting matrix is by multiplying $\boldsymbol{L}$ with corresponding expansion coefficients of a certain type of orthogonal polynomials will yield the Taylor series coefficients. For example, assume an arbitrary continues function $g(\xi)$, its Hermite and Taylor series expansion coefficients with respect to ξ are $\boldsymbol{g}_H^\xi = [\hat{g}_{H,0}^\xi, \hat{g}_{H,1}^\xi, \cdots, \hat{g}_{H,M}^\xi]$ and $\boldsymbol{g}_T^\xi = [\hat{g}_{T,0}^\xi, \hat{g}_{T,1}^\xi, \cdots, \hat{g}_{T,M}^\xi]$ respectively, we will have the following relationship:

$$\boldsymbol{L}_H^\xi \boldsymbol{g}_H^\xi = \boldsymbol{g}_T^\xi \tag{A.1}$$

where the subscript H and T are used to distinguish for which expansion base, i.e. Hermite polynomial and Taylor series, the convert matrix and/or coefficients are, and the superscript indicates which parameters the convert matrix and/or coefficients are respected to. In order to achieve $\boldsymbol{L}$ such function, its entries must satisfy:

$$[\boldsymbol{L}]_{i+1,j+1} = \hat{\phi}_{j,i} \tag{A.2}$$

where $\hat{\phi}_{j,i}$ is the Taylor expansion coefficients for i_{th} moment of polynomial of order j, more specific

$$\phi_j(\xi) = \sum_i \hat{\phi}_{j,i}\xi^i \tag{A.3}$$

The relation in (A.2) can be verified easily by exam the principle of multiplication between a matrix and a vector. As the coefficient $\hat{\phi}_{j,i}$ can be obtained by using the three term recurrence relation, so this convert matrix can be generated easily with the computer program. The Pseudo-code for obtaining matrix $\boldsymbol{L}$ with maximum order of M are as follows:

- $\boldsymbol{L}$=zeros(M+1,M+1).

  Generate a matrix $\boldsymbol{L}$ of size $M+1$ by $M+1$, with all its entries equals to 0.

- $[\boldsymbol{L}]_{1,1} = 1$

  $\phi_0(\xi) = 1 \Longrightarrow \hat{\phi}_{0,0} = 1,\ \hat{\phi}_{0,i} = 0 (i \geq 1)$

- $[\boldsymbol{L}]_{1,2} = -g_0$ and $[\boldsymbol{L}]_{2,2} = a_0$

  $\phi_1(\xi) = a_0\xi - g_0 \Longrightarrow \hat{\phi}_{1,0} = -g_0,\ \hat{\phi}_{1,1} = a_0,\ \hat{\phi}_{1,i} = 0 (i \geq 2)$

- for i=2:M

- $[\boldsymbol{L}]_{(:,i+1)} = a_i[\boldsymbol{L}]_{(:,i)}$

  Copy all the values in i^{th} column to the $i+1^{th}$ column after multiply with a_i, which is equivalent to $\phi_{n+1}(\xi) = a_n\phi_n(\xi)$

- Shift all the entries in $i+1^{th}$ column one unit down.

  Equivalent to $\phi_{n+1}(\xi) = a_n\xi\phi_n(\xi)$

- $[\boldsymbol{L}]_{(:,i+1)} = [\boldsymbol{L}]_{(:,i+1)} - g_i[\boldsymbol{L}]_{(:,i)}$

  Multiply i^{th} column with $-g_i$ and add it to $i+1^{th}$ column, which is equivalent to $\phi_{n+1}(\xi) = a_n\xi\phi_n(\xi) - g_n\phi_n(\xi)$

- $[\boldsymbol{L}]_{(:,i+1)} = [\boldsymbol{L}]_{(:,i+1)} - b_i[\boldsymbol{L}]_{(:,i-1)}$

  Multiply $i-1^{th}$ column with $-b_i$ and add it to $i+1^{th}$ column , which is equivalent to $\phi_{n+1}(\xi) = a_n\xi\phi_n(\xi) - g_n\phi_n(\xi) - b_n\phi_{n-1}(\xi)$

For better illustrating, consider an example of a Hermite expansion with the expansion coefficients $\boldsymbol{X}_H^{\xi} = [1, 2, 0, 1]^T$. The Taylor coefficients can be obtained by substitute the coefficients back to the polynomials

$$1H_0(\xi) + 2H_1(\xi) + 0H_2(\xi) + 1H_3(\xi) = 1 + 2\xi + 1(\xi^3 - 3\xi) = \xi^3 - \xi + 1$$

which provide us the Taylor coefficients of $\boldsymbol{X}_T^{\xi} = [1, 0, -1, 1]^T$. On the other hand, the three term recurrence relationship of Hermite polynomial is given by:

$$\begin{aligned} H_0(\xi) &= 1 \\ H_1(\xi) &= \xi \\ H_{n+1}(\xi) &= \xi H_n(\xi) - nH_{n-1}(\xi) \quad (n \geq 1) \end{aligned}$$

Thus the convert matrix has the form of:

$$\boldsymbol{L}_H^{\xi} = \begin{bmatrix} 1 & 0 & -1 & 0 \\ 0 & 1 & 0 & -3 \\ 0 & 0 & 1 & 0 \\ 0 & 0 & 0 & 1 \end{bmatrix} \tag{A.4}$$

The Taylor expansion coefficients $\boldsymbol{X}_T^{\xi}$ can be obtained by using the converting matrix:

$$\boldsymbol{X}_T^{\xi} = \boldsymbol{L}_H^{\xi}\boldsymbol{X}_H^{\xi} = \begin{bmatrix} 1 & 0 & -1 & 0 \\ 0 & 1 & 0 & -3 \\ 0 & 0 & 1 & 0 \\ 0 & 0 & 0 & 1 \end{bmatrix} \times \begin{bmatrix} 1 \\ 2 \\ 0 \\ 1 \end{bmatrix} = \begin{bmatrix} 1 \\ -1 \\ 0 \\ 1 \end{bmatrix}$$

which has the exact same result.

The above relationship provides an easy way to convert the expansion coefficient from non-Askey-Wiener polynomials , i.e. Chebyshev expansion coefficients, to gPC basis expansion coefficients :

$$\boldsymbol{X}_{gPC} = {\boldsymbol{L}_{gPC}^{\boldsymbol{\xi}}}^{-1}\boldsymbol{L}_{nAW}^{\boldsymbol{\xi}}\boldsymbol{X}_{nAW}^{\boldsymbol{\xi}} \tag{A.5}$$

where $\boldsymbol{X}_{gPC}$ represent the gPC basis expansion coefficients and $\boldsymbol{X}_{nAW}^{\boldsymbol{\xi}}$ represent the expansion coefficients of non-Askey-Wiener polynomials. Moreover, notice that the convert matrix $\boldsymbol{L}$ always has an upper triangular structure, which means the conversion can be down with only a backward substitution.For the general multi-random variables problem, the convert matrix can be described by the follow theorem:

Theorem 4.

$$\bar{\boldsymbol{L}} = \boldsymbol{L}^{\xi_1} \otimes \boldsymbol{L}^{\xi_2} \otimes \cdots \otimes \boldsymbol{L}^{\xi_d} \tag{A.6}$$

where $\boldsymbol{L}^{\xi_i}$ is the convert matrix correspond to i^{th} RV.

Proof. To fulfill its function, the entries in matrix $\bar{\boldsymbol{L}}$,similar to equation (A.2), must satisfy the condition:

$$[\bar{\boldsymbol{L}}]_{|\boldsymbol{\alpha}|+1,|\boldsymbol{\beta}|+1} = \hat{\phi}_{|\boldsymbol{\beta}|,|\boldsymbol{\alpha}|} \tag{A.7}$$

where $|\boldsymbol{\beta}|$ is the rank of multi-indices whose definition can be found in (2.1), $|\boldsymbol{\alpha}|$ is the rank of Taylor series which has the same way of ranking as $|\boldsymbol{\beta}|$. And $\hat{\phi}_{|\boldsymbol{\beta}|,|\boldsymbol{\alpha}|}$ is the Taylor series coefficients of the moment $\prod_{i=1}^{d}\xi_i^{\alpha_i}$ for the multi-dimensional polynomial $\phi_{\boldsymbol{\beta}}(\boldsymbol{\xi})$. Hence the proof of theorem 4 can be carried out by proof all the entries obtained by (A.6) are equivalent to (A.7).

Given two arbitrary multi-indices $\boldsymbol{\alpha} = [\alpha_1, \alpha_2, \cdots, \alpha_d]$ and $\boldsymbol{\beta} = [\beta_1, \beta_2, \cdots, \beta_d]$, the corresponding entries obtained with (A.6) is given by:

$$[\bar{\boldsymbol{L}}]_{|\boldsymbol{\alpha}|+1,|\boldsymbol{\beta}|+1} = [\boldsymbol{L}^{\xi_1} \otimes \boldsymbol{L}^{\xi_2} \otimes \cdots \otimes \boldsymbol{L}^{\xi_d}]_{|\boldsymbol{\alpha}|+1,|\boldsymbol{\beta}|+1} \tag{A.8}$$

Applying the result of (4.6) in lemma 1 to the above equation results:

$$[\bar{\boldsymbol{L}}]_{|\boldsymbol{\alpha}|+1,|\boldsymbol{\beta}|+1} = \prod_{i=1}^{d}[\boldsymbol{L}^{\xi_i}]_{\alpha_i+1,\beta_i+1} \tag{A.9}$$

Next, by substituting (A.2) into (A.9) yields:

$$[\bar{\boldsymbol{L}}]_{|\boldsymbol{\alpha}|+1,|\boldsymbol{\beta}|+1} = \prod_{i=1}^{d}[\boldsymbol{L}^{\xi_i}]_{\alpha_i+1,\beta_i+1} = \prod_{i=1}^{d}\hat{\phi}_{\beta_i,\alpha_i} \tag{A.10}$$

On the other hand, the entries for the same index $\boldsymbol{\alpha}$ and $\boldsymbol{\beta}$ obtained from (A.7) is $\hat{\phi}_{|\boldsymbol{\beta}|,|\boldsymbol{\alpha}|}$, which its closed form expression can be obtain by first recall the expression of multi-dimensional polynomial in (3.33):

$$\phi_{\boldsymbol{\beta}}(\boldsymbol{\xi}) = \prod_{i=1}^{d}\phi_{\beta_i}(\xi_i)$$

Followed by applying (A.3) on above equation, which is:

$$\phi_{\boldsymbol{\beta}}(\boldsymbol{\xi}) = \prod_{i=1}^{d}\left(\sum_{j_i}\hat{\phi}_{\beta_i,j_i}\xi_i^{j_i}\right) = \sum_{j_1}\sum_{j_2}\cdots\sum_{j_d}\prod_{i=1}^{d}\hat{\phi}_{\beta_i,j_i}\xi_i^{j_i} \tag{A.11}$$

It is obvious the Taylor series coefficients for the moment $\prod_{i=1}^{d}\xi_i^{\alpha_i}$ in the above equation is $\prod_{i=1}^{d}\hat{\phi}_{\beta_i,\alpha_i}$, which is exact the same as (A.10). This shows that the matrix $\bar{\boldsymbol{L}}$ in (A.6) satisfy the condition as a convert matrix and here finish the proof of theorem 4. □

References

[1] G. S. Fishman, *Monte Carlo: Concepts, Algorithm and Applications*. New York: Springer, 1996.

[2] D. Xiu and G. E. Karniadakis, "The Wiener–Askey polynomial chaos for stochastic differential equations," *SIAM J. Sci. Comput.*, vol. 24, no. 2, pp. 619–644, Feb. 2002.

[3] S. Vrudhula, J. Wang, and P. Ghanta, "Hermite polynomial based interconnect analysis in the presence of process variations," *Computer-Aided Design of Integrated Circuits and Systems, IEEE Transactions on*, vol. 25, no. 10, pp. 2001 –2011, Oct. 2006.

[4] I. Stievano, P. Manfredi, and F. Canavero, "Stochastic analysis of multiconductor cables and interconnects," *Electromagnetic Compatibility, IEEE Transactions on*, vol. 53, no. 2, pp. 501 –507, May 2011.

[5] D. Spina, F. Ferranti, T. Dhaene, L. Knockaert, G. Antonini, and D. Vande Ginste, "Variability analysis of multiport systems via polynomial-chaos expansion," *Microwave Theory and Techniques, IEEE Transactions on*, vol. 60, no. 8, pp. 2329 –2338, Aug. 2012.

[6] M. Rufuie, E. Gad, M. Nakhla, and R. Achar, "Generalized hermite polynomial chaos for variability analysis of macromodels embeddedin nonlinear circuits," *Components, Packag-*

ing and Manufacturing Technology, IEEE Transactions on, vol. 4, no. 4, pp. 673–684, April 2014.

[7] A. Biondi, D. Ginste, D. De Zutter, P. Manfredi, and F. Canavero, "Variability analysis of interconnects terminated by general nonlinear loads," *Components, Packaging and Manufacturing Technology, IEEE Transactions on*, vol. 3, no. 7, pp. 1244–1251, 2013.

[8] J. Tao, X. Zeng, W. Cai, Y. Su, D. Zhou, and C. Chiang, "Stochastic sparse-grid collocation algorithm (SSCA) for periodic steady-state analysis of nonlinear system with process variations," in *Proceedings of the 2007 Asia and South Pacific Design Automation Conference*, ser. ASP-DAC '07. Washington, DC, USA: IEEE Computer Society, 2007, pp. 474–479.

[9] Z. Zhang, T. El-Moselhy, I. M. Elfadel, L. Daniel *et al.*, "Stochastic testing method for transistor-level uncertainty quantification based on generalized polynomial chaos," *Computer-Aided Design of Integrated Circuits and Systems, IEEE Transactions on*, vol. 32, no. 10, pp. 1533–1545, 2013.

[10] H. C. Elman, C. W. Miller, E. T. Phipps, and R. S. Tuminaro, "Assessment of collocation and galerkin approaches to linear diffusion equations with random data," *International Journal for Uncertainty Quantification*, vol. 1, no. 1, 2011.

[11] C. Sandu, A. Sandu, and M. Ahmadian, "Modeling multibody systems with uncertainties. part II: Numerical applications," *Multibody System Dynamics*, vol. 15, no. 3, pp. 241–262, 2006.

[12] T.-A. Pham, E. Gad, M. Nakhla, and R. Achar, "Efficient Hermite-based variability analysis using approximate decoupling technique," in *Signal and Power Integrity (SPI), 2013 IEEE 17th Workshop on*, 2013, pp. 111–114.

[13] M. R. Rufuie, E. Gad, M. Nakhla, R. Achar, and M. Farhan, "Fast variability analysis of general nonlinear circuits using decoupled polynomial chaos," in *Signal and Power Integrity (SPI), 2014 IEEE 18th Workshop on*, May 2014, pp. 1–4.

[14] X.C.Liu and E.Gad, "Statistical analysis via generalized decoupled polynomial chaos," in *Electrical Performance of Electronic Packaging and Systems (EPEPS), 2015 IEEE 24th Conference on*, Oct. 2015, pp. 17–19.

[15] X. C. Liu and E. Gad, "Variability analysis via decoupled generalized polynomial chaos using the galerkin projection technique," *Components, Packaging and Manufacturing Technology, IEEE Transactions on*, submitted.

[16] C.-W. Ho, A. Ruehli, and P. Brennan, "The modified nodal approach to network analysis," *Circuits and Systems, IEEE Transactions on*, vol. 22, no. 6, pp. 504 – 509, Jun. 1975.

[17] P. Galko, *Stochastic Processes*. uOttawa docu centre, 2014.

[18] R. V. Hogg and A. T. Craig, *Introduction to Mathematical Statistics,*, 3rd ed. New York: Macmillan, 1971.

[19] D. Xiu, "Fast numerical methods for stochastic computations: A review," *Commun. Comput. Phys.*, vol. 5, no. 2-4, pp. 242–272, Feb. 2009.

[20] A. Singhee and R. A. Rutenbar, "Why quasi-monte carlo is better than monte carlo or latin hypercube sampling for statistical circuit analysis," *Computer-Aided Design of Integrated Circuits and Systems, IEEE Transactions on*, vol. 29, no. 11, pp. 1763–1776, Nov. 2000.

[21] N. Wienner, "The homogeneous chaos," *American Journal of Mathematics*, vol. 60, no. 4, pp. 897–936, Oct. 1938.

[22] A. J. Chorin, "Gaussian fields and random flow," *J. Fluid Mech*, vol. 63, pp. 21–32, Jul 1973.

[23] S. A. Orszag and L. R. Bissonnette, "Dynamical properties of truncated wiener-hermite expansions," *Phys. Fluids*, vol. 10, pp. 2603–2613, Dec 1967.

[24] G. Dattoli, H. M. Srivastava, and K. Zhukovsky, "Orthogonality properties of the hermite and related polynomials," *J. Comput. Appl. Math.*, vol. 182, pp. 163–172, Oct. 2005.

[25] W. H. Press, S. A. Teukolsky, W. T. Vetterling, and B. P. Flannery, *Numerical Recipes: The Art of Scientific Computing.*, 3rd ed. New York: Cambridge University Press, 2007.

[26] P. Manfredi, "High-speed interconnect models with stochastic parameter variability," Ph.D. dissertation, Politecnico di Torino, 2013.

[27] M. Abramowitz and I. A. Stegun, *Handbook of Mathematical Functions*. New York: Dover, 1972.

[28] M. S. Eldred, "Recent advances in non-intrusive polynomial chaos and stochastic collocation methods for unvertainty analysis and design," in *50th AIAA/ASME/ASCE/AHS/ASC structures, Structurak Dynamics and Materials Conference*, May 2009.

[29] I. Babuska, F. Nobile, and R. Tempone, "A stochastic collocation method for elliptic pparti differential equations with random input data," *SIAM J. Numer. Anal.*, vol. 45, pp. 1005–1034, May 2007.

[30] D. Xiu and S. Hesthaven, "High-order collocation methods for differential equations with random inputs," *SIAM J. Sci. Comput.*, vol. 27, pp. 1118–1139, 2005.

[31] D. Xiu, *Numerical Methods for Stochastic Computations: A Spectral Method Approach*. Princeton University Press, 2010.

[32] S. A. Smolyak, "Quadrature and interpolation formulas for tensor products of certain classes of dunctions," *Soviet Math. Dokl*, vol. 4, pp. 240–243, 1963.

[33] I. S. Gradshteyn and I. M. Ryzhik, *table of Integrals, Series and Products 7th edition*. San Diego: Academic press, 2007.

[34] J. A. Gaunt, *The triplets of Helium*. Philosophical Transactions of the Royal Society of London, 1929.

[35] M. N. T.-A. Pham, E. Gad and R. Achar, "Decoupled polynomial chaos and its applications to statistical analysis of high-speed interconnects," *IEEE Transaction on Components, Packaging and Manufacturing Technology*, vol. 4, no. 10, pp. 1634–1647, Oct 2014.

[36] C. F. Dunkl and Y. Xu, *Orthogonal Polynomials of Several Variables*, ser. Encyclopedia of Mathematics and its Applications. Cambridge, 2001.

[37] D. Bernstein, *Matrix Mathematics. Theory, Facts, and Formulas with Applications to Linear Systems Theory*. Princeton University Press, 2005.

[38] I. Stievano, P. Manfredi, and F. Canavero, "Carbon nanotube interconnects: Process variation via polynomial chaos," *IEEE Trans. Electromagn. Compat.*, vol. 54, no. 1, pp. 140–148, Feb 2012.